

Head-mounted Sensory Augmentation System for Navigation in Low Visibility Environments



Hamideh Kerdegari

Supervisors:

Prof. Tony Prescott

Dr. Yeongmi Kim

The University of Sheffield

Thesis Submitted for the Degree of
Doctor of Philosophy

March 2017

Dedicated to

My parents and sister

*for their support and encouragement, and
for always being there for me despite the distance.*

My beloved husband Saeid

for his endless love and support.

Abstract

Sensory augmentation can be used to assist in some tasks where sensory information is limited or sparse. This thesis focuses on the design and investigation of a head-mounted vibrotactile sensory augmentation interface to assist navigation in low visibility environments such as firefighters' navigation or travel aids for visually impaired people.

A novel head-mounted vibrotactile interface comprising a 1-by-7 vibrotactile display worn on the forehead is developed. A series of psychophysical studies is carried out with this display to (1) determine the vibrotactile absolute threshold, (2) investigate the accuracy of vibrotactile localization, and (3) evaluate the funneling illusion and apparent motion as sensory phenomena that could be used to communicate navigation signals. The results of these studies provide guidelines for the design of head-mounted interfaces.

A 2nd generation head-mounted sensory augmentation interface called the Mark-II Tactile Helmet is developed for the application of firefighters' navigation. It consists of a ring of ultrasound sensors mounted to the outside of a helmet, a microcontroller, two batteries and a refined vibrotactile display composed of seven vibration motors based on the results of the aforementioned psychophysical studies.

A 'tactile language', that is, a set of distinguishable vibrotactile patterns, is developed for communicating navigation commands to the Mark-II Tactile Helmet. Four possible combinations of two command presentation modes (continuous, discrete) and two command types (recurring, single) are evaluated for their effectiveness in guiding users along a virtual wall in a structured environment. Continuous and discrete presentation modes use spatiotemporal patterns that induce the experience of apparent movement and discrete movement on the forehead, respectively. The recurring command type presents the tactile command repeatedly with an interval between patterns of 500 ms while the single command type presents the tactile command just once when there is a change in the command. The effectiveness of this tactile language is evaluated according to the objective measures of the users' walking speed and the smoothness of their trajectory parallel to the virtual wall and subjective measures of utility and comfort employing Likert-type rating scales. The Recurring Continuous (RC) commands that exploit the phenomena of apparent motion are most effective in generating efficient routes and fast travel, and are most preferred.

Finally, the optimal tactile language (RC) is compared with audio guidance using verbal instructions to investigate effectiveness in delivering navigation commands. The results show that haptic guidance leads to better performance as well as lower cognitive workload compared to auditory feedback.

This research demonstrates that a head-mounted sensory augmentation interface can enhance spatial awareness in low visibility environments and could help firefighters' navigation by providing them with supplementary sensory information.

Acknowledgements

I would like to express my gratitude to my supervisor, Prof. Tony Prescott, for giving me the opportunity to work with him, for his guidance, patience, and advice to keep me motivated throughout my PhD study.

I would like to thank Dr. Yeongmi Kim and Dr. Sean Anderson for their support during my PhD, for sharing their valuable experience and for providing me with invaluable feedback.

I would also like to acknowledge all the participants who graciously agreed to participate in my experiments.

Undoubtedly, I would like to thank my family and particularly my husband, Saeid, without whose love and encouragement, the completion of this thesis would not have been possible.

Finally, I gratefully acknowledge the University of Sheffield Cross-Cutting Directors of Research and Innovation Network (CCDRI), Search and Rescue 2020 project which provided full funding for this work.

Declaration

I hereby declare that the contents of this thesis are my original work and have not been submitted for any other degree or any other university. I have designed and built all of the sensory augmentation device described in this thesis. Some parts of the work described in Chapters 3, 4, 5 and 6 have been published in a journal article or conference proceedings as given below. I have received permission from their publishers to use them in my thesis.

1. **H. Kerdegari**, Y. Kim and Tony J. Prescott, “Head-mounted Sensory Augmentation Device: Designing a Tactile Language,” *IEEE Transactions on Haptics*, vol. 9, no. 3, pp. 376–386, 2016.
2. **H. Kerdegari**, Y. Kim and Tony J. Prescott, “Head-mounted Sensory Augmentation Device: Comparing Haptic and Audio Modality,” in *Biomimetic and Biohybrid Systems*, Springer, pp. 107–118, 2016. (Poster presentation)
3. **H. Kerdegari**, Y. Kim and Tony J. Prescott, “Tactile Language for a Head-mounted Sensory Augmentation Device,” in *Biomimetic and Biohybrid Systems*, Springer, pp. 359–365, 2015. (Poster presentation)
4. **H. Kerdegari**, Y. Kim, T. Stafford, and T. J. Prescott, “Centralizing Bias and the Vibrotactile Funneling Illusion on the Forehead,” in *Proceedings of Eurohaptics*, Springer, pp. 55–62, 2014. (Oral presentation)

Table of Contents

List of Figures	xv
List of Tables	xxi
Abbreviations	xxiii
1 Introduction	1
1.1 Motivation	3
1.1.1 Enhanced awareness for firefighters	4
1.2 Problem statement	6
1.3 Objectives	6
1.4 Contributions	7
1.5 Thesis outline	9
2 Background and Related Work	13
2.1 The sense of touch in humans	15
2.1.1 Skin physiology	15
2.2 Vibrotactile perception	19
2.2.1 Sensory parameters	20
2.2.2 Sensory phenomena	27
2.2.2.1 Funneling illusion	28
2.2.2.2 Sensory saltation	31
2.2.2.3 Apparent movement	33
2.3 Tactile display technology	35
2.4 Vibrotactile actuators	37
2.5 Tactile display applications	39
2.5.1 Sensory substitution	40

2.5.2	Sensory augmentation	43
2.5.3	Spatial orientation and navigation	46
2.6	Tactile language	48
2.6.1	Distance encoding	50
2.6.2	Direction encoding	53
2.7	Head-mounted vibrotactile displays	55
2.8	Wall-following navigation	60
3	Vibrotactile Headband Display	65
3.1	Methods	66
3.1.1	Participants	66
3.1.2	Apparatus	66
3.1.3	General procedure	68
3.2	Experiments	70
3.2.1	Vibrotactile absolute threshold	70
3.2.2	Vibrotactile Localization	75
3.2.3	Effect of inter-tactor spacing on the funneling illusion	78
3.2.4	Effect of SOA and inter-tactor spacing on apparent motion	80
3.3	Summary	84
4	Design of a Head-mounted Sensory Augmentation System	87
4.1	System overview	88
4.1.1	Ultrasound sensor	89
4.1.2	Inertial Measurement Unit (IMU)	91
4.1.3	Vibrotactile display	92
4.1.4	Controlling unit and power supply	93
4.2	System data flow	94
5	Designing a Tactile Language for a Head-mounted Sensory Augmentation System	97
5.1	Experimental design	98
5.2	Methods	102
5.2.1	Participants	102

5.2.2	Apparatus and materials	102
5.2.3	Procedure	105
5.3	Results	111
5.4	Summary	116
6	Evaluation of Navigation Performance in a Physical Environment	119
6.1	Haptic and audio guidance	120
6.2	Experimental design	121
6.3	Methods	122
6.3.1	Participants	122
6.3.2	Apparatus and material	123
6.3.3	Procedure	123
6.3.4	A multi-layer perceptron classifier for computing navigation commands	125
6.3.4.1	Data collection procedure	125
6.3.4.2	Proposed MLP algorithm	126
6.4	Results	130
6.5	Summary	133
7	Conclusion and Future Work	135
7.1	Reviewing the scope of the thesis	135
7.2	Answer to research questions	142
7.3	Future work	144
	References	147
	Appendix A Participant consent forms	169
A.1	Consent form I	169
A.2	Consent form II	171
A.3	Consent form III	173
A.4	Consent form IV	174
	Appendix B Hardware specification	177
B.1	I2CXL-MaxSonar-EZ2 Ultrasound Sensor	178

B.2	IMU	180
B.3	310-113 Vibration Motor	186
B.4	Arduino Yún microcontroller	187
B.5	ADXL325 Accelerometer	189
B.6	Schematic of the Mark-II Tactile Helmet	191
Appendix C Questionnaires		193
C.1	Likert Scale Questionnaire	194
C.2	NASA Task Load Index Questionnaire	195

List of Figures

1.1	Three network projects and their interrelationship.	2
1.2	(a) Firefighters' mission in a burning building, (b) Firefighters' navigation through keeping contact with a guided rope by moving their hands, source from Fischer et al. [10]	5
2.1	A diagram of the employed technical approach in this thesis.	14
2.2	Cross section of hairy and glabrous skin showing skin layers and its mechanoreceptors. Source from [15].	16
2.3	Two-point discrimination thresholds for different parts of the body. Source from Weinstein [20].	18
2.4	The sensory homunculus on the somatosensory cortex. The size of each area represents the perception sensitivity. Source from Betts et al. [22].	19
2.5	Threshold frequency characteristics measured on the fingertip [24], forearm [16], and abdomen [25]. Source from Jones et al. [23].	20
2.6	Difference thresholds as a function of frequency for the forearm (filled squares [27], open squares [18]), finger (filled circles [28], open circles [29]), and hand [30]). Source from Jones et al. [23].	21
2.7	Vibrotactile enhancement effect. (a) Spatial summation: refers to an increasing number of stimulated nerved fibers that result in a perception of increasing intensity, (b) Temporal summation: refers to an increasing number of impulses along a single fiber which causes a perception of increasing intensity. Source from Guyton [58].	28

2.8	Funneling illusion with: (a) Same intensities, (b) Different intensities. Source from Cha et al. [65].	29
2.9	Illustration of using funneling illusion to create a continuous movement sensation. Source from Barghout et al. [68].	30
2.10	An explanation of stimulation pattern (top) vs. the perceived sensation pattern (bottom) for sensory saltation. Source from Tan et al. [42].	32
2.11	Illustration of Duration of Stimulus (DoS) and Stimulus Onset Asynchrony (SOA). Source from Niwa et al. [76].	34
2.12	Sample actuators for vibrotactile display. S: Five solenoids of varying sizes. VC: A commercial voice coil without bearings. Sp: Two audio speakers. C2: A C2 tactor from EAI. Haptuator: A Haptuator from Tactile Labs, Inc. Tactaid: One complete Tactaid from AEC and one opened to show the suspension inside. E: Five shafted/cylindrical eccentric rotating mass motors. P: Three shaftless/pancake eccentric rotating mass motors. A U.S. quarter appears at bottom right for scale. Source from Choi et al. [87].	38
2.13	Sensory substitution structure. Source from Visell [83].	40
2.14	(a) A Tactile Visual Sensory Substitution (TVSS) device, source from Batch-y-Rita [90]. (b) The Tongue Display Unit (TDU) as an electrotactile sensory substitution device, source from Batch-y-Rita et al. [91].	41
2.15	(a) Optacon device is used to read a text by visually impaired individuals. (b) A close up of the tactile array. Source from Stronks et al. [94].	42
2.16	(a) Augmented spatial awareness. (b) Avoiding an unseen object with Haptic Radar. Source from Cassinelli et al. [5].	44
2.17	Balance prostheses sensory augmentation devices. (a) A waist-mounted vibrotactile display, source from Wall et al. [111]. (b) A foot-mounted vibrotactile display, source from Priplata et al. [112].	46

2.18	The Mark-I Tactile Helmet [6] was composed of a ring of ultrasound sensors and four actuators inside the helmet and was designed to help firefighters' navigation inside smoked-filled buildings.	59
2.19	Block diagram of the wall-following controller employed by Freire et al. [158].	61
2.20	A fuzzy wall-following controller.	63
3.1	(a): Eccentric Rotating Mass (ERM) vibration motor (Model 310-113 by Precision Microdrives), (b): Vibrotactile headband interface, (c): A participant wearing the vibrotactile headband interface.	67
3.2	Overview of the experimental setup.	68
3.3	A participant in the experiment room sitting in front of the mirror, PC, mouse, and footswitch while doing the experiment.	69
3.4	A participant is pointing to the perceived location(s) of stimulation on his forehead. (a): pointing on one location, (b): pointing on two locations.	70
3.5	Graphical User Interface (GUI) for vibrotactile absolute threshold measurement experiment.	71
3.6	Histogram of frequency of detection for the employed PWM intensities, n=200 samples.	73
3.7	An ADXL325 accelerometer was mounted on top of an ERM vibration motor to measure the unit of intensity.	74
3.8	Acceleration values equivalent of PWM intensity of 1-255.	75
3.9	GUI for vibrotactile localization experiment.	76
3.10	Localization mean error for seven factor locations, n=1050 samples. Error bars show standard error.	77
3.11	Localization mean error for left and right side pointings, n=1050 samples. Error bars show standard error.	77
3.12	Percentage of pointing to one and two locations for different inter-tactor spacings, n=900 samples. Error bars show standard error.	79

3.13	Perceived and actual inter-tactor spacing, n=900 samples. Error bars show standard error.	80
3.14	Employed GUI in apparent motion experiment.	81
3.15	Two stimuli are presented one after the other with a time interval between sequences, source from Niwa et al. [76]. . .	82
3.16	Subjective rating for stimuli patterns, n=540 samples. Bars show median value and error bars indicate standard error. .	83
4.1	The Mark-II Tactile Helmet configuration.	88
4.2	Ultrasound sensor range measurement principle.	89
4.3	(a): Ultrasound sensor (Model I2CXL-MaxSonar-EZ2 by MaxBotic), (b): Ultrasound sensors arrangement on the Mark- II Tactile Helmet.	91
4.4	(a): Eccentric Rotating Mass (ERM) vibration motor (Model 310-113 by Precision Microdrives (see Appendix B.3), (b): Vibrotactile display interface, (c): Vibrotactile display po- sition inside the helmet, (d): Microcontroller, IMU, sound card, and batteries position inside the helmet.	93
4.5	Data flow diagram of the Mark-II Tactile Helmet.	95
5.1	Vibrotactile patterns for turn-left, turn-right and go-forward commands in the tactile display.	99
5.2	Schematic representation of the tactile language employed in this study. (a) Continuous presentation. (b) Discrete presentation. (c) Single cue. (d) Recurring cue.	100
5.3	Basic Vicon system structure.	103
5.4	3D perspective of the capture room from the perspective of the Vicon Tracker software [187] and representation of the Mark-II Tactile Helmet as an object within the capture room (bottom left). Ten cameras (green boxes) cover the experimental environment with the size of $3 \times 5 \text{ m}^2$	104
5.5	Schematic of the virtual walls and the user in the right and left side of them.	105

5.6	Experimental environment: 3×5 m ² free space. A volunteer is walking along a virtual wall in the capture room.	106
5.7	An example of the left out-corner wall following of one participant. Dashed lines show the user's head trajectory and arrows show the user's head orientation while receiving the related command.	110
5.8	(a) Recognition accuracy (%) for each condition, (b) Reaction time (s) for each condition, n=1296 samples. Error bars indicate standard error.	112
5.9	(a) Smoothness of users' trajectory measured by Mean Absolute Deviation (MAD), (b) Walking speed for each condition, n=1296 samples. Error bars indicate standard error.	113
5.10	Users' trajectory with: (a) Recurring Continuous (RC), (b) Recurring Discrete (RD), (c) Single Continuous (SC), and (d) Single Discrete (SD) command. Blue lines show users' Motion Trajectory (MT) and red dashed lines show users' Expected Trajectory (ET). In each command, the presented trajectories were chosen randomly from each of 18 participants.	114
6.1	(a) Overhead view of the experimental set-up consisting of cardboard walls and motion capture cameras, position 1 and 2 show the trial stating points. The length of the walls from the start point to the end is 20 m. (b) A participant is navigating along the wall.	123
6.2	Sketch of the data collection environment. Experimenter's start position for collecting data in anti-clockwise (1) and clockwise (2) direction is presented.	126
6.3	The structure of the proposed MLP. It consists of 12 input neurons, 15 hidden neurons and 3 outputs.	127
6.4	Mean Squared Error (MSE) as a function of hidden neurons.	128
6.5	The MLP best validation performance.	129

-
- 6.6 Objective measures. (a) Task completion time, (b) Travel distance, (c) Route deviation, n=40 samples. The unit of task completion time is in the minute and unit of travel distance and route deviation is in the meter. Error bars show standard error. 131
- 6.7 Questionnaire feedback. The first six bar plots represent the NASA TLX score for the audio and haptic guidance. The rating scale is 1-21, where 1 represents no mental, physical and temporal demand, best performance, no effort required to complete the task and, no frustration. The last bar plot shows the participants' preference for navigation with the haptic guidance. The error bars indicate standard error. . . 132

List of Tables

2.1	Characteristics of skin mechanoreceptors [17].	17
3.1	Post hoc test for SOA and inter-tactor spacing comparison for perceived apparent motion (AP)	84
5.1	User's experience evaluation for 18 participants.	108
5.2	Post hoc test for condition types comparison in terms of being easy to distinguish and effective for navigation.	115
6.1	Performance of the trained MLP with different transfer functions. Std and perf stand for standard deviation and performance, respectively.	128
6.2	Precision and recall of the MLP algorithm for recognizing the go-forward, turn-left and turn-right commands.	130

Abbreviations

ADC Analog to Digital Converter

CCDRI Cross-Cutting Directors of Research & Innovation Network

DCT DC motor Tactor

DoF Degrees of Freedom

DoS Duration of Stimulus

ERM Eccentric Rotating Mass

ET Expected Trajectory

GUI Graphical User Interface

IMU Inertial Measurement Unit

ISI Inter-Stimulus Interval

Logsig Log-sigmoid

MAD Mean Absolute Deviation

MANOVA Multivariate Analysis of Variance

MLP Multi-Layer Perceptron

MT Motion Trajectory

PWM Pulse Width Modulation

RA Rapid Adaptors

RC Recurring Continuous

RD Recurring Discrete

SA Slow Adaptors

SC Single Continuous

SD Single Discrete

SOA Stimulus Onset Asynchrony

SYFR South Yorkshire Fire and Rescue

TDU Tongue Display Unit

TLX Task Load Index

TOF time-of-flight

TSAS Tactile Situation Awareness System

TVSS Tactile Visual Sensory Substitution

Tansig Hyperbolic tangent sigmoid

VCT Voice Coil Tactor

Chapter 1

Introduction

The research presented in this thesis is undertaken as part of a network project ‘Search and Rescue 2020’ funded by The University of Sheffield whose aim is to develop novel assistive technologies to enhance and complement the capabilities of humans in search and rescue missions conducted in the year 2020. This network project consists of three interdisciplinary and interlinked projects that brings together researchers from different departments at The University of Sheffield such as Psychology (PSY), Automatic Control & Systems Engineering (ACSE), Computer Science (COM), and Architecture (ARCH). The three network projects, their interrelationship and which of the challenges they address are highlighted in [Figure 1.1](#).

Each of the projects will address a key technological challenge in the area of search and rescue. However, an overarching theme of the project is the development of technologies that aid the overall command and control in search and rescue by providing more accurate and timely sensing, situational awareness and support to the search and rescue workers. This thesis focuses on ‘Wearable computing for sensing and navigation’ as a part of this network project by developing and investigating a head-mounted sensory

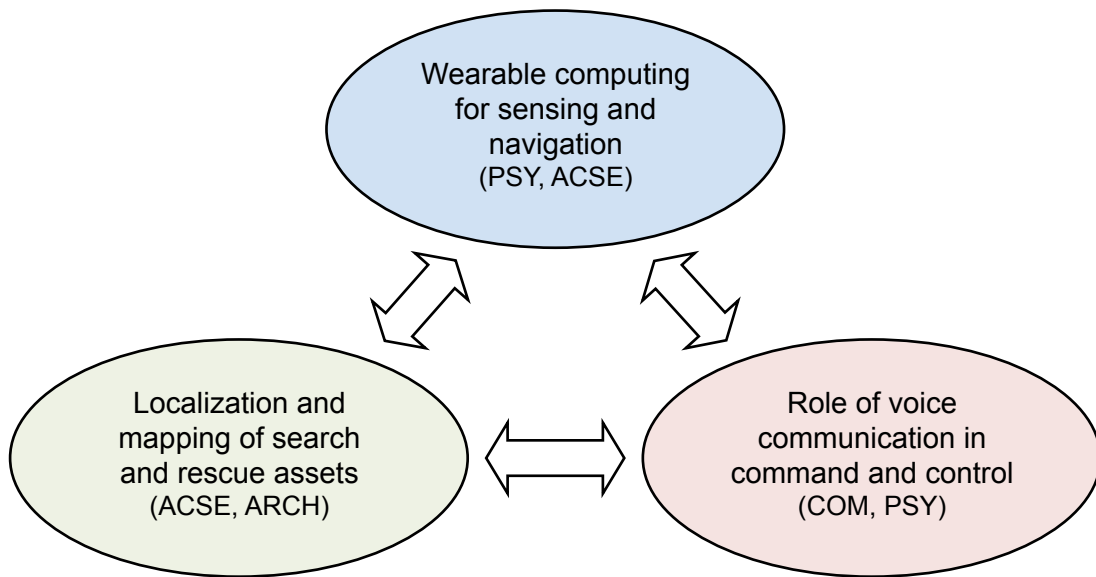


Fig. 1.1 Three network projects and their interrelationship.

augmentation system to enhance rescue workers' spatial awareness and navigation in low visibility environments such as smoke-filled buildings.

The rest of this chapter is organised as follows: the motivation that supports the investigations, designs and implementations of this thesis is presented in Section 1.1. The problems that require to be addressed through this research is described in Section 1.2. The principal aim and objectives to be accomplished in this work are presented in Section 1.3. The contributions from the investigations performed in this thesis are described in Section 1.4. Finally, Section 1.5 presents the organisation of the chapters that build the rest of this thesis.

1.1 Motivation

This thesis explores the exciting possibility of augmenting the human senses to create new ways of experiencing and understanding the world particularly through the sense of touch. The idea of using touch as a medium for communication has drawn the attention of researchers over many years. Geldard [1] was one of the first people to propose using the sense of touch as a communication channel. He emphasized the different capabilities of touch including temporal and spatial discrimination, capturing attention, the existence of large areas of skin for stimulation, and underutilization of this channel for information presentation [2].

The sense of touch is a unique communication channel. In contrast to visual and audio modalities, touch represents a proximal sense which means it senses objects that are in direct contact with the body [3]. Moreover, the proximal nature of touch allows for the creation of tactile displays/interfaces. Tactile displays offer an alternative channel through which information can be communicated when other channels such as vision and hearing are impaired or overloaded.

Initial investigations with tactile displays explored their potential to compensate for sensory loss or impairment [4]. Tactile displays support a variety of applications in sensory substitution [4] and sensory augmentation [5, 6] and may be particularly useful for tasks such as spatial orientation and navigation [7, 8]. Sensory augmentation as one application of tactile displays operates by synthesizing new information then displaying it through an existing sensory channel. It can be used to augment the spatial awareness

of people with impaired sensing or to assist in tasks where sensory information is limited or sparse, for example, when navigating in a low visibility environment.

1.1.1 Enhanced awareness for firefighters

Firefighters operate in low visibility environments with potentially noxious atmospheric conditions, high noise and extreme temperatures that are physically very hazardous (see Figure 1.2a). Navigation in such ever-changing environments with few supporting infrastructures is a common situation for firefighters. They usually need to enter into smoke-filled buildings, explore the environments to make a shared knowledge of the situation, and to define the intervention task [9]. During this reconnaissance mission which play a central role in firefighting practice, firefighters face a situation where orientation and navigation are key success factors. In order to navigate in such challenging environments, firefighters utilize the existing infrastructures such as walls and doors. These reference points help them to stay oriented and make a mental model of the environment [9].

Guide-rope or lifeline is one of the main tools used for navigation in the firefighters' practice which is latched at the belt of a firefighter and hold on the other end by the team leader. Firefighters use the guide-rope as a retreat path and as a way to define positions along their path using knots while navigating along the walls. Actually, firefighters are trained to make extensive use of their tactile sense to feel their way during navigation (see Figure 1.2b). Although details vary between countries, the universal best-practice method employed by firefighters traversing smoke-filled environments includes



Fig. 1.2 (a) Firefighters' mission in a burning building,¹ (b) Firefighters' navigation through keeping contact with a guided rope by moving their hands, source from Fischer et al. [10].

keeping contact with a guide-rope and exploring the interior of the building by moving with an extended hand or tool such as an axe [10].

In addition to the guide-rope as a physical guideline, firefighters are also given navigation information by a commander via radio communication. Communication with command centers is critical, but, in addition there should be navigation systems that augment firefighters' spatial awareness and allow them to work autonomously when communication channels such as vision and hearing are heavily loaded and compromised. Instead of replacing existing navigation tools such as a guide-rope, new navigation systems should improve and augment existing concepts and be constructed in a way that facilitates their appropriation.

Therefore, these challenges motivate this thesis to provide firefighters with a new sensory augmentation system that can assist

¹Source from Fire Engineering magazine: <http://community.fireengineering.com/photo>

them with navigation in low visibility environments by providing supplementary sensory information.

1.2 Problem statement

The main problems which require to be addressed in building a sensory augmentation system for enhancing navigation are designing an effective tactile display and the selection and specification of the tactile language that is used to present navigation information. This thesis addresses these problems, focusing on the following research questions:

- RQ1: What form of a head-mounted vibrotactile display will be effective as a haptic interface for head-mounted sensory augmentation systems?
- RQ2: Given an initial head-mounted sensory augmentation prototype device, how can we identify and overcome its limitations?
- RQ3: What are the vibrotactile parameters that can be manipulated to encode direction information as a tactile language for head-mounted sensory augmentation systems?
- RQ4: How should the proposed tactile language work in a navigation task?

1.3 Objectives

In light of the above problem definition, the overall aim of this thesis is to develop and investigate a head-mounted vibrotactile

interface for sensory augmentation in low visibility environments. The specific objectives are as follows:

- Investigate the human perception of tactile signals delivered by a head-mounted vibrotactile display using a series of psychophysical experiments focusing on the vibrotactile absolute threshold, vibrotactile localization, the funneling illusion and the apparent motion illusion.
- Develop a 2nd generation head-mounted sensory augmentation prototype to overcome some of the limitations of the earlier prototype developed by Bertram et al. [6], particularly the low resolution of the tactile display and the size and weight of the on- and off-board electronics.
- Investigate the design space for display of haptic commands as tactile language, specifically focusing on the potential of signals that can be interpreted quickly and intuitively, and in the context of designing haptic navigation aids for firefighters.
- Evaluate the effectiveness of the developed tactile language compared with audio guidance for navigation without vision.

1.4 Contributions

This thesis makes the following contributions:

- I describe a novel psychophysical investigation of a head-mounted vibrotactile display that resulted in the following original findings:

(i) Whereas vibrotactile localization error on the forehead is uniform, there is a bias towards the forehead midline in localizing tactors that are away from the center of the forehead.

(ii) The funneling illusion occurs mainly for shorter inter-tactor spacing on the forehead (e.g. 2.5 cm), however, two stimuli at wider spacings are consistently reported as being closer together than their actual distance, even when not experiencing the funneling illusion. Centralizing bias in the vibrotactile localization study could partly describe this consistent under-estimating of inter-tactor spacing in the funneling illusion study.

(iii) Stimulus Onset Asynchrony (SOA) and inter-tactor spacing both influence the perception of apparent motion illusion on the forehead. An inter-tactor spacing of 5 cm at 100 ms SOA showed the highest rate of apparent motion of the values tested.

As a theoretical contribution, these studies help in formulating guidelines for the design of head-mounted vibrotactile displays and also inform the wider understanding of tactile sensing. This contribution acts as a part of the basis that is used for the design of the practical studies in this thesis which resulted in the following contributions.

- The Mark-II Tactile Helmet as a head-mounted sensory augmentation prototype has been designed for firefighters' navigation. It is comprised of a ring of ultrasound sensors mounted to the outside of a helmet to sense the environment and a refined tactile display with a design based on the results of

the aforementioned psychophysical studies. This compact and lightweight system works as standalone using its embedded controlling unit and power supply system.

- A tactile language for communicating navigation commands to the Mark-II Tactile Helmet has been developed. The proposed tactile language, namely, Recurring Continuous (RC) command exploits the spatiotemporal patterns that induce the experience of apparent motion illusion while presenting the navigation commands repeatedly. To the best of my knowledge, this is the first tactile language that has been proposed specifically for the head-mounted vibrotactile displays.
- Navigation performance of the proposed tactile language (RC) when compared to that using auditory feedback demonstrated that haptic guidance leads to better performance as well as lower cognitive workload.

1.5 Thesis outline

This thesis is structured as follows:

- Chapter 2 provides a review of background material on various aspects of tactile communication including the tactile sense in humans and related sensory phenomena, tactile display technology and its application, tactile language for encoding navigation information, and head-mounted vibrotactile displays. Finally, a literature on wall-following methods employed in mobile robots is presented which can inform the design of guidance systems using sensory augmentation.

- Chapter 3 presents a psychophysical investigation of head-mounted vibrotactile interfaces for sensory augmentation. A 1-by-7 headband vibrotactile display was designed to provide stimuli on participants' forehead. Experiment I measures the vibrotactile absolute threshold on the forehead using the method of limits [11]. Experiment II evaluates the ability to identify the location of a vibrotactile stimulus presented to a single tactor in the display. Experiment III is designed to investigate the dependency of funneling illusion on inter-tactor spacing. Finally, experiment IV is performed to find the appropriate timing value and inter-tactor spacing that create apparent motion illusion on the forehead.
- Chapter 4 presents the design and development of the Mark-II Tactile Helmet as a 2nd generation head-mounted sensory augmentation prototype. The electronic components, the structure and data flow of the prototype system are described in this chapter.
- Chapter 5 presents a tactile language for communicating navigation commands to a head-mounted vibrotactile sensory augmentation prototype. Four possible combinations of two command presentation modes (continuous, discrete) and two command types (recurring, single) is tested to navigate users in a structured environment along a virtual wall. The effectiveness of this tactile language is evaluated according to the users' walking speed, smoothness of their trajectory parallel to the virtual wall and subjective measure using a Likert-type scale questionnaire.

-
- Chapter 6 compares and investigates the effectiveness of the proposed tactile language with audio guidance for navigation without vision. Participants are navigated along a wall in a structured environment relying on the haptic or audio feedback as navigation commands. Feedback is generated according to distance information measured from the wall using 12 ultrasound sensors placed around the Mark-II tactile Helmet and then a Multi-Layer Perceptron (MLP) neural network algorithm is used to determine appropriate guidance commands (i.e. go-forward, turn-right/left). The effectiveness of the haptic and audio guidance is evaluated according to the objective measures of task completion time, distance of travel and route deviation, and subjective measure of workload measurement using a NASA Task Load Index (TLX) questionnaire.
 - Chapter 7 summarizes the thesis, describes the limitation of this research and discusses a number of potential directions for future work.

Chapter 2

Background and Related Work

It is essential to gain an understanding of human perception of vibration stimuli before designing vibrotactile displays and subsequently tactile languages. Therefore, this chapter provides a description of the human tactile sense, its capabilities and potential applications in tactile displays.

The first part of this chapter (Sections [2.1](#) to [2.2.2](#)) contextualizes the work presented in this thesis by providing an overview of the sense of touch (Section [2.1](#)), then proceeding to the different parameters of vibration that can be manipulated to encode tactile information (Section [2.2.1](#)), and related phenomena in vibrotactile perception namely the funneling illusion (Section [2.2.2.1](#)), sensory saltation (Section [2.2.2.2](#)) and the apparent movement illusion (Section [2.2.2.3](#)).

A focused literature review on tactile displays is presented in the second part of this chapter (Sections [2.3](#) to [2.7](#)). It starts by discussing the two main categories of tactile displays such as electrotactile displays and vibrotactile displays in Section [2.3](#). Section [2.4](#) provides an overview of the most common actuators utilized in the vibrotactile displays, and discusses the choice of actuators for this research. The main applications of vibrotactile displays

such as sensory substitution, sensory augmentation and spatial orientation and navigation are reviewed in Section 2.5. A review of tactile languages for encoding distance and direction information is presented in Section 2.6. Section 2.7 introduces head-mounted vibrotactile displays for enhancing spatial awareness and navigation. Finally, Section 2.8 presents a review of wall-following approaches in mobile robots which is used in this thesis to simulate firefighters' wall-following behaviour during building exploration. Figure 2.1 shows a diagram of the employed technical approach in this thesis which this chapter reviews its related work in the following sections.

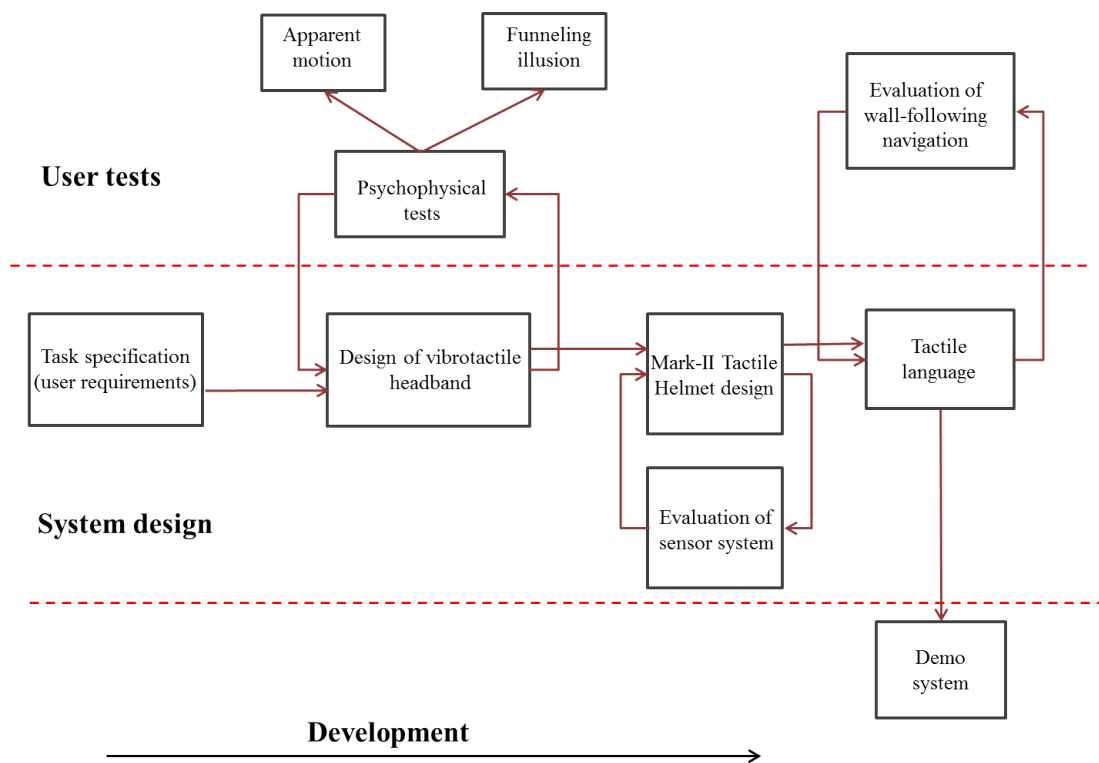


Fig. 2.1 A diagram of the employed technical approach in this thesis.

2.1 The sense of touch in humans

The human sense of touch consists of two main sensory systems — kinesthetic and cutaneous — which are characterized on the basis of their sensory inputs [12]. The kinesthetic sense receives sensory inputs from receptors within muscles, tendons, and joints while the cutaneous sense receives sensory inputs from receptors embedded in the skin. These two sensory systems are stimulated by two main categories of interfaces such as force feedback interface (by exerting forces to oppose movement) and tactile interface (by deforming the skin through vibration or pressure), respectively [12]. Furthermore, the sense of touch is multifunctional in that it supports both active and passive sensing [13]. Active sensing (touching) represents the exploratory action of touching [13], which generally involves both kinesthetic movements of the body and the cutaneous sense while passive sensing (being touched) refers to stimulation of the skin through external stimuli [13] which is associated purely with the cutaneous sense. This thesis covers both active and passive sensing. Chapter 3 is limited to passive sensing where the cutaneous sense on the forehead is stimulated by a tactile interface while Chapter 5 and 6 focus on a new kind distal active sense, by stimulating receptors on the forehead using body and head movement.

2.1.1 Skin physiology

The cutaneous sense is located in the skin as the largest human sensory organ. The sensations from the environment begin by contacting the skin that is embedded with different receptors responsible for the registration of different stimuli. These receptors are located

in various layers of the skin and are classified as mechanoreceptors (for pressure and vibration), nociceptors (for pain/damage) and thermoreceptors (for temperature) [14].

The focus of this thesis is on the perception of skin deformation sensed by mechanoreceptors. The mechanoreceptors provide a larger contribution to register mechanical distortion in the skin [14]. Four main kinds of mechanoreceptors - Meissner's Corpuscles, Merkel Disks, Ruffini Endings, and Pacinian Corpuscles - sense skin contacts and respond to various stimuli [14]. Figure 2.2 shows a cross section of the glabrous and hairy skin with different types of mechanoreceptors.

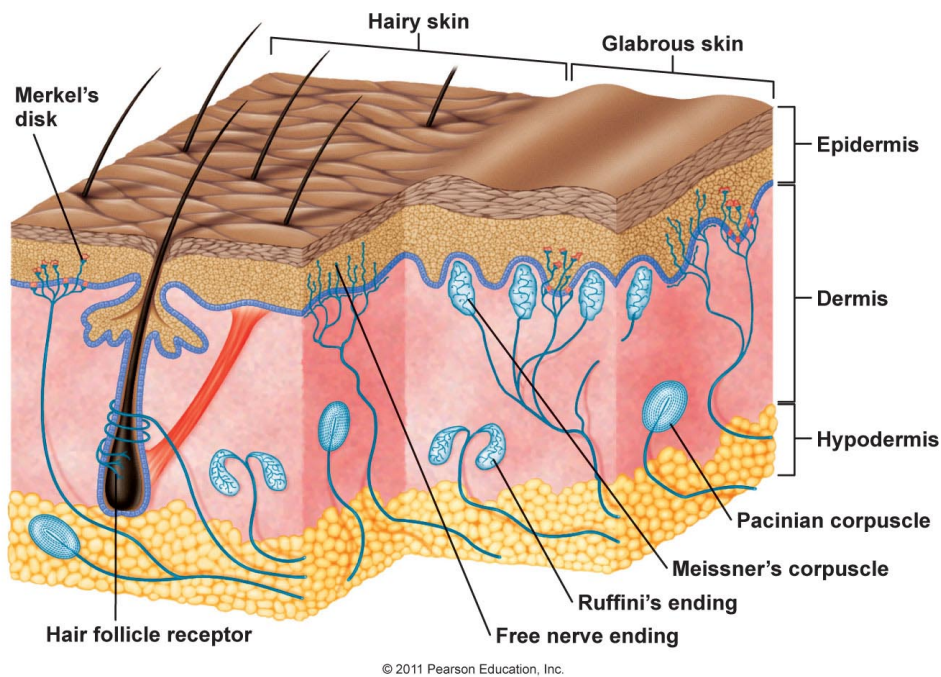


Fig. 2.2 Cross section of hairy and glabrous skin showing skin layers and its mechanoreceptors. Source from [15].

These mechanoreceptors are often categorized into classes depending on their receptive fields and the speed of excitation [14]. As shown in Table 2.1, they can be classified as Type I with small

Table 2.1 Characteristics of skin mechanoreceptors [17].

Receptor	Receptor type	Receptor field (mm)	Frequency range (Hz)	Response
Pacinian Corpuscle	RAII	10-1000	40-800	Vibration
Meissner's Corpuscle	RAI	1-100	10-200	Motion, vibration
Ruffini Endings	SAII	10-500	7	Pressure, Stretch
Merkel Disk	SAI	2-100	0.4-100	Pressure, texture

receptive fields; Type II with large receptive fields; Rapid Adaptors (RA) which respond to more rapidly changing stimuli; and Slow Adaptors (SA) which respond to slowly changing stimuli. For instance, the Pacinian Corpuscle, which responds to vibration stimuli, is classified as an RAI (rapid adaptors, typeI) mechanoreceptor as it responds to higher frequency stimulation and has large receptive fields.

Unlike glabrous skin which mediates the sense of touch through four mechanoreceptors, the tactile stimuli presented to hairy skin are processed through three mechanoreceptors called RAI, RAI and SAII [16]. Although glabrous and hairy skin are populated by various receptors, the Pacinian Corpuscle (RAII) as a mechanoreceptor responsible for perceiving high frequency vibration is available in both skin types. However, in hairy skin the Pacinian Corpuscle is located in deeper tissue compared to the glabrous skin [18]. Glabrous and hairy skin are also different in terms of detection threshold but vibrotactile frequency discrimination is very similar on both skin types [18]. This thesis is concerned with vibrotactile perception in hairy skin since the vibrotactile display considered in this research is mounted on the forehead.

The sensitivity of the skin to mechanical stimuli varies across the body [19]. Figure 2.3 shows the sensitivity of different body sites

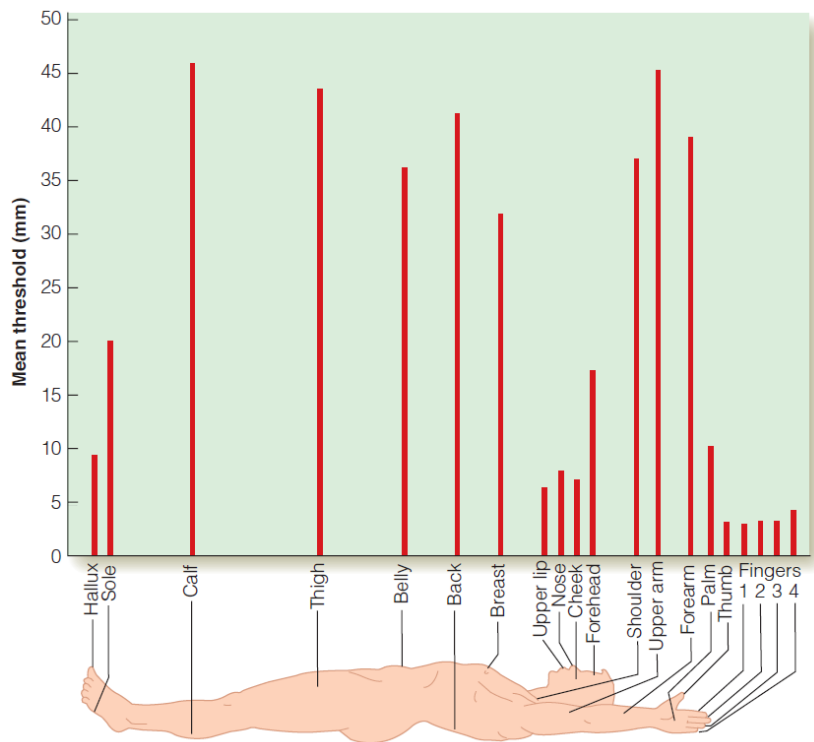


Fig. 2.3 Two-point discrimination thresholds for different parts of the body. Source from Weinstein [20].

that has been measured using the two-point threshold experiment that detects the smallest distinguishable separation of two points of stimulation [19]. The level of sensitivity is dependent on the number of touch receptors and the size of the receptive field, with the sensitivity inversely proportional to the size of the receptive field. Fingertips, lips, and palms have the densest concentrations of mechanoreceptors with small receptive fields and consequently are the most sensitive areas of the body.

When external stimuli interact with skin receptors, those receptors are stimulated and pass nerve signals to the brain. The somatosensory cortex in the brain receives these signals from the skin via the main sensory trigeminal pathway for the face and the medial lemniscal pathway for the body [21]. As shown in Figure 2.4, each

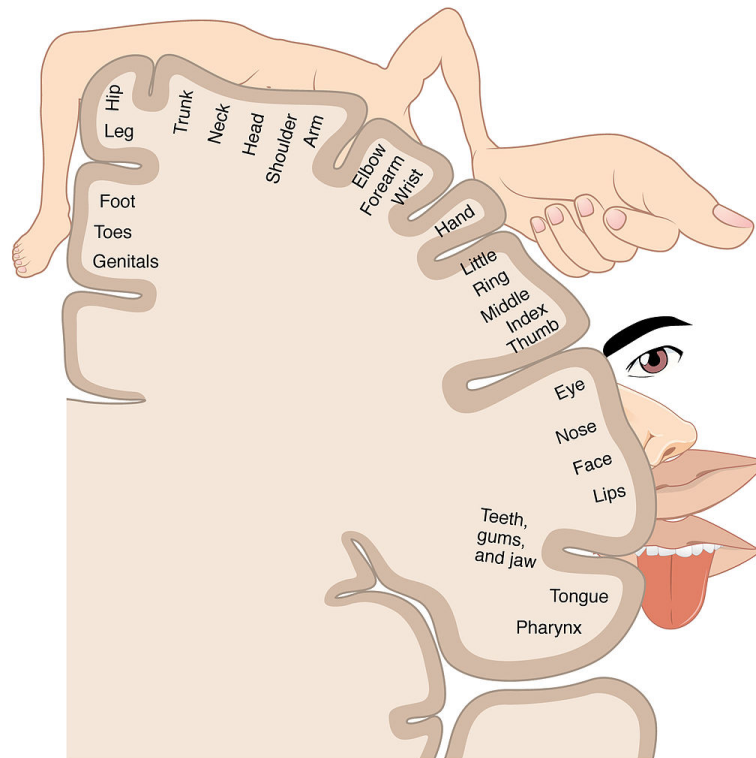


Fig. 2.4 The sensory homunculus on the somatosensory cortex. The size of each area represents the perception sensitivity. Source from Betts et al. [22].

area of the skin projects to specific regions of the somatosensory cortex. Some areas such as fingertips, palms, and lips which are embedded with more touch receptors are represented by larger areas in the somatosensory cortex. After processing the stimuli in the brain, the corresponding signals are sent back from primary motor cortex to control the different body areas [21].

2.2 Vibrotactile perception

Vibrotactile stimuli activate skin mechanoreceptors and their responses depend on various parameters such as amplitude, frequency, duration of vibration and the area of the contactor stimulating the

skin [23]. In the following sections, the perception of vibrotactile sensory parameters and related sensory phenomena are explained.

2.2.1 Sensory parameters

The perception of vibrotactile stimuli depends on the vibrotactile parameters that are manipulated to encode information, and the limitations and capabilities of the tactile sense to perceive these parameters. Vibrotactile stimuli are characterized by the following main parameters: frequency, amplitude, temporal, and spatial patterns of stimulation [23]. An overview of these parameters is presented in the following sections.

Vibrotactile frequency: Vibrotactile frequency as a tactile parameter refers to the rate of vibration. It is important to understand the sensitivity of human touch to changes in vibration frequency as a natural parameter for encoding information when using skin as a communication channel [23]. Threshold frequency has been measured in Figure 2.5 for the fingertip, forearm, and ab-

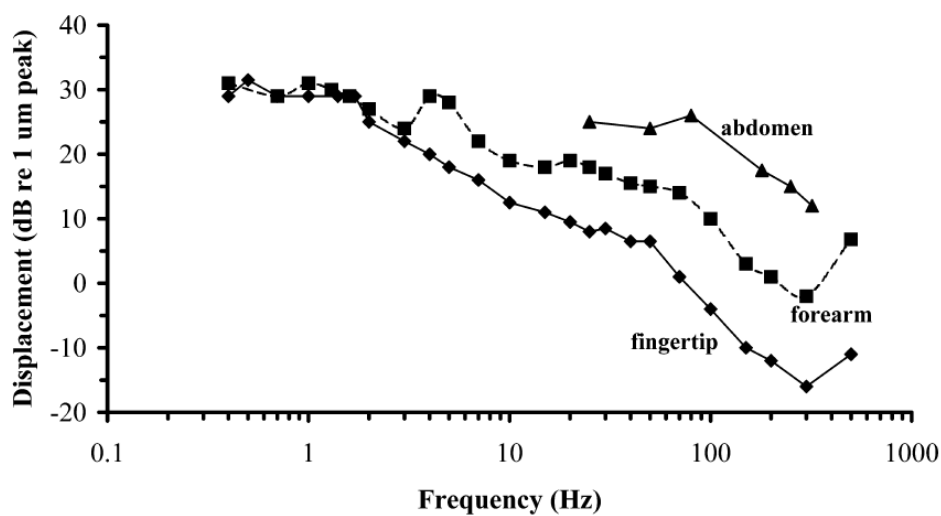


Fig. 2.5 Threshold frequency characteristics measured on the fingertip [24], forearm [16], and abdomen [25]. Source from Jones et al. [23].

domen at frequencies ranging from 0.4 to 1000 Hz. As shown in the figure, optimal sensitivity is achieved in the 150-300 Hz range, though it varies slightly depending on the site of stimulation on the body.

Vibrotactile frequency discrimination has been studied considerably less than the vibrotactile threshold as a function of frequency (e.g., Bolanowski et al. [16]) due to the interaction of frequency and amplitude. As the amplitude of vibration increases (at a constant frequency), there is a perceptible increase in frequency [26]. Figure 2.6 presents results of studies on vibrotactile frequency discrimination in different body sites. As shown in the figure, determining

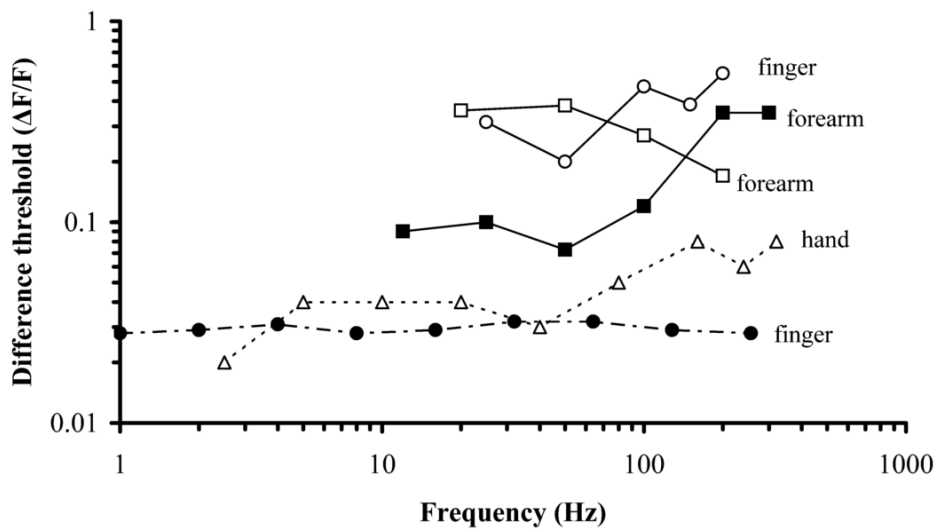


Fig. 2.6 Difference thresholds as a function of frequency for the forearm (filled squares [27], open squares [18]), finger (filled circles [28], open circles [29]), and hand [30]). Source from Jones et al. [23].

distinguishable frequency changes by people is difficult. Rothenberg et al. [27] suggested seven differentiable steps in vibrotactile frequency on the forearm and Sherrick et al. [31] proposed three to five distinguishable rates on the finger. However, due to the complex interaction between amplitude and frequency in vibrotactile

frequency discrimination, it is unclear whether vibration frequency is an effective parameter to vary [23] as already mentioned by Geldard [2] that frequency “would have to be handled gingerly in a tactile communication, especially if intensity were simultaneously manipulated as a variable” (p. 1586).

Vibrotactile amplitude: Amplitude or intensity as one of the vibrotactile stimuli attributes is often utilized to convey distance and obstacle information. Changes in amplitude at a constant frequency affect both the perceived amplitude and perceived frequency [32], therefore it is advisable that either amplitude or frequency be changed in encoding tactile information.

The absolute and difference thresholds for vibrotactile amplitude are used to determine the number of levels that can be uniquely identified and the amount by which the stimulus intensity can be altered for the user to distinguish a change, respectively.

In an absolute threshold experiment, Geldard [2] reported that around 15 levels of intensity can be discriminated by trained people, however, if users did not receive a great deal of training, a maximum of three steps, widely separated across the perceivable range of intensity, should be utilized. On the other hand, Cholewiak et al. [33] found that users could only absolutely distinguish three different levels of intensity.

A range of psychophysical studies has been performed to evaluate the difference threshold for intensity. A wide range of values has been reported; for example 0.4 dB (Weber ratio¹: 0.07) for the smallest value and 2.3 dB (Weber ratio: 0.4) as the largest value

¹The Weber ratio is calculated by dividing the intensity increment required to perceive a change by the existing intensity [34]

[35]. As the medium value, Sherrick et al. [34] found a Weber ratio of 0.2 which indicates an increase or decrease of 20% is necessary for a change in amplitude to be perceived.

Varying the number of factors concurrently active can also influence the perceived intensity of stimulation. For instance, using a tactile display on the thigh, Cholewiak [36] increased the factor count from 1 to 64 and found a linear increase in the perceived intensity of the vibrotactile stimulation.

Although amplitude is one of the vibrotactile parameters that is used widely for presenting distance information, Geldard [2] found it to be the least successful parameter. The first factor that influences the usefulness of this parameter is having different tactile sensitivity at different body locations which makes the user perceive amplitude differently. Furthermore, when stimuli are located on some parts of body like the chest, maintaining the contact between stimuli and skin is difficult due to chest movement as a result of breathing. The first constraint could be problematic for any body location but the second one can be reduced by using more suitable body locations [37].

Vibrotactile temporal pattern: Temporal variation of stimuli is another parameter that is utilized to encode tactile information. Temporal attributes include the duration of a stimulus, the Inter-Stimulus Interval (ISI), the repetition period and temporal pattern of the presented stimuli [38]. The duration of tactile stimuli mostly ranges from 80 to 500 ms and as it increases from 80 to 320 ms, tactile pattern recognition improves [39].

Rhythms as more complex stimuli can be formed by grouping pulses of varying durations together. Rhythms along with frequency

and amplitude were utilized by Summers et al. [39] to encode speech information. It was found that subjects obtained more information from rhythms than frequency and amplitude. This result indicates the effectiveness of rhythm for presenting information. In another study, Brown et al. [40] created a set of Tactons (tactile icons) by modulating three rhythms and three roughnesses created using amplitude modulated sinusoids. Results showed that subjects could recognize rhythms with an accuracy of 93% and roughness with an accuracy of 80% which indicates the usefulness of rhythm in Tactons.

Waveform is another complex parameter that refers to the shape of the vibration wave (for instance a sine wave or a square wave) and is used to create various tactile sensations. Waveform variation is perceived if the complexity of a waveform is varied by using amplitude modulated sinusoids as performed by Brown et al. [40]. They created waveforms that vary in roughness by modulating a 250 Hz signal at different frequencies. Subjects could recognize three levels of roughness which were used to create Tactons as explained above.

Vibrotactile spatial pattern: Since the locus of vibrotactile stimuli applied to the skin is represented in the central nervous system accurately [41], spatial information about the external world may be communicated via tactile stimulation of the skin. Vibrotactile spatial attributes include tactor location, inter-tactor spacing, stimulus area (size), number of tactors and their spatial arrangement [23].

The location of vibrotactile stimulation on different body sites can be utilized as a cue to provide spatial information about the external world, indicate the direction of navigation [7], or direct user's

attention to a visual target on a screen [42]. The ability to localize the site of stimulation varies as a function of the number and configuration of the tactors in the tactile display [43]. Perception of localized vibrotactile stimulation is also more accurate when presented near anatomical points of reference such as the spine, navel, elbow or wrist [25, 41, 44].

Vibrotactile localization has been studied using both one and two dimensional arrays mounted on different sites of body. Using a one dimensional tactile array, Cholewiak et al. [25] examined the ability to localize vibrotactile stimuli at sites around the abdomen using a cylindrical keyboard as a response device. The experiments were performed with a one dimensional tactile display comprised of a belt with 12, 8 or 6 tactors each with different spacing. They found that as the number of tactors increased from six to twelve, localization accuracy decreased from 97% to 74% correct. Van Erp [7] investigated the direction in the horizontal plane to which a specific torso location is mapped using a 15 tactor linear display. Participants indicated the external direction of a localized vibration applied around the torso by positioning a remotely controlled cursor. Consistent with the findings of Cholewiak et al. [44], it was found that localization accuracy was highest for stimuli presented in the midsagittal plane of the body. A one-dimensional eight-tactor display was introduced by Jones et al. [45] to present tactile cues to the waist. Results from spatial localization experiments showed that this tactile display can provide tactile cues that are perceived very accurately in terms of the location of stimulation with a 99% correct response rate.

Vibrotactile localization is dependant on inter-tactor spacing when stimuli are presented using two-dimensional tactile arrays. For example, using a 3-by-3 array on the back with a 60 mm inter-tactor spacing, on 84% of the trials participants could recognize the location of a single vibrotactile stimulus [46]. In contrast, Jones et al. [45] reported that with a 4-by-4 tactor array on the back with 60 mm inter-tactor spacing in the horizontal direction and 40 mm in the vertical direction, vibrotactile localization accuracy reduced to 59% correct. Additionally, participants were more accurate in identifying the correct column of the tactile display than the row. Similar results have been achieved from localization studies on the forearm in which the width of the forearm restricts the dimension of the display. Using a 3-by-3 tactile display on the dorsal surface of the forearm with a 25 mm inter-tactor distance, participants were able to identify the location of the vibrotactile stimulus on only 50% [47] and 53% of the trials [48]. In both of these studies, columns showed slightly better localization performance than rows on the forearm.

As explained in this section, vibrotactile localization as one of the spatial attributes is influenced by inter-tactor spacing, array configuration and the specific location of the body that tactile arrays are mounted. Therefore, these parameters should be considered in the design of the tactile displays utilized to present spatial information. It is also important to emphasize that the ability to localize a point of stimulation is unrelated to the vibrotactile sensitivity of the skin surface, varying vibrotactile frequency also has little effect [43].

Individual differences: Age and gender are other parameters that affect vibrotactile perception. Age has been investigated in

[49] and [4], and it was found that older people are less sensitive to tactile stimuli due to the loss of mechanoreceptors that occurs as we age. It was shown that tactile sensitivity differed according to gender and that women are more sensitive than men in pressure sensitivity, two-point discrimination and point localization at specific body locations [20].

2.2.2 Sensory phenomena

Manipulating temporal and spatial vibrotactile parameters can create various illusory phenomena such as masking, adaptation, enhancement, change blindness, and mislocalization illusions [50, 51].

Masking is a phenomenon whereby the presentation of a masker stimuli decreases the correct perception of a following target stimuli [52]. In order to avoid the masking effect, increasing the interval between two successive stimuli and the spatial distance between the masker and the target is recommended [53]. *Vibrotactile adaptation* refers to reduced perception of tactile stimuli caused by continuous exposure to an above-threshold stimulus. This effect is not permanent and can be avoided with proper time gaps between stimuli [54]. *Vibrotactile enhancement* [55] is defined as a perceived stimulus intensity magnification caused by spatial or temporal summation as illustrated in Figure 2.7. *Change blindness*, as a tactile equivalent of visual change blindness [56], is expressed by the failure to detect change between two consecutive stimuli [57]. Finally, *Mislocalization* of stimulation on the skin can occur as the result of well-known tactile illusions such as the funneling illusion, sensory saltation, and apparent motion which will be described in the next sections.

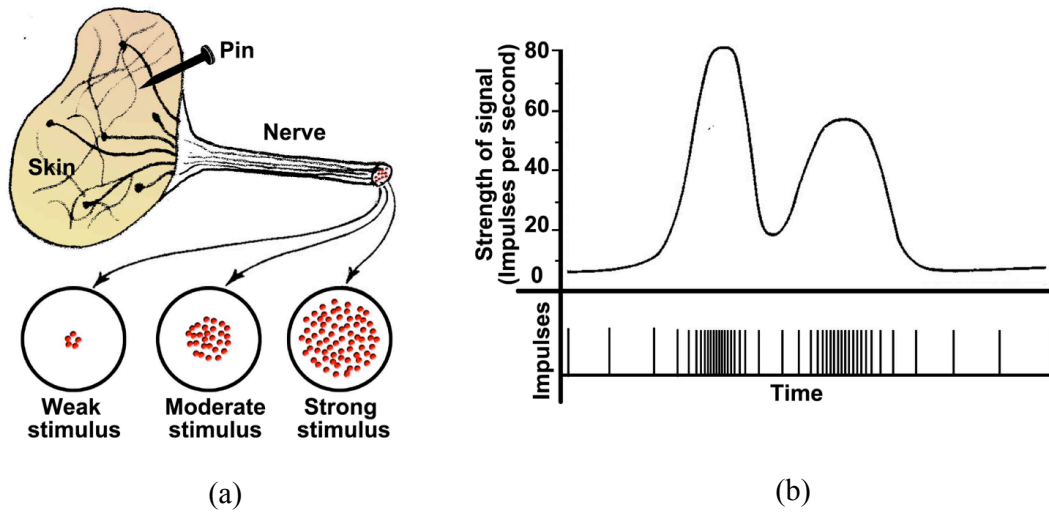


Fig. 2.7 Vibrotactile enhancement effect. (a) Spatial summation: refers to an increasing number of stimulated nerved fibers that result in a perception of increasing intensity, (b) Temporal summation: refers to an increasing number of impulses along a single fiber which causes a perception of increasing intensity. Source from Guyton [58].

2.2.2.1 Funneling illusion

Funneling is one of the perceptual illusion techniques which is used for vibrotactile feedback [59]. It refers to a sensory illusion that generates a midway phantom sensation between multiple stimuli when they are presented simultaneously at adjacent locations on human skin [60, 61]. The temporal order of the stimuli, their relative amplitudes, and the stimuli separation can affect this phantom sensation [61]. The location of the phantom sensation can be altered by adjusting the interstimulus interval or adjusting the intensities of the two stimuli. This effect is mediated by temporal inhibition and amplitude inhibition as discussed next [61, 62].

Temporal inhibition occurs as the interstimuli interval between two stimuli with the same intensities increases and the perceived location moves towards the earlier stimulus. However, when the

interstimuli interval reaches 8-10 ms, the funneling illusion disappears and the two stimuli are felt separately [61]. The effect of interstimuli interval on the funneling illusion by producing continuous motion was examined in a few studies [63, 64]. However, since the phantom sensation produced by the use of amplitude variation (or amplitude variation with interstimuli interval variation) is much more distinct than interstimuli interval variation, it has been utilized more to examine the funneling illusion [61].

In amplitude inhibition, if two stimuli have the same intensity (Figure 2.8a), the phantom sensation is created in the middle of them. However, if they have different intensities (Figure 2.8b), the sensation is funneled and shifted towards the stimulus with higher intensity [65]. Using two stimuli, this phantom sensation can be obtained anywhere on the body if two stimuli are within several inches of each other [65]. However, it has been shown that this phantom sensation is produced even when two stimuli are located as far apart as the fingertips of the opposite hands [66].

Using amplitude inhibition, Alles [61] has reported that the intensity of tactile stimuli can be varied linearly and logarithmically to provide continuous vibrotactile motion. Rahal et al. [67] exploited

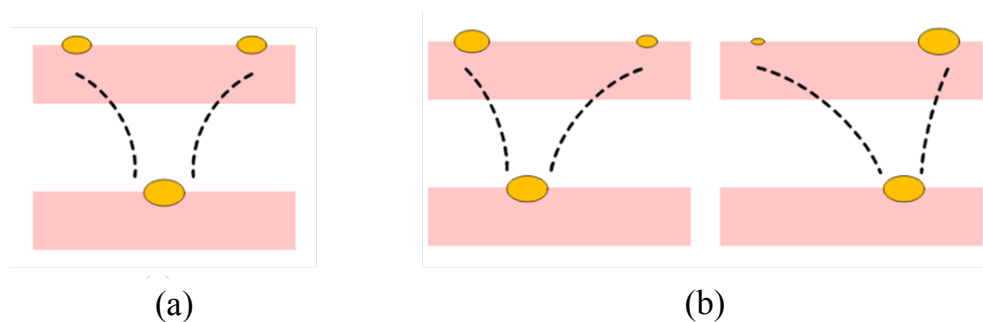


Fig. 2.8 Funneling illusion with: (a) Same intensities, (b) Different intensities. Source from Cha et al. [65].

amplitude inhibition to produce a funneling illusion by making use of linear and logarithmic intensity variations to display continuous tactile sensations on the human skin. Psychophysical experiments have shown relationships between orientation, duration of the vibrotactile actuators, and gender, combined with preferred intensity variation, in mediating funneling illusion effect. Figure 2.9 shows an illustration of the funneling illusion used to create a continuous movement sensation. As shown in the figure, by continuously changing the intensities of two adjacent actuators in opposite direction, a continuous sensation moving from one actuator location to the other is produced. Note that this is a different sensory phenomenon from the apparent motion discussed in Section 2.2.2.3 below.

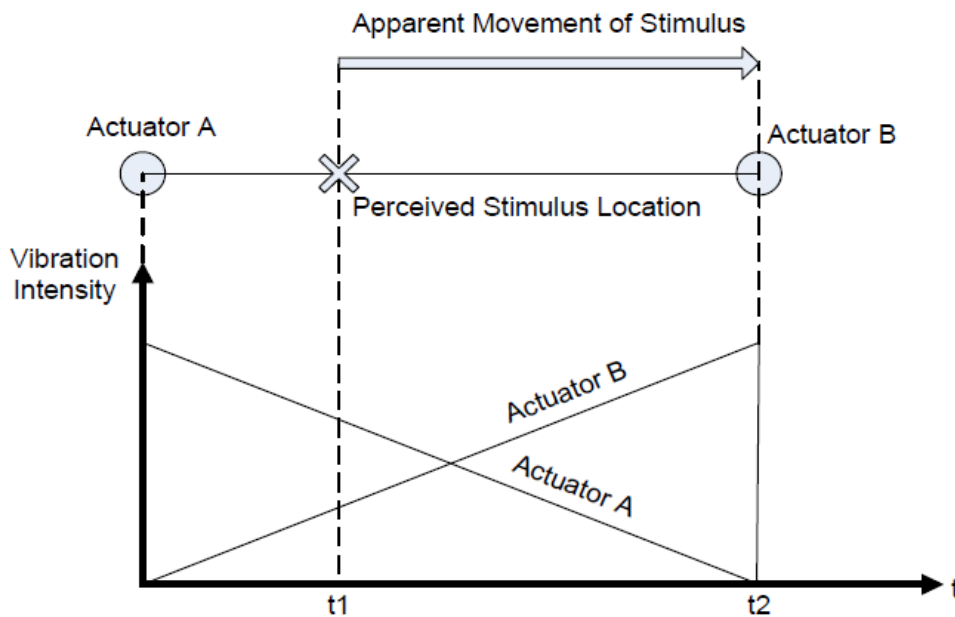


Fig. 2.9 Illustration of using funneling illusion to create a continuous movement sensation. Source from Barghout et al. [68].

The separation of stimuli also influences the funneling illusion. Cha et al. [65] showed that distances between the two stimuli on the dorsal forearm should be between 40-80 mm to produce a contin-

uous sensation. Using the inter-tactor spacing of 80 mm, Barghout et al. [68] investigated the spatial resolution of vibrotactile perception on the forearm when applying multiple funneling stimuli. The best localization accuracy was found around the joints such as the elbow and wrist using both stationary and moving vibrotactile stimuli. This thesis focuses on the effect of inter-tactor spacing on the forehead funneling illusion as explained in Chapter 3.

2.2.2.2 Sensory saltation

Sensory saltation or cutaneous rabbit [64] is a type of tactile illusion created by rapidly stimulating multiple body locations sequentially. This illusion is demonstrated by placing three stimulators at equally spaced locations on the skin- such as the forearm or back [63, 42] - and presenting three brief pulses at the first stimulator, followed by three pulses at the second stimulator and finally at the third stimulator. Rather than sensing separate presentations solely at each stimulator site, the observer perceives that pulses are evenly distributed across the skin surface [23]. Figure 2.10 shows the actual stimulation and the perceived sensation during sensory saltation.

Temporal separation between the bursts of vibration is a parameter that determines the perceived spatial layout in sensory saltation [23]. The stimuli are perceived as being spatially distributed across the skin when the interstimulus intervals are between 20 and 300 ms [23]. Geldard [64] and Sherrick [69] showed that producing sensory saltation on the back needs inter-tactor spacing no greater than 100 mm and a number of pulses of between three and six. Cholewiak et al. [63] compared saltatory presentations with veridical presentations on the back and found that both presentation modes produce

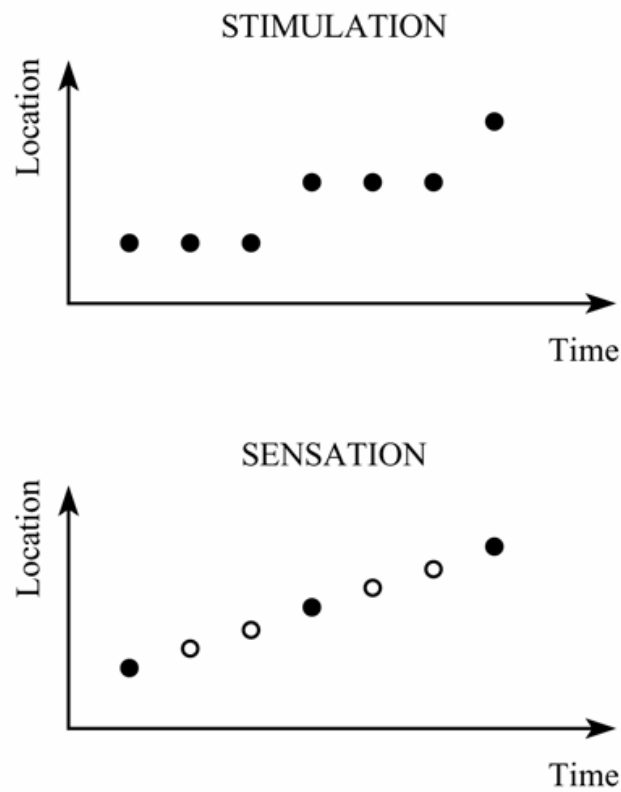


Fig. 2.10 An explanation of stimulation pattern (top) vs. the perceived sensation pattern (bottom) for sensory saltation. Source from Tan et al. [42].

equivalent sensations. However, Roady et al. [70] showed that with more complex signals, the saltatory presentations show the greatest accuracy and faster response times.

Sensory saltation allows a user to perceive higher resolution linear signals from point stimuli that communicate movement direction. For example, Tan et al. [42] utilized sensory saltation to display directional information using a 3×3 haptic back display. Sensory saltation can also create ‘out of the body’ tactile experiences as discovered by Miyazaki et al. [71]. They demonstrated that when a stick was laid across the tips of the index fingers and rapid sequential taps were delivered to the left and right index fin-

gers, illusory taps in the space between the actual stimulus positions were reported. Furthermore, Lee et al. [66] showed the existence of this phenomenon for interaction with virtual objects but with reduced effects.

2.2.2.3 Apparent movement

The sense of motion generated across a field of tactors (vibration motors) is one attribute of vibrotactile cues that could be applied to allow users to better disambiguate tactile commands [72]. Specifically, when two or more tactors are activated sequentially with a certain timing value, an illusory sensation that the stimulus is traveling smoothly and continuously from one position to another is perceived. This phenomenon is called the apparent motion illusion or phi illusion [73–75].

Various parameters have been found to affect the perception of apparent motion such as timing [74], number of tactors [76] and inter-tactor spacing [77].

The timing parameters that influence feelings of apparent motion include the Duration of Stimulus (DoS) and the Stimulus Onset Asynchrony (SOA) [74]. As shown in Figure 2.11, DoS refers to the amount of activation to a given tactor per display period, while SOA refers to the interval between the sequential activation of two tactors. In order to induce the perception of tactile apparent movement, the activation period of consecutive tactors should overlap which means that SOA should be shorter than DoS.

Kohli et al. [72] investigated the use of apparent movement at various speeds (produced by using different DoS and SOA values) for information display on the upper arm. Results indicated that

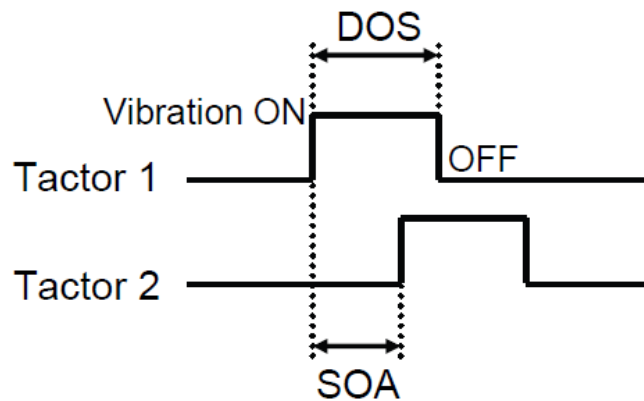


Fig. 2.11 Illustration of Duration of Stimulus (DoS) and Stimulus Onset Asynchrony (SOA). Source from Niwa et al. [76].

absolute apparent motion speed recognition was difficult but that at least two speeds were easily distinguishable. Niwa et al. [78] examined the occurrence of apparent movement by using DC motor Tactors (DCT) and Voice Coil Tactors (VCT). While the DoS was longer than 200 ms, no significant difference was found between two tactor types in producing apparent motion. However, the response time of DCT became slower when DoS was shorter than 200 ms; therefore, the VCT tactor was to be preferred as it can cover a wider range of DoS and SOA for presenting apparent motion to subjects. Israr et al. [77] measured the SOA space for moving sensations when direction of motion and spacing between actuators were varied. They found that the SOA space was influenced by both the direction and spacing on the forearm while it was only affected by the direction of actuation on the back. Niwa et al. [76] determined that a time interval greater than 400 ms, before repeating the directional sequence, is required in order to correctly identify linear apparent motion on the upper arm over a range of DoS and SOA values.

Tactor number also affects the feeling of apparent motion. Niwa et al. [76] found that four or more tactors should be used as the minimum adequate number of tactors to correctly identify the direction of circular apparent motion on the upper arm. Kirman [79] showed that four stimulators produced more frequent reports of apparent movement than did two stimulators, regardless of the stimulus duration.

Distance between tactors is a parameter where there have been contradictory findings regarding its effect on the perception of apparent motion. For instance, Sherrick [80] found that varying the inter-tactor spacing has no significant effect on the perception of apparent motion. Similarly, Harrar et al. [81] failed to find a significant effect of inter-tactor spacing. In contrast to these findings, Israr et al. [77] found that spacing as an effective parameter in the perception of apparent motion on the forearm. Earlier research by Gibson [82] also stressed the strong influence that interstimulus distance had on the perception of apparent motion. In this thesis, the effect of SOA and inter-tactor spacing on forehead apparent motion is investigated in Chapter 3.

2.3 Tactile display technology

Tactile displays communicate through the sense of touch. As a wearable device that stimulates the skin, tactile displays should be small, lightweight and have low power consumption. Tactile displays can be distinguished from each other based on the sensations that they produce on the skin and the actuators required to produce those sensations [83]. Electrotactile and vibrotactile displays

are two widespread classes of tactile displays which use the skin as a medium of communication.

Electrotactile displays stimulate the skin by passing current via surface electrodes such as gold, platinum, silver or stainless steel. This current excites the afferent nerve fibers directly [23]. The felt sensation is described as a tingle, itch, buzz, or sharp and burning pain, depending on the stimulating voltage, current and waveform, the electrode size, skin location, and degree of hydration of the skin [84]. Electrotactile displays have been developed as sensory aids for those with hearing [85] and visual disabilities [86]. In order to make electrotactile displays practical, several difficulties must be solved [83]. One disadvantage of electrotactile displays is the challenge of current control. For instance, poor contact between the skin and an electrode will result in a higher current density and stronger sensation of a sharp pain [84]. More generally, a significant limitation of electrotactile displays is the small dynamic range available to present cues. The range from threshold to a maximal level that is comfortable and not painful depends on the individual, skin location, skin hydration and oiliness, electrode type, and waveform used [84]. Thus, controlling the sensation at a comfortable level is challenging in the design of electrotactile displays.

Vibrotactile displays, as the most popular type of tactile displays, stimulate the skin mechanically using an actuator that converts electrical energy into a mechanical displacement of either the whole actuator or a contactor pad at frequencies ranging from 10 to 500 Hz [23]. Unlike electrotactile displays which stimulate afferent nerves, vibrotactile displays stimulate mechanoreceptors. Their sensation is felt as a bump, a vibration, a texture or a material quality

[83]. Their robust operation and easy fabrication result in delivering a reliable tactile perception. Vibrotactile displays have vast applications in compensating sensory impairments and assisting in navigation through sensory substitution or augmentation that will be discussed further in Section 2.5. The focus of this thesis is on the vibrotactile displays and next section reviews the most widely used vibrotactile actuators in vibrotactile displays.

2.4 Vibrotactile actuators

A wide range of vibrotactile actuators can be utilized to provide an oscillating movement across the human skin. The most common types of actuators are rotary electromagnetic actuators (Eccentric Rotating Mass (ERM) actuators), linear electromagnetic actuators, and nonelectromagnetic actuators [87]. Figure 2.12 shows examples of the mentioned vibrotactile actuators.

In the rotary electromagnetic actuators (ERM actuators), the vibration is caused by the movement of an off-center mass and the entire case in which the mass housed. When a constant voltage or current is applied to these actuators, they rotate continuously. Their design couples both the frequency and amplitude of the resulting vibration to the motor's rotational speed which makes it impossible to render vibration at arbitrary combinations of frequency and amplitude. In addition, when the applied voltage is very small, their internal static friction prevents these actuators from rotating which results in a delay in the start of the vibrotactile cue. The simplicity of these actuators makes them a popular choice despite these rendering limitations. Three main categories of commercially available Eccentric Rotating Mass (ERM) motors are: shafted motors

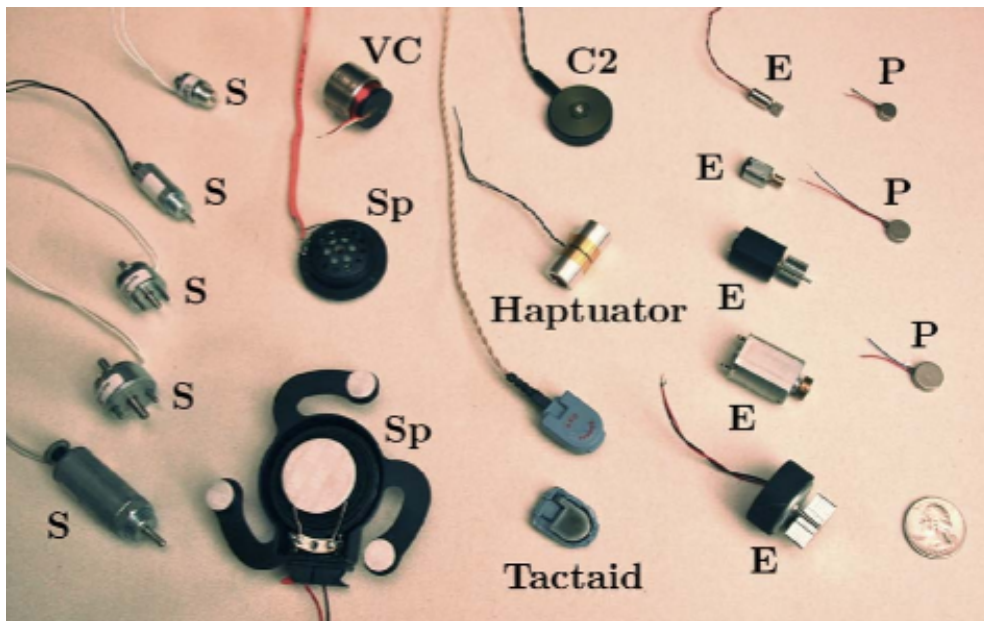


Fig. 2.12 Sample actuators for vibrotactile display. S: Five solenoids of varying sizes. VC: A commercial voice coil without bearings. Sp: Two audio speakers. C2: A C2 tactor from EAI. Haptuator: A Haptuator from Tactile Labs, Inc. Tactaid: One complete Tactaid from AEC and one opened to show the suspension inside. E: Five shafted/cylindrical eccentric rotating mass motors. P: Three shaftless/pancake eccentric rotating mass motors. A U.S. quarter appears at bottom right for scale. Source from Choi et al. [87].

where the eccentric mass is visible (Figure 2.12.E), encapsulated cylindrical motors where the rotating shaft is covered to prevent interference with surrounding items (Figure 2.12.E), and shaftless motors (Figure 2.12.P) where the eccentric mass is fully enclosed.

Unlike ERM actuators, vibration in the linear electromagnetic actuators is caused only by moving a contactor (contact point with the skin) which is located outside the case. In these actuators, passing a current through the coil (located in a magnetic field) pushes the coil along its axis causing the contactor to vibrate in a linear motion against the skin. Linear actuators can produce frequencies within the range 0.1 Hz to 300 Hz that are appropriate for tactile perception applications [33]. However, they cannot be easily ap-

plied in wearable tactile displays due to their large size, weight and high power consumption. The solenoids, voice coil, C2, haptuator and tactaid shown in Figure 2.12 are commercially available linear actuators.

Piezoceramic actuators are nonelectromagnetic actuators that take advantage of the piezoelectric effect to produce the vibrotactile sensation. In these actuators, piezoceramic materials change their shape depending on the polarity of the voltage applied to the material. Vibrotactile display applications such as the Sony TouchEngine [88] utilized Piezoceramic actuators effectively. Although these actuators respond to applied inputs quickly, requiring the input voltages on the order of 100 V makes them an unsuitable choice for wearable tactile displays [87].

Considering the limitations of the mentioned vibrotactile actuators, shaftless ERM motors are a reasonable choice for designing the vibrotactile head-mounted display described in this thesis. Detailed information about the type of actuator and the design of the vibrotactile display will be presented in Chapter 3.

2.5 Tactile display applications

Tactile displays provide an alternative way of communicating various kind of information and may be particularly useful when other communication channels, such as vision and hearing, are overloaded or compromised [2]. Consequently, tactile displays have been utilized to support a variety of applications including sensory substitution [4], sensory augmentation [5, 6], spatial orientation and navigation [7, 8] and exploration of virtual environments [46]. A comprehensive review of sensory substitution and sensory augmentation

is described in [89]. The following sections present an overview of tactile display applications.

2.5.1 Sensory substitution

Initial investigations with tactile displays come back to sensory substitution where tactile stimuli is used to represent the experience of an absent visual or auditory sense through the sense of touch [4]. Figure 2.13 shows the structure of a sensory substitution system that translates the sensory information that is normally available via one sense to another.

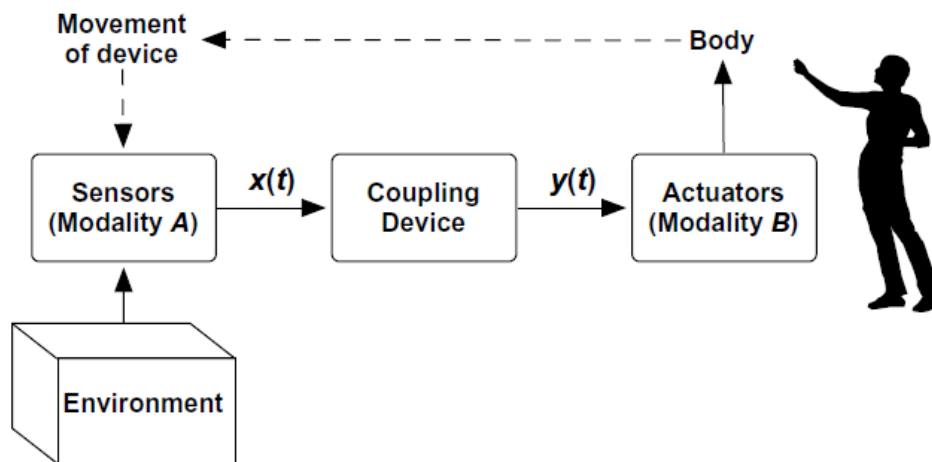


Fig. 2.13 Sensory substitution structure. Source from Visell [83].

Sensory substitution devices were first developed to compensate sensory impairments for visually impaired people [4, 90]. Tactile Visual Sensory Substitution (TVSS) studies have been carried out using vibrotactile and electrotactile sensory substitution devices. For example, Batch-y-Rita [90] transmitted camera signals to a grid of back-mounted vibrotactile stimulators which enable visually impaired users to recognize simple visual patterns (see Figure 2.14a).

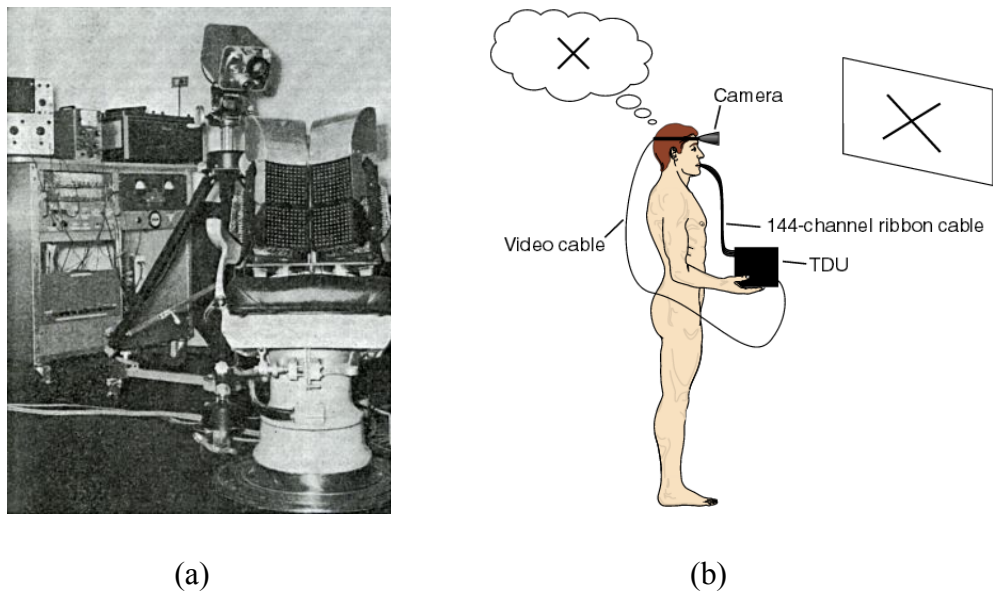


Fig. 2.14 (a) A Tactile Visual Sensory Substitution (TVSS) device, source from Batch-y-Rita [90]. (b) The Tongue Display Unit (TDU) as an electro-tactile sensory substitution device, source from Batch-y-Rita et al. [91].

The Tongue Display Unit (TDU) shown in Figure 2.14b is an example of electro-tactile sensory substitution device [91] that transmits the video data captured by a head-mounted camera to an electro-tactile display mounted on the tongue. In order to present basic navigation commands to the visually-impaired, an electro-tactile display that stimulates the roof of the mouth was designed by Tang et al. [92]. Optacon [93], a reading device for visually-impaired people, is another example of TVSS that converts optical data to a tactile array onto which the person places his/her index finger (see Figure 2.15). Vibrotactile sensory substitution devices have also been used to cue the presence of other persons to blind users using a vibrotactile belt display [95], to encode Braille characters through a wearable finger vibrotactile display [96], and to assist navigation using vibration insoles [97] and the ‘enactive torch’ [98].

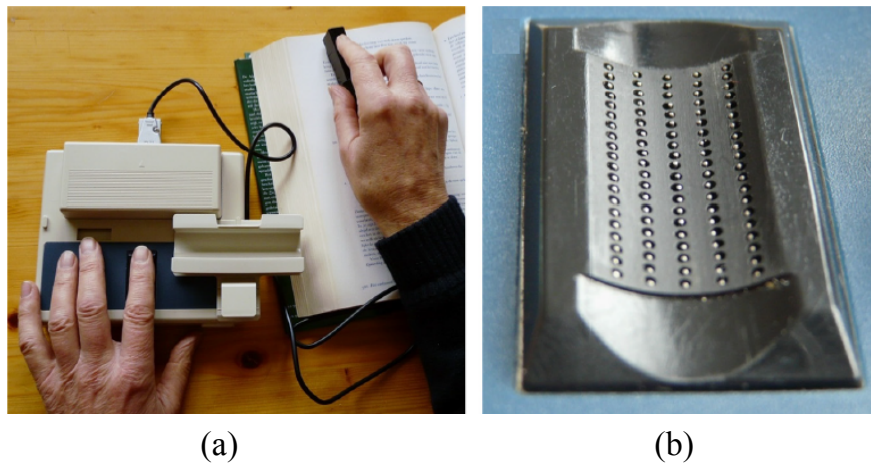


Fig. 2.15 (a) Optacon device is used to read a text by visually impaired individuals. (b) A close up of the tactile array. Source from Stronks et al. [94].

Sensory substitution devices can also assist speech comprehension for people with hearing impairments using electrotactile or vibrotactile displays. Positional encoding of frequency information in the speech signal, inspired by models of the cochlea, is applied in most tactile audio sensory substitution devices [23]. For example, Teletactor [99] was an electrotactile auditory prosthesis that transformed the speech sound into a tactile pattern using a belt consisting of 32 electrotactile actuators worn around the abdomen. Results showed that the speech recognition of deaf children improved. Furthermore, it was found to assist in auditory comprehension in older adults [100]. As a vibrotactile audio sensory substitution device, Tactaid [101] encodes properties of the acoustic signal by variation in the amplitude, location, duration, and frequency of the vibrotactile inputs to assist in speech comprehension for people with hearing impairments.

2.5.2 Sensory augmentation

Unlike sensory substitution that translates the form of one modality into the form of another, sensory augmentation adds new synthesized information to an existing sensory channel. The additional senses provided by sensory augmentation can be used to augment the spatial awareness of people with impaired vision [38, 102] or for people operating in environments where visual sensing is compromised such as smoked-filled buildings [5, 6, 103], and to improve balance for individuals with impairments such as vestibular dysfunction [104].

As a spatial awareness enhancement device for visually impaired people, Gallo et al. [105] developed an augmented white cane navigation aid. This device integrated ultrasound and infrared sensors to detect distant objects and convey this information through a vibrotactile interface to the user's hand. Nagel et al. [106] and Kaspar et al. [107] investigated magnetoreception ability (understanding magnetic north) using vibrotactile stimulation around the user's waist provided by a modified belt. This research indicated that new sensorimotor contingencies [108] can be learned and integrated into behaviour to some extent. Karcher et al. [102] showed that this kind of sensory augmentation device can be used by people with visual impairments to maintain their heading direction over long distances. Furthermore, Heever [109] reported that a magnetoreception belt that presented tactile sensation corresponding to directional information can increase spatial sensitivity.

In order to enhance the spatial awareness of operators who are working in dark environments, Carton et al. [103] developed a

sensory augmentation glove for distance display in a low vision search context for firefighters. Their glove mapped an ultrasonic rangefinder to a pair of vibration motors on the dorsal surface of the hand. Furthermore, a glove-mounted tactile display has also been developed to allow temperature readings from the surface of a firefighter's glove to a wrist-mounted tactile display [110]. Augmentation of spatial awareness in hazardous working environments (Figure 2.16a), has been investigated by Cassinelli et al. [5] using the Haptic Radar as the first head-mounted sensory augmentation device. Here, several infrared sensor-tactor modules were mounted together on a band wrapped around the head and a one-to-one mapping was created between an infrared distance sensor and a tactor mounted directly beneath it. As shown in Figure 2.16b, users intuitively responded to objects moving close to the sensor by tilting

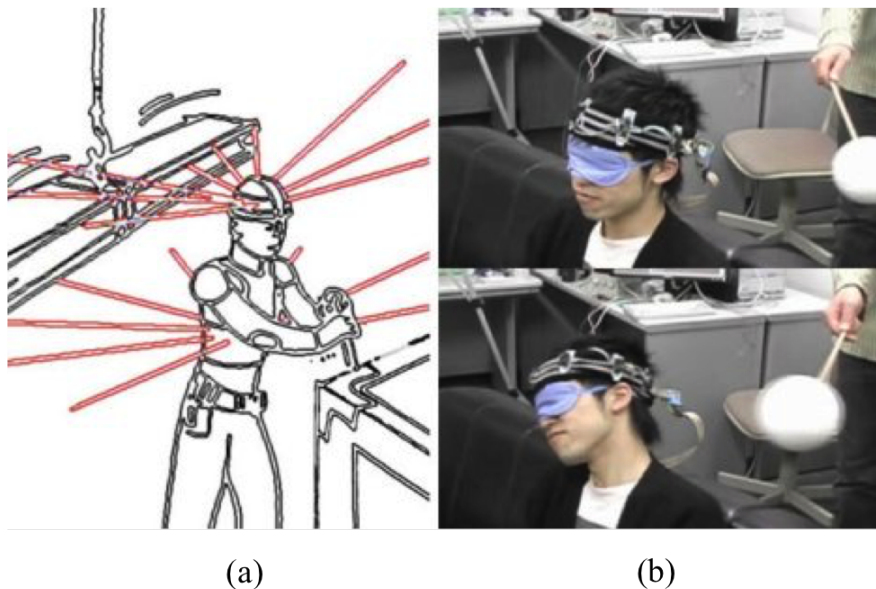


Fig. 2.16 (a) Augmented spatial awareness. (b) Avoiding an unseen object with Haptic Radar. Source from Cassinelli et al. [5].

away from the direction of the stimulus, showing that the device could be useful for avoiding collisions.

The Mark-I Tactile Helmet [6] is a prototype sensory augmentation device that was developed to help firefighter's navigation inside smoked-filled buildings. It consisted of a 1-by-4 tactile display connected to an external array of ultrasound sensors, converting ultrasound distance signals to nearby surfaces, such as walls, into a vibrotactile display pattern on the area of the head closest to the nearest surface. Unlike Haptic Radar, the Mark-I Tactile Helmet was non-modular, allowing direction signals from the array of sensing elements to be combined into an appropriate display pattern to be presented to the user. A more detailed explanation is presented in Section 2.7.

Sensory augmentation is also utilized to improve standing balance for people with vestibular dysfunction [104]. In one application as shown in Figure 2.17a, body tilt information acquired by inertial sensors was represented via a vibrotactile display around the torso to improve postural stability in people with balance impairment [111]. It was found that this system significantly reduced the magnitude of body sway in people with vestibular dysfunction. In another application, tactile displays were embedded in gel insoles worn on the feet (see Figure 2.17b). The insoles presented tactile noise to the somatosensory system to improve balance control and postural stability [112]. Similar to Wall et al. [111], results indicated that postural sway was decreased when vibration was applied to the body. In addition to standing balance, sensory augmentation improves walking balance [113, 114] for individuals with vestibular

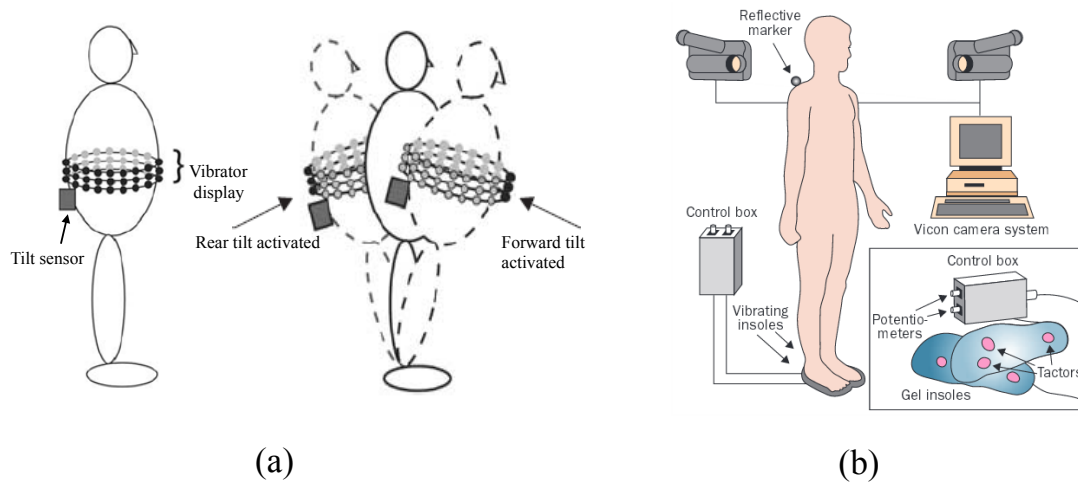


Fig. 2.17 Balance prostheses sensory augmentation devices. (a) A waist-mounted vibrotactile display, source from Wall et al. [111]. (b) A foot-mounted vibrotactile display, source from Priplata et al. [112].

loss and is used for rehabilitation of people with some neurological diseases [115, 116].

Sensory augmentation has also been used for object localization and shape recognition. For example, Jeffs et al. [117] developed an electrotactile array mounted on the tongue surface to augment user's shape recognition and object tracking. 'Whisking' as a new sensory modality has been evaluated by [118] using an apparatus attached to the subjects' fingers that emulated the movements of the long facial whiskers found on many small mammals. Users were able to localize objects and recognize shapes with high accuracy.

2.5.3 Spatial orientation and navigation

An important application of tactile displays is to assist in spatial orientation and navigation in situations where human operators can become disoriented. Examples of these situations include flying under high G-load conditions [119, 120], working in weightless

environments in space [121, 122] and moving through unfamiliar environments [123, 124]. In these applications, vibrotactile stimuli are utilized to present information about the intended direction of personal or vehicle movement, the pitch and roll of an aircraft, and waypoint locations in the environment [23]. The Tactile Situation Awareness System (TSAS) [120] is a navigation aid for pilots that assists spatial awareness and orientation using vibrotactile feedback. It consists of a 8-by-5 torso-mounted vibrotactile display (tactor type: miniature electromechanical speakers) and an gyroscope that detects the orientation of the pilot. If the device identifies unbalanced movements, the pilot is alerted by activating a tactor on the body where the disorientation has occurred. The TSAS has shown that tactile signals presented to the torso can be used to control a vehicle and maintain spatial orientation.

To provide a navigation aid for moving through unfamiliar terrain, Van Erp et al. [7] made extensive use of torso-mounted vibrotactile displays to present directional or position cues. They investigated the direction in the horizontal plane to which a specific torso location is mapped using a 15 tactor (tactor type: minivib-4 vibration motor) linear display. Applications from their work include displaying orientation information via a wearable tactile vest for astronauts in zero gravity [119], displaying directional information for pedestrian wayfinding [125], and vehicle navigation [126]. Results showed that a vibrotactile display mounted on the torso can effectively convey navigation cues. Jones et al. [8] used a wirelessly controlled 4-by-4 vibrotactile display (tactor type: pancake type vibration motor) mounted on the back to provide direction of movement information outdoors. The required direction movement

was sent through a PC wirelessly to the display. Each direction was generated using all 4 tactors through spatiotemporal patterns, e.g. tactors vibrating from bottom to top conveyed North. Similar to Van Erp et al. [7], participants could use the vibrotactile display as an effective navigation device with minimal training.

In addition to spatial orientation and navigation, tactile displays are also applied in the exploration of virtual environments. One such application is presenting collision information during interaction with virtual objects or providing rumble vibration in driving simulators [23]. These devices range from displays attached to a chair which stimulate the back [46] to a glove that stimulates the hand whenever it interacts with a virtual object [127].

This thesis focuses on sensory augmentation to enhance firefighters' navigation in low visibility environments using a head-mounted sensory augmentation interface as described in Chapter 4.

2.6 Tactile language

As discussed above, tactile displays are applied to provide different kinds of information for applications including navigation, spatial orientation, notification and high-level messaging [70]. One of the challenges in using tactile displays is determining what vibrotactile patterns should be employed to convey information effectively [128]. Of the four vibrotactile parameters available for creating communication signals namely frequency, amplitude, duration and location, the latter two are the most promising candidates for a simple tactile language/vocabulary [128]. Due to the interaction between amplitude and frequency (discussed in Section 2.2.1) which causes frequency changes as a result of amplitude changes, these two pa-

rameters are used less than duration and location in creating tactile languages.

The first tactile language, Vibratese, was designed by Geldard [1]. Vibratese was composed of 45 basic elements (the tactile equivalent of numbers and letters) that changed along three amplitudes, three durations and five locations on the chest. Results showed that participants learned the language quickly and could recognize up to 38 words per minute. Tadoma [129] is another tactile language designed for people with severe visual and hearing impairments. It included placing a hand on the speaker's face and monitoring actions associated with speech production. Tadoma users were able to understand speech with high accuracy and even recognize the accent. Brewster et al. [130] proposed 'Tactons' as structured tactile messages for non-visual information display. They showed that different vibrotactile parameters such as frequency, amplitude, duration of a tactile pulse, rhythm, and location can be used to construct Tactons. The effectiveness of Tactons was evaluated by Brown et al. [40] using two experiments: the first investigated perception of vibrotactile roughness (created using amplitude modulated sinusoids), and the second evaluated a set of Tactons created using roughness and rhythm. Results indicated that Tactons could be a successful means of communicating information in user interfaces, with an overall recognition rate of 71%, and recognition rates of 93% for rhythm and 80% for roughness. The following sections describe some available tactile languages applied for presenting navigation information such as distance and direction.

2.6.1 Distance encoding

Distance as one kind of navigation information is a parameter that cannot be communicated directly and the preferred distance encoding scheme is not clear a priori [125]. All of the above mentioned vibrotactile parameters can be used to encode distance information, however, among them, amplitude and frequency seem to offer limited possibilities of encoding information [131]. The restricted number of perceptually distinguishable intensity levels between the detection threshold and the maximum comfort level, and restricted number of frequency levels between the lower and upper frequency limit make these two parameters less suited to coding distance information [131].

Distance encoding schemes have been evaluated in a number of studies to present user's distance to obstacles, to the next waypoint in waypoint navigation task and to turning points in car navigation.

Riener et al. [132] developed a vibrotactile waist belt consisting of eight tactors for distance information encoding. Variations in vibration intensity and vibration frequency were used to notify the changing distances between a person and an obstacle. Evaluation results indicated that distance estimation using vibration intensity was more intuitive than vibration frequency. In a second study, Riener et al. [133] applied variation of vibration frequency with a carrier frequency of 250 Hz for distance encoding in a boundary detection task. Results indicated that their system would increase safety in close proximity to obstacles by reducing movement speed compared to walking under poor visibility condition without tactile feedback.

A 2D tactile vocabulary for blind navigation was proposed by Dakopoulos et al. [134]. The vocabulary was associated to a 4×4 tactile array consisting of 16 vibration motors placed around a user's abdomen. The 3D space of the user's field of view was captured by a camera and represented through the tactile array. The activation of each vibration motor represented the location of a detected obstacle and its frequency represented the distance of the object. Results showed that subjects could detect safe navigation paths with an average accuracy of 92.5%.

A tactile vocabulary was designed by Oliveira et al. [135] to aid navigation in underground mines. Using a vibrotactile belt display consisting of eight vibration motors, obstacle, destination, course, warning and itinerary information were presented to users by manipulating the location and frequency of vibration. It was shown that tactile feedback facilitated navigation in a virtual underground mine. Carton et al. [103] presented a vibrotactile glove for distance display in low vision search contexts such as firefighting applications. The glove mapped an ultrasonic rangefinder value (distance) to a pair of vibrating motors on the dorsal surface of the hand by changing the intensity of vibrating motors (closer distances were mapped to a longer pulse width). Results showed that participants detected the presence and absence of obstacles in a gap-detection task with 93% accuracy and relative changes in the proximity of an obstacle with 74% correct identification. However, mapping tactile stimuli to the absolute position was more challenging, with an accuracy rate of 57%.

Straub et al. [136] investigated distance encoding using a vibrotactile waist belt in a waypoint navigation task. Four distance

encodings based on the parameters of intensity, frequency, position (which factor), and pattern were used. Results indicated that adding distance information had no meaningful effect on walking speed and accuracy. Van Erp et al. [125] evaluated distance information encoding using a vibrotactile waist belt in a waypoint navigation experiment. The location of the next waypoint that subjects had to walk toward determined the specific factor activation and its vibration rate. Similar to [136], results indicated that providing distance feedback to the next waypoint did not have any significant effect on participants' walking speed.

In a car navigation experiment, Asif et al. [137] investigated three vibrotactile distance encodings based on rhythm, rhythm and intensity, and rhythm and duration using a tactile belt. The continuous distance information was presented to users in four categories: very far (200-150 meters), far (100-80 meters), near (50-30 meters) and turn-now (given at 10 meters from the waypoint). It was found that rhythm and duration were the most effective parameters for distance information encoding. Boll et al. [138] introduced a vibrotactile waist belt for a turn-by-turn car navigation application to reduce the driver's cognitive load. They presented a series of vibrotactile patterns for turning instructions, where the number of repetition of discrete pulses corresponded to distance indicators. It was found that cognitive load of the tactile navigation system was not higher than with a classical car navigation system.

The above studies have employed the four vibrotactile parameters to encode distance information for different navigation tasks. The next section describes how tactile languages have been used to encode direction information which is the focus of this thesis.

2.6.2 Direction encoding

Of the four vibrotactile parameters, location (spatial pattern) is the first choice to code direction information by activating a single tactor that is positioned on the body close to the intended direction [125]. Many application scenarios such as waypoint navigation and maintaining spatial awareness present directions by mapping them to body locations.

For example, Nagel et al. [106] and Tan et al. [139] utilized a wearable tactile belt consisting of several tactors, together with a compass, to calculate and display cardinal directions by mapping them to body locations. The tactor that pointed most closely north was always activated allowing users to gain a sense of their global orientation. Karcher et al. [102] showed that this kind of augmentation device can also be used by people with visual impairments to maintain a heading direction over long distances. The ‘active belt’, developed by Tsukada and Yasumura [140], provided users with directional information via eight tactors distributed around the waist. A target destination was displayed in a discrete fashion by activating the tactor closest to its direction. Van Erp et al. [125] evaluated a similar discrete direction encoding using a vibrotactile waist display where the location of the next waypoint determined the specific tactor that was active at any given time.

Although participants were able to navigate effectively in the above studies, the discrete number of displayable directions limits the resolution with which directional information can be conveyed and could lead to suboptimal routes. This has encouraged the development of more continuous forms of direction display that in-

volve activating multiple tactors. For example, Heuten et al. [141] developed a belt-type display that guided pedestrians by indicating a continuous range of directions and deviations from the path. Similarly, Pielot et al. [142] developed a presentation method that displayed direction by interpolating the intensity of two adjacent tactors in a tactile belt with six tactors. Interpolated presentation was found to be more accurate than discrete presentation and improved the accuracy of perceived directions.

Whilst location of activation is clearly an intuitive way to present direction, the possibility also exists to communicate navigation instructions through the temporal pattern. For example, Cosgun et al. [143] showed that displaying a rotating pattern of activation on a belt with eight tactors could usefully indicate an intended direction for whole-body rotation.

Different combinations of spatial and temporal patterns are also possible and may be useful for displaying richer instructional cues [144]. For instance, Tan et al. [42] and Ross et al. [145] developed a 3-by-3 haptic back display for directional cueing. Each direction was generated as a simulated line using three tactors, e.g. tactors vibrating in the middle vertical row of the array from bottom to top conveyed North. Similarly, Jones et al. [8] investigated spatiotemporal patterns for presenting direction information for outdoor navigation using a 4-by-4 tactile display mounted on the torso. Results showed that subjects could navigate through the course with perfect accuracy using the proposed direction encoding method.

The design of tactile display signals for use as navigation commands can also exploit sensory phenomena such as the apparent motion illusion (see Section 2.2.2.3). Roady et al. [70] compared

the effectiveness of static (single or multiple factors activated together), dynamic (factors activated in sequence but no temporal overlap), and saltatory (overlapping sequential stimuli) vibrotactile patterns in a task in which participants were asked to draw the stimulation pattern using pen and paper. Results showed that saltatory presentation mode, which induced an apparent motion effect, outperformed dynamic display in terms of response time and accuracy, and was easier to interpret than static displays for more complex patterns. Murata et al. [146] proposed an automotive 8-direction warning system that informed drivers of hazardous traffic situations using tactile apparent movement. The effectiveness of the proposed system was compared with simultaneous two-point stimulation and a system without warning. Results showed that apparent movement led to faster reaction time and higher hit rate (for front and rear hazard) as compared with the simultaneous two-point stimulation and without warning system.

This thesis focuses on the design of a tactile language for presenting direction information on the forehead that will exploit the efficacy of apparent motion as a direction cue. Detailed information about the design and investigation of the employed tactile language is presented in Chapter 5.

2.7 Head-mounted vibrotactile displays

As noted in Section 2.1.1, different parts of the human body display differing levels of sensitivity to vibrotactile commands [20] which could influence vibrotactile pattern recognition. For example, Jones et al. [147] showed that the ability to identify tactile patterns presented on the back is higher than forearm indicating that the back

may be a more effective location for presenting vibrotactile navigation cues.

Back and waist-mounted vibrotactile displays are used extensively for presenting navigation information as explained earlier in this chapter. Wrist-mounted vibrotactile displays have been investigated less than the waist and back displays, partly due to the limited skin area and lower tactile sensitivity of the wrist [148]. Nevertheless, if the nature of the information being conveyed is relatively simple, wrist displays can still be effective. ‘Gentleguide’ [149] and ‘VibroTac’ [150] are two examples of the wrist-mounted vibrotactile displays that provide an intuitive means to deliver directional information to guide pedestrians, and spatial guidance for translating and rotating virtual objects, respectively.

An alternative body location that has the potential to provide a reasonably high resolution for tactile discrimination and sensitivity is the forehead. Compared to a wrist- or waist-mounted tactile display, a head-mounted display can allow faster reactions to unexpected obstacles since tactile response latencies are approximately linear in distance from the brain [151]. The reaction time at five body locations such as the head, the outside of the thigh, the temples, the forehead and the back of the head has been investigated by Stafford et al. [151]. They found comparable levels of sensitivity in the fingertips and temples, but quicker speed of response for stimulation sites on the head. In other words, the skin around the forehead and temples provides a sensitive and rapidly responsive site to transmit tactile information which we take advantage of with the Mark-II Tactile Helmet in this thesis. A head-mounted display may also be intuitive for navigation since a relatively straightforward

mapping can be created between sensed objects (such as obstacles) and stimulation of the head in the direction of that object.

Several studies have investigated head-mounted vibrotactile displays for enhancing spatial awareness and navigation. One of the first as previously discussed in Section 2.5.2 was the ‘haptic radar’, created by Cassinelli et al. [5], that linked infrared sensors to a head-mounted vibrotactile display allowing users to perceive and respond simultaneously to multiple spatial information sources. Mann et al. [152] developed a vibrotactile helmet consisting of a Kinect camera and a vibrotactile array around the forehead to display visual information for the application of blind navigation. HapticHead as a head-mounted display was designed by Kaul et al. [153] for 3D guidance and target acquisition. It consisted of a bathing cap with 20 vibration motors distributed in three concentric ellipses around the head and an Oculus Rift. For target acquisition task, the three closest motors to the target were activated with an interpolated intensity to show the closeness to the target. It was found that haptic feedback is faster and more precise than audio feedback for finding virtual objects around users. However, presenting haptic feedback to the hairy part of the head reduced the tactile stimuli perception depending on the thickness of the users’ hair. ProximityHat [154], a head-mounted sensory augmentation device, was designed based on the spatially extended skin paradigm [5] to augment the spatial awareness of the user. It detected the distance to surrounding objects with ultrasonic sensors and displayed this information to users via tactile pressure actuators rather than vibrotactile actuators. Marsalia [155] evaluated the effectiveness of a head-mounted display in improving hazard recognition for distracted pedestrians

using a driving simulator. Results showed that response hit rates improved and response times were faster when participants had a display present.

The above studies indicate the value of head-mounted vibrotactile displays for alerting wearers to possible threats. The close proximity of the display to the brain can allow a fast response with the direction of the threat displayed in an intuitive way by the position of the activated tactor(s). The Mark-I Tactile Helmet [6] was a prototype sensory augmentation device, developed at the University of Sheffield, that aimed to be something more than a hazard detector — a device for guiding users within unsafe, low-visibility environments such as burning buildings. A head-mounted vibrotactile display was selected as this facilitates rapid reactions [151], can easily fit inside a modified firefighter helmet, and leaves the hands of the firefighters free for tactile exploration of objects and surfaces. The first generation device (see Figure 2.18) comprised a ring of eight ultrasound sensors on the outside of a firefighter's

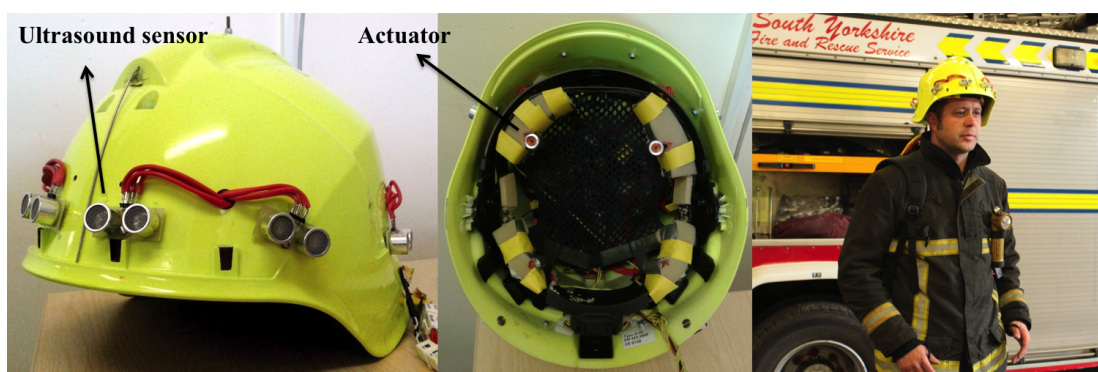


Fig. 2.18 The Mark-I Tactile Helmet [6] was composed of a ring of ultrasound sensors and four actuators inside the helmet and was designed to help firefighters' navigation inside smoked-filled buildings.

safety helmet with four voice coil-type vibrotactile actuators fitted to the inside headband. Ultrasound distance signals from the sensors were converted into a pattern of vibrotactile stimulation across all four actuators.

One of the goals of the Mark-I Tactile Helmet was to have control over the information displayed to the user, and, in particular, to avoid overloading tactile sensory channels by displaying too much information at once. This is particularly important in the case of head-mounted tactile displays, as vibration against the forehead is also detected as a sound signal (buzzing) in the ears; too much vibrotactile information could therefore be confusing, or irritating, or could mask important auditory stimuli. Despite seeking to provide better control over the signal display, field tests with the Mark-I Tactile Helmet, conducted at a training facility for South Yorkshire Fire and Rescue (SYFR), showed that a design that directly converted local distance information into vibration on multiple actuators generated too much stimulation in confined situations such as a narrow corridor.

These tests therefore established the need to better regulate the tactile display of information, to ensure clearer signals and to minimize distracting or uninformative signals. Following on from these field tests, the psychophysical studies described in Chapter 3 were conducted to investigate how to best optimize head-mounted vibrotactile displays to relay effective information to the user. In order to overcome some of the limitations of the Mark-I Tactile Helmet, particularly the low resolution of the tactile display and the size and weight of the on- and off-board electronics, the Mark-II Tactile Helmet was developed as described in Chapter 4.

2.8 Wall-following navigation

This thesis will develop a haptic guidance system for navigation that is inspired, in part, by robot wall-following algorithms that are therefore briefly reviewed here. Wall-following navigation is a type of robot motion that navigates the robot to move along a wall in a certain direction while keeping a constant distance away from the wall [156]. In order to design a controller for wall-following navigation, either traditional control techniques or soft computing algorithms could be employed. With traditional methods, it is difficult to deal with nonlinear and dynamic nature of the wall-following navigation [157]. Thus, this encourages the application of soft computing techniques such as neural networks, fuzzy logic or some combination of these two to solve this problem.

Artificial neural networks have been used widely for mobile robots navigation. As a wall-following controller, neural networks associate sensory input patterns with actions to be taken by a robot. For example, Freire et al. [158] evaluated the performance of four neural network classifiers – logistic perceptron, multilayer perceptron, mixture of local experts and elman recurrent network – as controllers for a robot wall-following navigation. Ultrasound sensor data collected after navigating in a room by following walls provided the network inputs, and the output was selected from the discrete commands such as move forward, slight right-turn, sharp right-turn and slight left-turn (see Figure 2.19). Results showed that the multilayer perceptron achieved the best performance among other classifiers with 97.6% success rate.

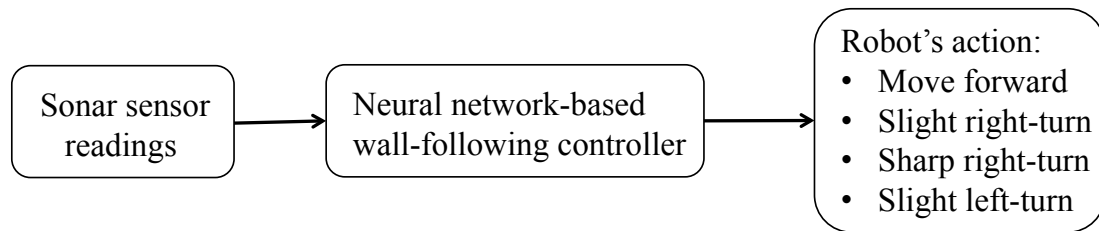


Fig. 2.19 Block diagram of the wall-following controller employed by Freire et al. [158].

The dataset collected by Freire et al. [158] is available in the UCI machine learning repository [159] and has been used as a benchmark by the following studies. Dash et al. [160] developed a three-layer MLP neural network controller for navigation of a wall-following robot. The controller classified the sonar data into four classes – move-forward, slight-right-turn, sharp-right-turn and slight-left-turn – to determine the robot’s next move. Experimental results showed that the proposed algorithm controlled the robot with 92.7% accuracy which is lower than the reported accuracy with MLP controller in [158]. In another study, Dash et al. [161] used a feed-forward neural network based on gravitational search [162] for controlling navigation of a wall-following mobile robot. The gravitational search algorithm was used to enhance the performance of the neural network by setting the weights optimally. Results indicated that the network achieved lower decision accuracy compared to the MLP controller in their previous study [160]. ‘Adaptive Resonance Theory-1’, a biological inspired neural network developed by [163], was utilized by [164] for navigation of a wall-following mobile robot. Compared to the above studies, this controller achieved 99.6% of maximum decision accuracy.

Wang et al. [165] proposed a modular navigation controller based on Spiking Neural Networks for a mobile robot that employed a reactive architecture containing three sub-controllers: obstacle-avoidance, wall-following, and goal-approaching. The navigation controller was able to control a mobile robot to reach a target successfully while following the wall and avoiding obstacles.

Fuzzy logic is another soft computing approach that provides promising solution to handle real world uncertainty by mimicking human experience in the form of rules [166]. Fuzzy logic is well suited for controlling mobile robots and many researchers have utilized it for developing controllers for robot wall-following. For example, Antonelli et al. [167] proposed a path following approach for mobile robots based on a fuzzy logic technique that emulated human driving behaviour. The inputs to the fuzzy system were curve and distance information which were extracted using a vision-based system and the corresponding output was the cruise velocity that the vehicle needed to attain in order to safely drive on the path (see Figure 2.20). Lo et al. [168] performed wall-following based on a differential velocity control using fuzzy logic for a wheeled mobile robot equipped with IR and sonar sensors. Their system was tested

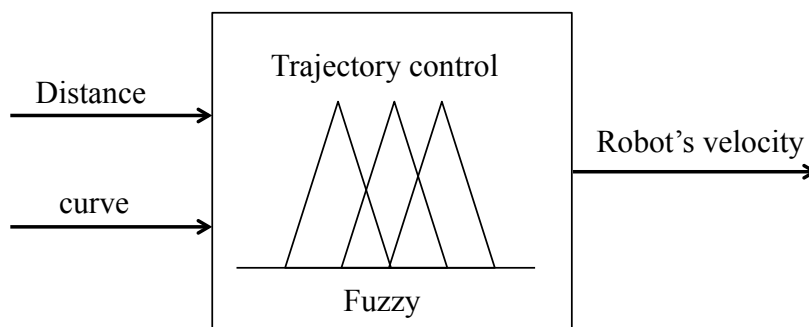


Fig. 2.20 A fuzzy wall-following controller.

with a mobile robot for an indoor surveillance task of polygon terrain using right wall-following and was demonstrated to work effectively. A wall-following fuzzy controller for a car-like mobile robot was designed by Li et al. [169]. The robot's infrared sensors were used to generate two inputs to the fuzzy controller including relative distance and orientation of the robot to the wall with the output of the system being the steering angle. In another work [170], a fuzzy logic algorithm has been used to guide a corridor-cleaning robot successfully to move along a wall in a desired direction by keeping a constant distance from the wall.

One of the limitations of the fuzzy logic approach for robot navigation is the difficulty of finding appropriate fuzzy rules to navigate robots in complex environments [171]. To address this issue, some studies have suggested neuro-fuzzy approaches that tune the fuzzy parameters with the help of neural networks [172–175]. Results showed that robots could avoid obstacles and generate smooth trajectories toward targets in various situations. Genetic based fuzzy logic is another approach for tuning the fuzzy parameters that has been employed by [176, 177] for a wall-following mobile robot.

The effectiveness of fuzzy logic and neural network algorithms for mobile robot navigation has been compared in a number of studies. Nijhuis et al. [178] performed a comparative study of fuzzy logic and neural network controller on a mobile robot obstacle avoidance task. Results indicated that the obstacle avoidance problem can be successfully solved by both algorithms, however, the neural network was easier to design as hidden relationships between different sensory signals can be extracted, whereas the fuzzy logic requires an explicit transformation of the data into linguistic variables. Tsui et

al. [157] compared the usefulness of fuzzy logic and a neural network algorithm for a car-like mobile robot in a wall-following navigation task. It was found that the neural network provided good tracking behaviour with smaller tracking trajectory error compared to the fuzzy logic controller.

The design of a human feedback system could benefit from robot wall-following navigation to navigate users in a trajectory parallel to the wall. This thesis employs the wall-following approach inspired by mobile robots to simulate firefighters' wall-following behaviour [9] by navigating users along a wall. Detailed information about the wall-following navigation algorithm in this thesis is described in Chapter 6.

Chapter 3

Vibrotactile Headband Display

A better understanding of how people perceive tactile stimuli is important in addressing the challenge of designing vibrotactile interfaces. As already explained in Section 2.7, head-mounted vibrotactile interfaces facilitate rapid reactions, can easily fit inside a modified firefighter's helmet, and leave the hands of the firefighter free for tactile exploration of objects and surfaces. In order to aid in the design of head-mounted vibrotactile displays and subsequent design of the Mark-II Tactile Helmet, a better understanding of tactile sensing on the forehead is required. This chapter explains the design of a vibrotactile headband display and four psychophysical experiments that have been performed to test the perception of different vibrotactile stimuli on the forehead.

Section 3.1 as experimental methods describes participants, the vibrotactile headband display, and the procedures employed in the experiments. Using the vibrotactile headband display, four experiments are carried out on the forehead to (1) measure vibrotactile absolute threshold (Section 3.2.1), (2) investigate vibrotactile localization accuracy (Section 3.2.2), and (3) evaluate two sensory phenomena: the funneling illusion (Section 3.2.3) and apparent motion

(Section 3.2.4). Finally, a summary of this chapter is presented in Section 3.3.

3.1 Methods

3.1.1 Participants

Ten participants - 3 men and 7 women, average age 24 - were included in the experiments in Section 3.2.1, Section 3.2.2, and Section 3.2.3. Another ten participants - 6 men and 4 women, average age 23 - took part in the experiment in Section 3.2.4. All participants were university students and staff. None of the participants reported any known abnormalities with haptic perception. The experiments were approved by the University of Sheffield Ethics Committee and all participants signed an informed consent form before being enrolled in the studies (see Appendix A.1 and Appendix A.2 for consent forms). Participation in these experiments was voluntarily and participants were informed that they could withdraw at any time.

3.1.2 Apparatus

An easy-to-wear, lightweight vibrotactile headband display was designed to provide stimuli on the participants' forehead. The vibrotactile headband consisted of seven vibration motors (tactors) with 2.5 cm inter-tactor spacing attached to a Velcro strip that can easily be worn as a headband and that can be adjusted according to head size. The tactors used in the experiments were Eccentric Rotating Mass (ERM) vibration motors (Figure 3.1a) with 10 mm diameter,

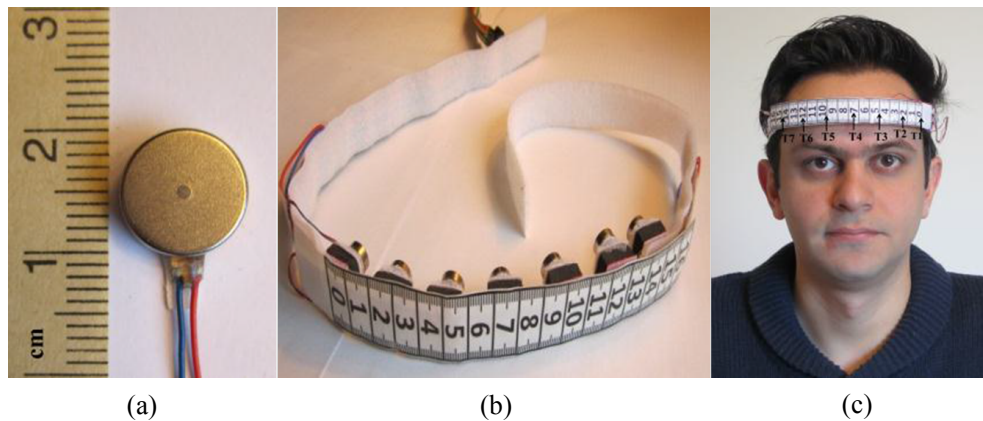


Fig. 3.1 (a): Eccentric Rotating Mass (ERM) vibration motor (Model 310-113 by Precision Microdrives), (b): Vibrotactile headband interface, (c): A participant wearing the vibrotactile headband interface.

3.4 mm thickness, 3 V operating voltage and about 200 Hz operating frequency at 3 V (see Appendix B.3).

A paper ruler was attached on the outer side of the headband to aid accurate measurement of the stimulus position. The seven tactors were attached at positions 0, 2.5, 5, 7.5, 10, 12.5 and 15 cm relative to the ruler and are referred as tactors 1 (0 cm) to 7 (15 cm). Figure 3.1b shows the headband, and Figure 3.1c a participant wearing the vibrotactile display such that tactor 1 is on the far left of the forehead and tactor 4 is aligned with the forehead midline. In order to control the intensity of the tactors, a microcontroller, ATmega32u4 was used to generate Pulse Width Modulation (PWM) signals. As illustrated in Figure 3.2, the microcontroller was connected to a PC through an RS232 serial port to transfer the command data to the tactors.

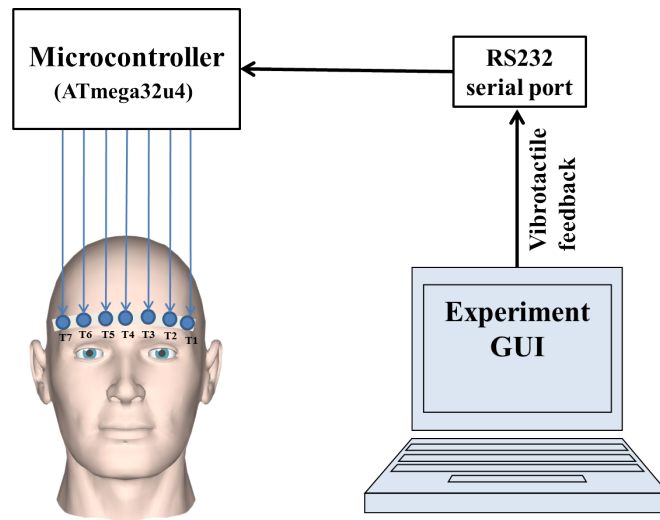


Fig. 3.2 Overview of the experimental setup.

3.1.3 General procedure

At the beginning of the experiment, each participant was invited into the experiment room. Participants were seated comfortably in front of the computer screen, camera, mirror, mouse and footswitch while the vibrotactile display was worn on the forehead. As shown in Figure 3.3, a mirror was positioned so that participants were able to see the headband, and a mouse button and footswitch were provided for participants to initiate each trial and trigger data capture by interacting with a Graphical User Interface (GUI) displayed on the computer monitor. A short practice session was provided to allow some familiarity with the experimental set-up. Once the participant felt comfortable, the trial phase was started. During the experiment, participants wore headphone playing white noise to mask any sounds from the tactors.

Each trial consisted of the participant clicking the GUI start button. After experiencing a vibration stimulus (experiment 3.2.2), or

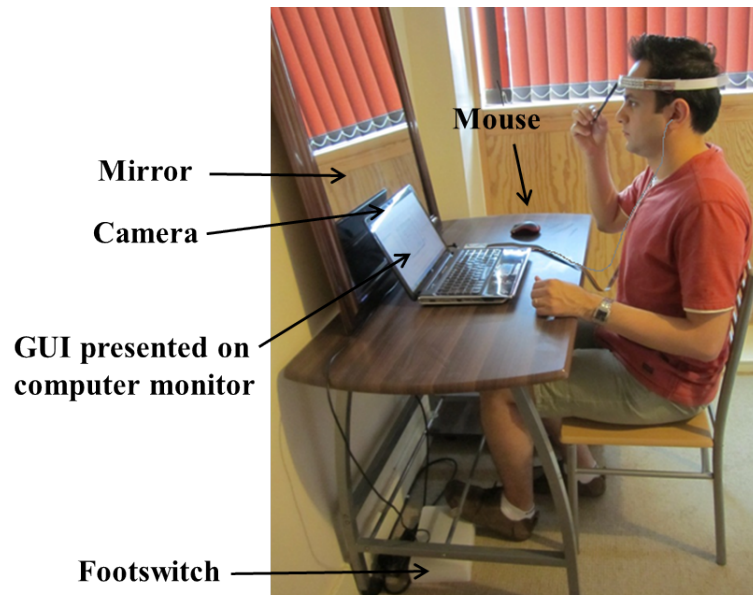


Fig. 3.3 A participant in the experiment room sitting in front of the mirror, PC, mouse, and footswitch while doing the experiment.

two simultaneous stimuli (experiment 3.2.3), the participant was asked to respond appropriately by pointing to the perceived location(s) of stimulation on their forehead using one or two thin pointers and while looking into the mirror as illustrated in Figure 3.4. By pressing the ‘Next’ button in the GUI, a snapshot was captured with the digital camera recording the indicated position. A shutter sound played after image capture to indicate to that the trial was complete, and that the next trial was ready to commence after 2 seconds. In experiments 3.2.1 and 3.2.4, participants responded to the stimuli by choosing the appropriate answer button in the GUI. Participants interacted with the GUI using a mouse in the experiments described in Section 3.2.1, 3.2.2 and 3.2.4, and with a footswitch in experiment 3.2.3 when both hands were needed for pointing.

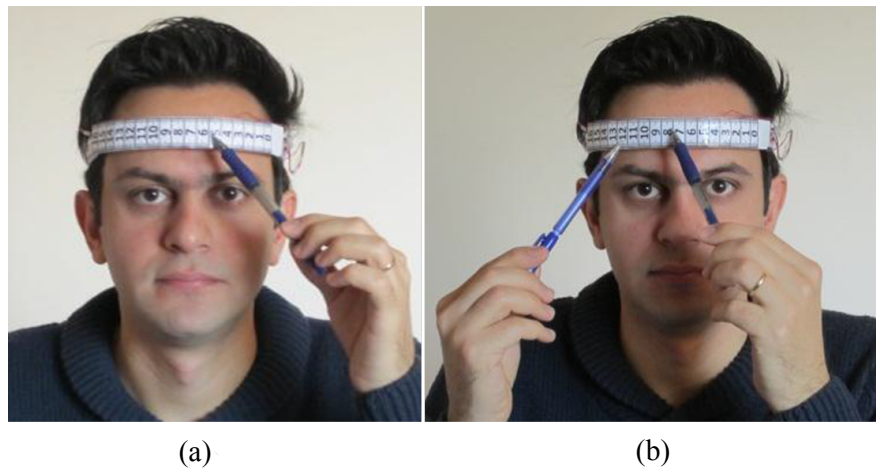


Fig. 3.4 A participant is pointing to the perceived location(s) of stimulation on his forehead. (a): pointing on one location, (b): pointing on two locations.

3.2 Experiments

3.2.1 Vibrotactile absolute threshold

As explained in Chapter 2, the characteristics of the body skin vary greatly in different body sites due to different density of skin mechanoreceptors and properties of surrounding tissues. Therefore, it is important to measure vibrotactile threshold on the forehead to find how forehead features might influence detection sensitivity and the subsequent test of vibrotactile localization [25]. The aim of this experiment was to measure vibrotactile absolute threshold on the forehead. Based on a preliminary test, I expected that a PWM value between 96/255 to 100/255 could be the vibrotactile absolute threshold on the forehead.

In order to measure vibrotactile absolute threshold on the forehead, the method of limits which is one of the most frequently used techniques for determining sensory thresholds was employed [11].

In this method, stimuli are presented in a descending and ascending series a number of times beginning with a stimulus either well above or well below the anticipated threshold. In the descending series, the trial stops when the participant reports that the stimulus is no longer perceived and in the ascending series the trial stops when the participant first indicates the presence of the stimulus. A number of ascending and descending series are presented and the absolute threshold is defined as the mean of the transition points in each of the series presented [179].

Method

The experiment was performed by presenting the vibrotactile stimuli to the participant's forehead using the forth tactor at position 7.5 cm in the vibrotactile display. Fifteen levels of intensities (equivalent to PWM 90/255-104/255) which are well below or well above the anticipated threshold (PWM 96/255-100/255) were considered. As shown in Figure 3.5, a GUI was designed as an experimental interface for this experiment. By pressing the 'Start' button, the experiment started with the descending series. A vibration well above the threshold was presented to the participant for 1000 ms.

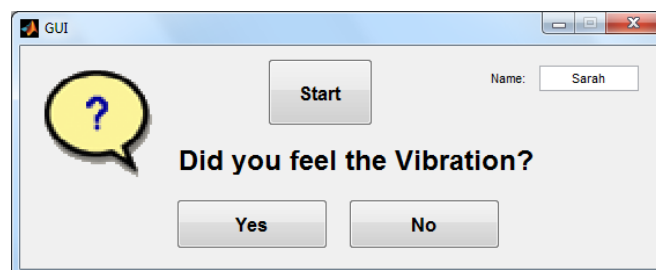


Fig. 3.5 Graphical User Interface (GUI) for vibrotactile absolute threshold measurement experiment.

The intensity of the vibration was decreased step by step until the participant reported the disappearance of the sensation by pressing the ‘No’ button in the GUI. At this point, the descending series were terminated and the ascending series were started. In ascending series, first a very weak subthreshold vibration was presented to the participant. Then the intensity of vibration was increased step by step until the participant reported the appearance of sensation by pressing the ‘Yes’ button in the GUI. The transition points that were obtained from these ascending and descending series were recorded and next trial started again with descending series.

During the experimental session, a total of twenty series were considered with alternate ascending and descending series. The mean transition points for all twenty series was designated as the absolute threshold. A similar procedure was applied in a practice session in which reduced ascending and descending series consisting of five series were presented to each participant. The maximum duration of the whole experiment was approximately 15 minutes.

Two common errors in the method of limits which can influence the obtained results are the error of habituation and the error of expectation [11]. To prevent the error of habituation which can cause a tendency for participants to repeat the same response, relatively short trial series were employed. The error of expectation which causes participants to anticipate a change in the stimuli was prevented by varying the starting points for the ascending and descending series. This means that each ascending and descending series started in each trial with three different levels of intensity selected randomly to be below (PWM 87/255-89/255) and above

(PWM 105/255-107/255) of the minimum and maximum of the defined fifteen levels of intensity, respectively.

Results

By averaging the transition points in each of these twenty series, level 9 (intensity equal to PWM 98/255) was identified as the vibrotactile absolute threshold value on the forehead. Figure 3.6 shows a histogram of detection frequency for PWM intensities employed in this experiment.

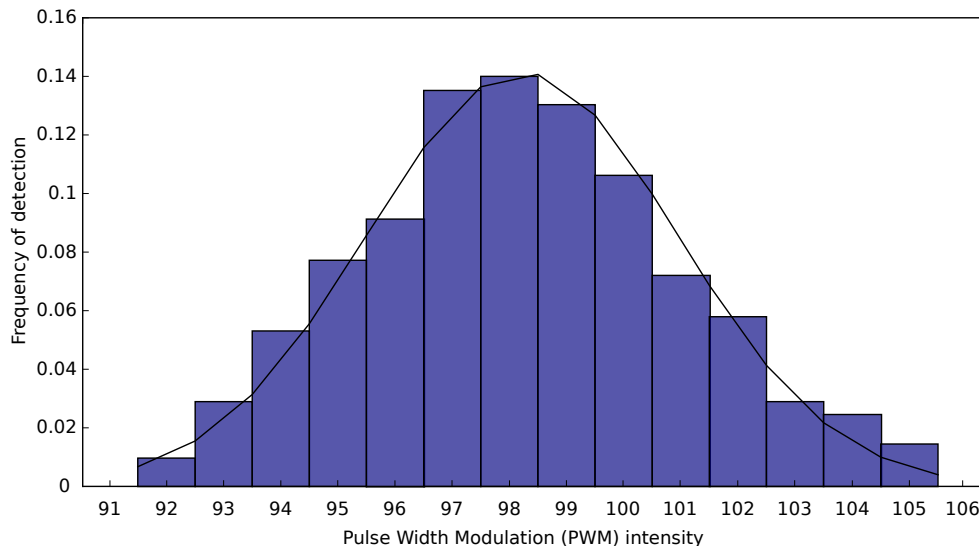


Fig. 3.6 Histogram of frequency of detection for the employed PWM intensities, $n=200$ samples.

In order to quantify the intensity, an ADXL325 three-axis accelerometer (see Appendix B.5) was mounted on top of a similar vibration motor to that utilized in the vibrotactile display (see Figure 3.7) and hung out from a desk to move freely after applying the vibration. Acceleration values were then recorded for each level of intensity from the minimum to maximum values (PWM 1-255), 1000 samples at each level, with the ATmega32u4 microcontroller.

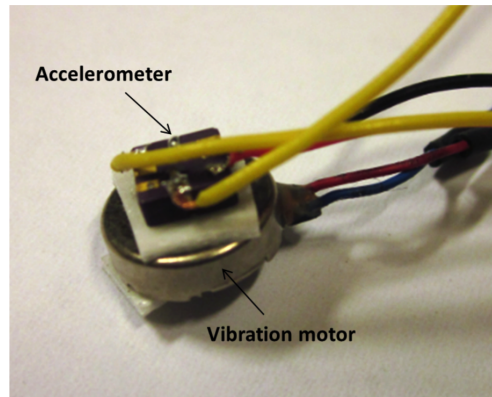


Fig. 3.7 An ADXL325 accelerometer was mounted on top of an ERM vibration motor to measure the unit of intensity.

The acceleration value (Acc) for each axis (x, y and z axis) was calculated using the following formula:

$$Acc = \left(\frac{Raw \times ADC_{ref}}{ADC_{res}} - zero_g \right) / sensitivity \quad (3.1)$$

where Raw is the raw Analog to Digital Converter (ADC) value of the accelerometer at x, y and z axis, ADC_{ref} is the conversion range for the ADC, ADC_{res} represents the ADC resolution¹, $zero_g$ indicates 0 g voltage at x, y and z output, and $sensitivity$ indicates the sensitivity at x, y and z output. The overall acceleration value was obtained by computing the magnitude of sum vector of acceleration at x, y and z axis.

Figure 3.8 shows acceleration values for each level of intensity from PWM 1 to 255. As shown in the figure, the applied fifteen levels of intensity (PWM 90/255-104/255) start from 0.18 g and range through 0.27 g. Level nine (PWM 98/255) as the vibrotactile abso-

¹The resolution of a n-bit ADC is a function of how many parts the maximum signal can be divided into. The formula to calculate resolution is 2^n [180]. Here, a 10 bit ADC has a resolution of $2^{10} = 1024$.

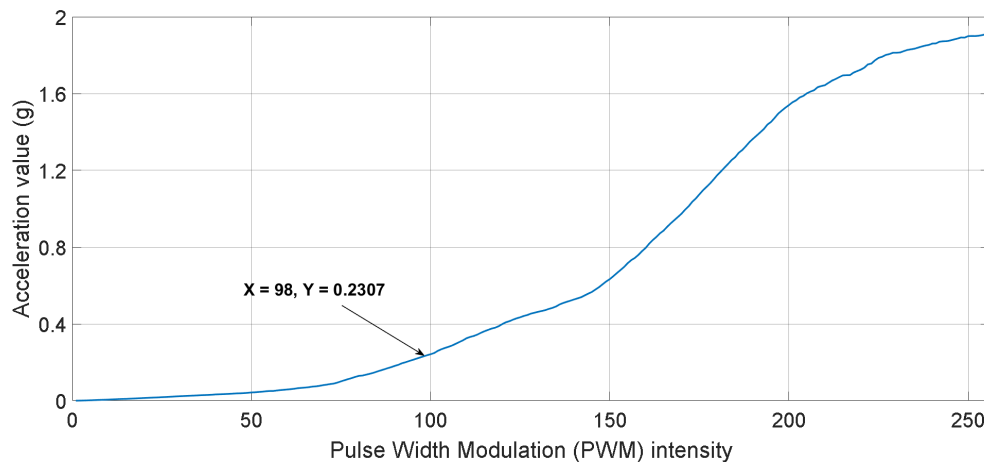


Fig. 3.8 Acceleration values equivalent of PWM intensity of 1-255.

lute threshold on the forehead is therefore equal to an acceleration of 0.23 g.

3.2.2 Vibrotactile Localization

Activation of vibrotactile stimulators at specific locations on the body can provide a spatial cue to the location of an object or event in the environment or show a navigation direction [7]. The number and configuration of the vibrotactile stimulators in the tactile display are known to play an important role in vibrotactile localization accuracy [43] although increasing array granularity does not necessarily improve localization ability [25, 45]. The objective of this experiment was to determine vibrotactile localization accuracy for vibrotactile stimuli on the forehead. Since the midsagittal plane of the body can simplify the ability to localize a point of stimulation [44, 7], I expected that vibrotactile localization accuracy would be higher for the forehead midline where tactor 4 is placed.

Method

A GUI as shown in Figure 3.9 was used for this experiment. It allowed participants to enter their personal information and provided a ‘Start’ button for starting the experiment and a ‘Next’ button for presenting the next stimuli. Each trial consisted of the participants pressing the ‘Start’ button, by using a mouse to begin the trial, followed by vibration being displayed in a pseudo-random order to each tactor with 255 PWM intensity for 1000 ms.

During the experimental session, a total of 105 trials were presented in a random order to each participant, 15 for each tactor. A practice session consisting of 5 randomly selected trials per tactor was provided before starting the experimental phase. The maximum duration of the experiment was approximately 15 minutes.

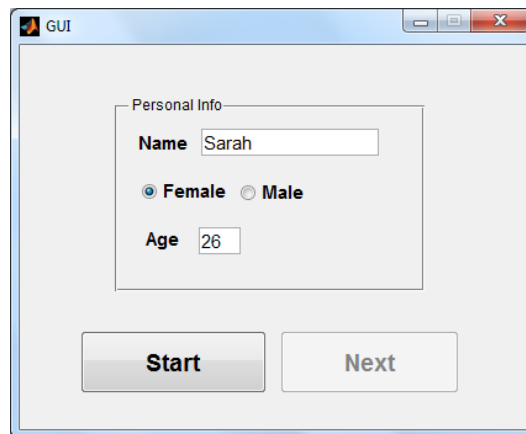


Fig. 3.9 GUI for vibrotactile localization experiment.

Results

Localization mean error with standard deviation for each of the seven tactor positions is shown in Figure 3.10. As can be seen, this varies from 0.51 cm for tactor 4 to 0.76 cm for tactor 3. It

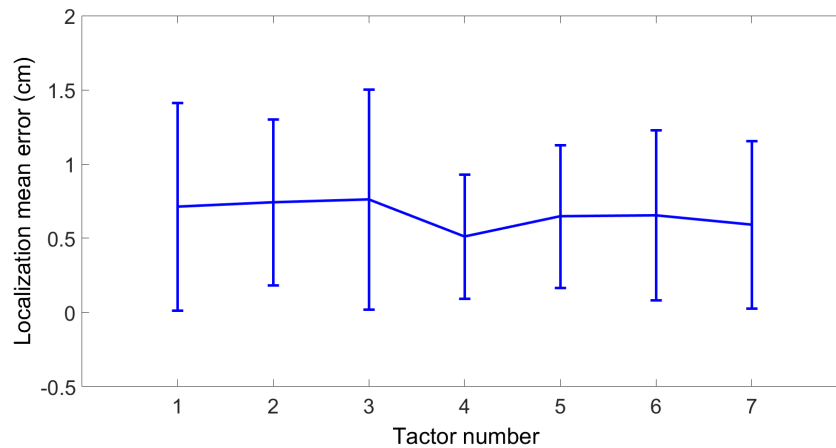


Fig. 3.10 Localization mean error for seven tactor locations, $n=1050$ samples. Error bars show standard error.

means that participants could recognize the tactor 4 with least error and tactor 3 with the maximum error. An ANOVA showed no significant difference in localization mean error across the seven positions ($F(6, 63) = 0.882, p = 0.513$), although, consistent with my hypothesis, the data indicate that the lowest error occurs above the midline. Figure 3.11 shows the localization mean error for left and right side pointings for each tactor. Moving from position 1 to

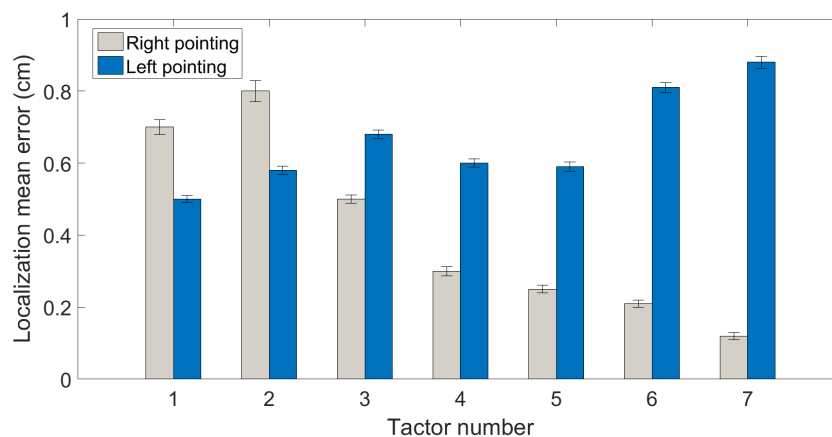


Fig. 3.11 Localization mean error for left and right side pointings, $n=1050$ samples. Error bars show standard error.

7 (from left to right), the error shifts from being strongly biased to the right to being strongly biased to the left. In other words, the perceived location of stimulation is biased towards the forehead midline for the outermost tactor locations.

3.2.3 Effect of inter-tactor spacing on the funneling illusion

The funneling illusion as a human sensory phenomenon can be used to improve the resolution of a vibrotactile display by generating a midway phantom sensation between two stimuli when they are presented simultaneously to adjacent and separate locations on the skin. As described in Chapter 2, this midway phantom sensation is affected by the separation of the stimuli, their temporal order, and their relative amplitude [61]. The aim of this experiment was to investigate the effect of inter-tactor spacing on the funneling illusion as it is important in helping to decide the positioning of tactors on the forehead.

Method

In order to perform this experiment, a similar GUI to the previous experiment (Figure 3.9) was used as an experimental interface. Each trial consisted of the participants pressing the ‘Start’ button by using a mouse to begin the trial, followed by vibration stimuli being displayed at one of the following tactor combinations $\{(1, 4), (2, 3), (4, 7), (5, 6), (2, 6), (3, 5)\}$ with both tactors activated simultaneously with 255 PWM intensity for 1000 ms. The tactor combinations were chosen in a symmetric form to cover possible distances on the forehead. After displaying the vibration stimuli,

participants indicated whether they perceived one or two vibration stimulation on the forehead using a thin pointer for one vibration stimulus and two thin pointers for two stimuli (see Figure 3.4).

During the experimental session, a total of 90 trials were presented in a random order to each participant, 15 for each factor combination. Before the experimental session, a practice session consisting of 5 randomly selected trials per factor combination was presented to each participant. The maximum duration of the experiment was approximately 15 minutes.

Results

Figure 3.12 shows that by increasing the distance between tactors the percentage of pointing to one location decreases while the percentage of pointing to two locations increases. Tactor combinations with the inter-tactor spacing of 2.5 cm showed the highest rate of pointing to one location while tactor combination with an inter-tactor spacing of 10 cm revealed the highest rate of pointing to two

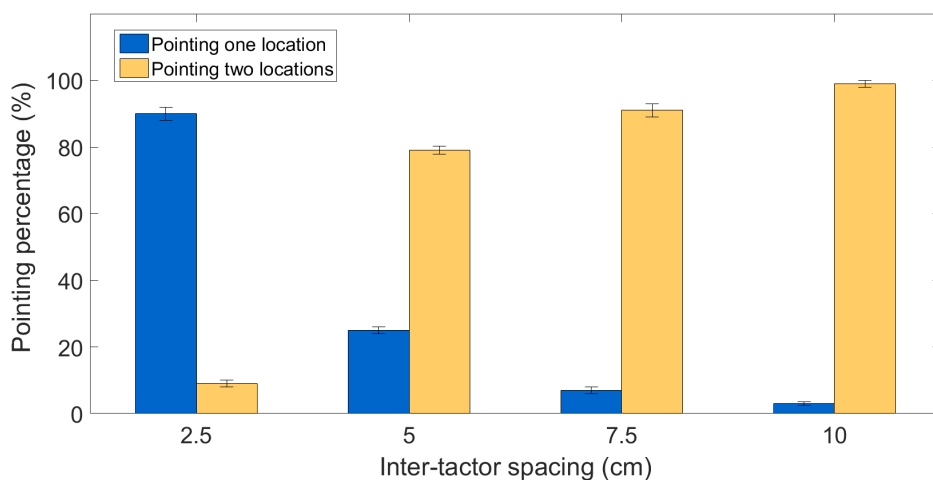


Fig. 3.12 Percentage of pointing to one and two locations for different inter-tactor spacings, $n=900$ samples. Error bars show standard error.

locations.

An ANOVA showed that the likelihood of judging the stimulation as coming from 2 sources rather than 1 source differed significantly by stimulation distance ($F(3, 27) = 92.426, p < 0.0001$). By visual inspection, it is clear that the likelihood of perceiving one source was only more probable for the shortest stimulation distance. Figure 3.13 shows that participants consistently indicated two stimuli as being closer together than their actual distance, even when not experiencing the funneling illusion.

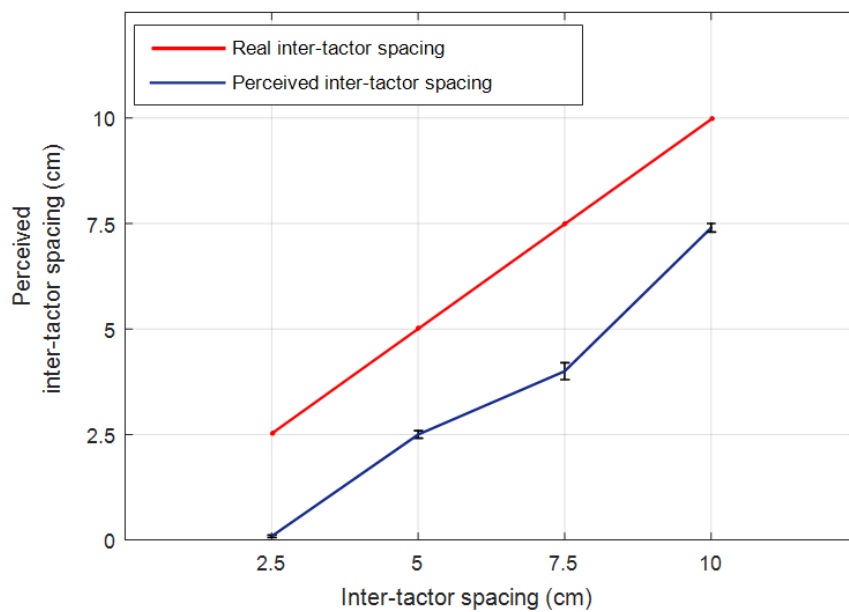


Fig. 3.13 Perceived and actual inter-tactor spacing, $n=900$ samples. Error bars show standard error.

3.2.4 Effect of SOA and inter-tactor spacing on apparent motion

Apparent motion as a type of human sensory illusion produces continuous moving sensation on the skin which is an effective way to provide directional cue using vibrotactile displays [77]. As ex-

plained in Chapter 2, various parameters have been found to affect the perception of apparent motion such as timing values (DoS and SOA) [74], inter-tactor spacings [77] and the number of tactors [76]. The objective of this experiment was to find the optimum SOA value and inter-tactor spacing to create apparent motion on the forehead.

Before running the experiment, a pilot study was performed to determine an approximate range of SOA values that would result in a sense of apparent motion. Stimuli with various DoS/SOA combinations were presented to the participants' forehead, and their responses were collected as to whether they perceived the stimulus as an apparent movement. Based on these responses, DoS of 400 ms and SOA with three levels (50 ms, 100 ms, and 200 ms) were selected as appropriate timing values for this experiment.

Method

As shown in Figure 3.14, a GUI was used for entering participants' personal information, starting the experiment, rating the perceived

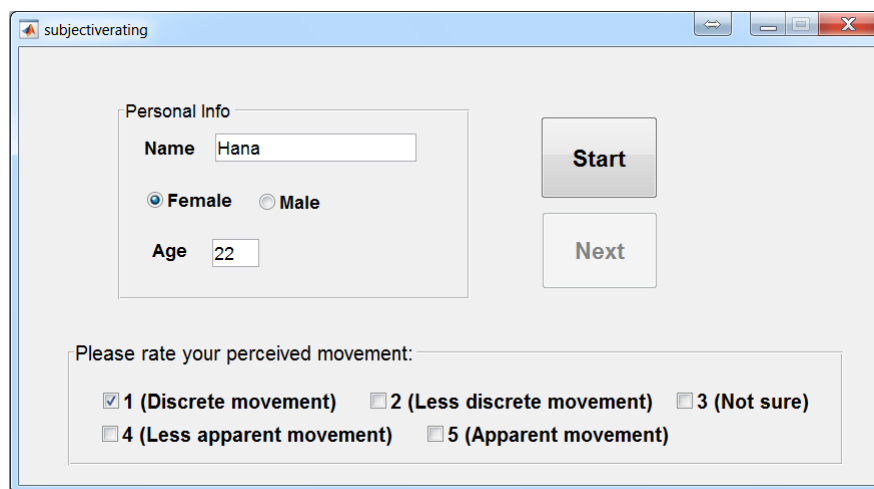


Fig. 3.14 Employed GUI in apparent motion experiment.

stimuli on a scale of 1 to 5, and presenting the next stimuli. Participants started the trial by pressing the GUI ‘Start’ button using a mouse with their left/right hand. Afterwards, a stimulus set consisted of two identical stimuli was presented one after the other at similar tactor locations and SOA values (see Figure 3.15). The stimulus is presented twice in order to ensure that it is notified by the participants. The time interval between presentation of the first stimulus and the second one was one second. This value was chosen as Niwa et al. [76] have previously shown that an inter-stimuli set interval of greater than 400 ms creates the feeling of apparent motion.

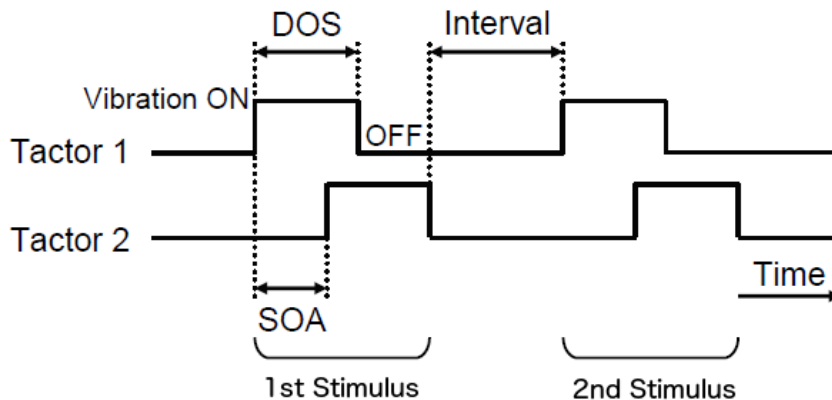


Fig. 3.15 Two stimuli are presented one after the other with a time interval between sequences, source from Niwa et al. [76].

The stimulus set was displayed randomly to one of the following tactor combinations $\{(1, 4), (2, 3), (4, 7), (5, 6), (3, 5)\}$ with 400 ms DoS and different SOA values of 50 ms, 100 ms, and 200 ms. The tactor combinations covered distances of 2.5 cm, 5 cm and 7.5 cm on the forehead. After displaying the stimulus set, participants rated the perceived stimuli by choosing one of five buttons

in the GUI. By pressing the next button in the GUI, their response was recorded and after 2 seconds the next stimuli were presented.

During the experimental session, a total of 54 trials (3 inter-tactor spacings \times 3 SOA values \times 6 times) were presented in a random order to each participant. Before starting the experiment, a practice session including shorter trials was provided to familiarize participants with the experiment procedure.

Results

Figure 3.16 shows the subjective rating for 9 stimuli patterns created using different combinations of 3 inter-tactor spacings and 3 SOA values. The subjective rating of 1 corresponded to ‘Discrete movement’ and 5 corresponded to ‘Apparent movement’. As shown in the figure, the median rating of 5 was achieved for inter-tactor spacing of 5 cm at 100 ms SOA which shows that it is producing a strong impression of apparent movement on the forehead.

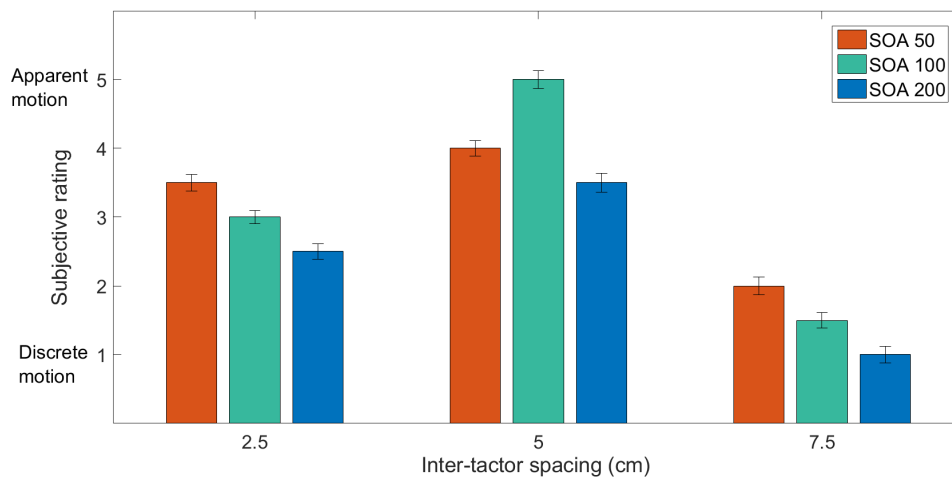


Fig. 3.16 Subjective rating for stimuli patterns, $n=540$ samples. Bars show median value and error bars indicate standard error.

A Friedman test showed that there was a statistically significant difference in perceived apparent motion depending on SOA values ($\chi^2(2) = 19$, $p < 0.001$) and inter-tactor spacings ($\chi^2(2) = 19.538$, $p < 0.001$). Post hoc analysis with Wilcoxon signed-rank tests was conducted with a Bonferroni correction applied, resulting in a significance level of $p = 0.016$ (calculated by utilizing Sidak Correction [181]). As shown in Table 3.1, there is a significant difference in perceived apparent motion between all the SOA values and between all the inter-tactor spacings.

Table 3.1 Post hoc test for SOA and inter-tactor spacing comparison for perceived apparent motion (AP)

<i>SOA(ms)</i>	Perceived AP	<i>Inter-tactor spacing(cm)</i>	Perceived AP
50/100	Z=-2.670, p=0.008*	2.5/5	Z=-2.812, p=0.005*
50/200	Z=-2.807, p=0.005*	2.5/7.5	Z=-2.673, p=0.008*
100/200	Z=-2.675, p=0.007*	5/7.5	Z=-2.820, p=0.005*

3.3 Summary

This chapter has provided a psychophysical investigation of head-mounted vibrotactile interfaces. A 1-by-7 vibrotactile headband display was designed to conduct four psychophysical experiments on the forehead. First, the vibrotactile absolute threshold was measured using the method of limits. Fifteen level of intensities (90/255 - 104/255 PWM) were presented in a descending and ascending series to the forth tactor in the vibrotactile display. It was found that level 9 equal to PWM 98/255 and acceleration 0.23 g is the vibrotactile absolute threshold value on the forehead. Second, the ability to identify the location of a vibrotactile stimulus presented

to a single tactor in the display was investigated. Results indicated that localization error is uniform but biased towards the forehead midline. The dependency of the funneling illusion on inter-tactor spacing was evaluated in a third experiment. Participants reported the funneling illusion mainly for the shortest inter-tactor spacing. Furthermore, they consistently indicated two stimuli as being closer together than their actual distance, even when not experiencing the funneling illusion. Finally, the fourth experiment was designed to evaluate the optimum SOA value and inter-tactor spacing for producing an apparent motion illusion on the forehead. Various stimulus patterns with different SOA and inter-tactor spacing were presented and participants were asked to rate them on a scale of 1-5 (1: Discrete motion, 5: Apparent motion). Results showed that participants reported the strongest impression of apparent motion for inter-tactor spacing of 5 cm at 100 ms SOA.

The results of this chapter should help formulate guidelines for the design of the vibrotactile headband displays. Specifically, PWM 98/255 (equal to an acceleration value of 0.23 g) as the vibrotactile absolute threshold was identified based on experiment [3.2.1](#), inter-tactor spacing of 2.5 cm was determined based on experiment [3.2.3](#) and apparent motion can be used to indicate direction with inter-tactor spacing of 5 cm at 100 ms SOA based on experiment [3.2.4](#).

Chapter 4

Design of a Head-mounted Sensory Augmentation System

The Mark-I Tactile Helmet, designed by Bertram et al. [6] and described in Chapter 2, was developed as a prototype sensory augmentation device to help firefighters' navigation in smoked-field buildings during search and rescue missions. As noted in Section 2.7, the objective of this system was to have control over the information displayed to the user, and particularly to avoid overloading tactile sensory channels by displaying too much information at once. However, field tests performed at the South Yorkshire Fire and Rescue (SYFR) training facility indicated that tuning the device to suit user needs and situation was problematic. Specifically, a design that directly converted local distance information into vibration on multiple actuators generated too much stimulation in confined situations such as a narrow corridor. Therefore, a 2nd generation tactile helmet called the Mark-II Tactile Helmet is developed, in this thesis, to address this issue and overcome some of the other limitations of the Mark-I Tactile Helmet particularly the low resolution of the tactile display and the size and weight of the on- and off-board electronics.

This chapter describes the design of the Mark-II Tactile Helmet. First, an overview of the prototype system is presented in Section 4.1. Following that, the main electronic components of the Mark-II Tactile Helmet including ultrasound sensor (4.1.1), Inertial Measurement Unit (IMU) (4.1.2), vibrotactile display (4.1.3) and controlling unit (4.1.4) are explained. Finally, a data flow diagram for the prototype system is presented in Section 4.2.

4.1 System overview

The Mark-II Tactile Helmet is a wearable sensory augmentation system comprising an array of 12 ultrasound sensors mounted evenly 30 degrees apart around a helmet, an Inertial Measurement Unit (IMU), a vibrotactile display composed of 7 vibration motors (tactors) positioned on the forehead, a controlling unit, a sound card and two small battery packs to provide the system power. Figure 4.1

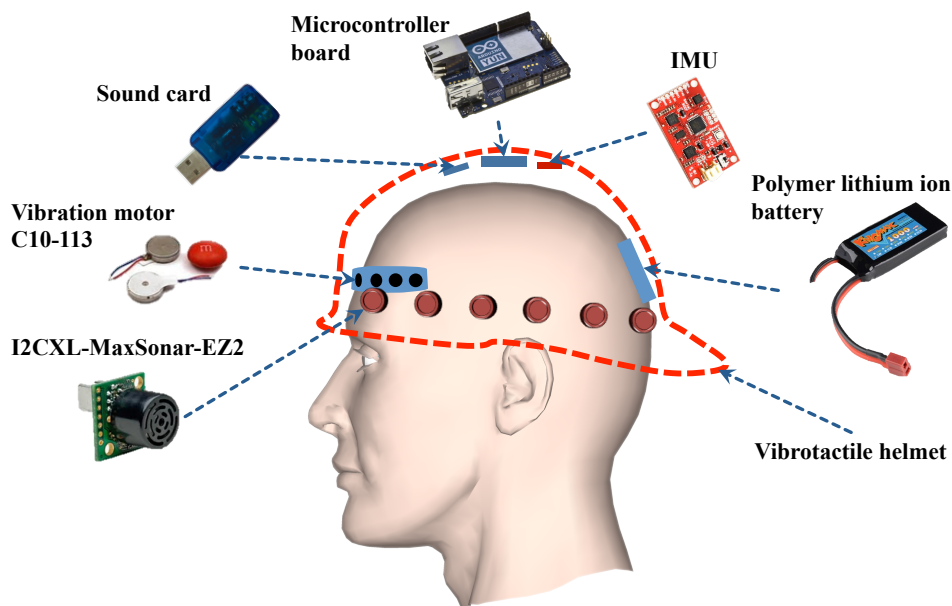


Fig. 4.1 The Mark-II Tactile Helmet configuration.

shows the configuration of the prototype system. The following sections describe these different components and their characteristics.

4.1.1 Ultrasound sensor

Ultrasound sensors are generally utilized for a wide variety of proximity and distance measuring applications. As a robust sensing modality suited to low visibility environments like smoked-filled buildings [182], ultrasound sensors employ high frequency acoustic sound (approximately 40 kHz) to measure the distance to nearby objects, typically by measuring time-of-flight (TOF) for sound to be transmitted, and then reflected back [183]. Figure 4.2 shows a simplified sonar system which uses the TOF for object detection.

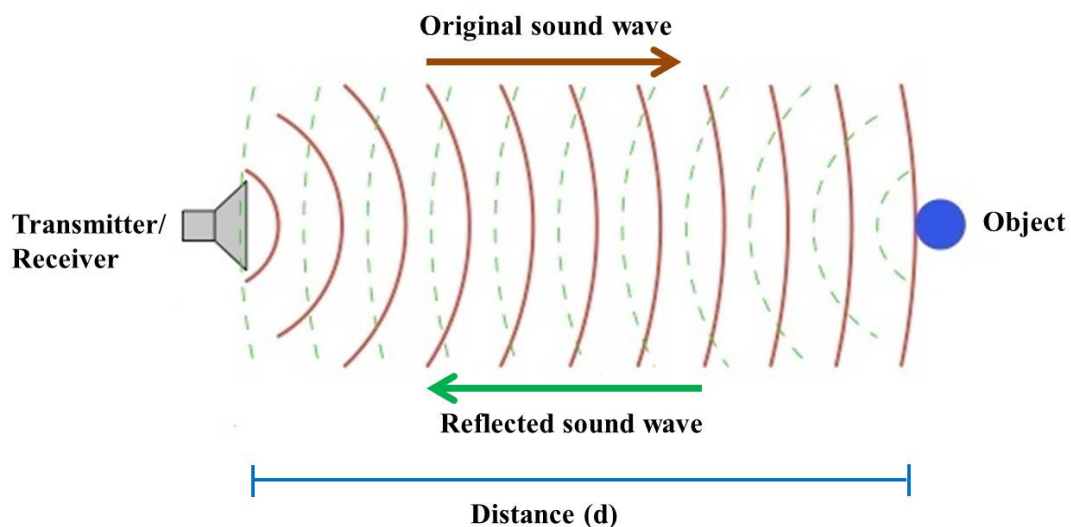


Fig. 4.2 Ultrasound sensor range measurement principle.

As shown in the figure, the ultrasound transmitter emits a short burst of ultrasonic sound toward an object within the sensor beam. The object reflects the sound back to the ultrasound receiver. The echo travel time (t), commonly called the time-of-flight (TOF) is

measured from the sound transmission time. The object distance (d) is computed from t using:

$$d = \frac{c \times t}{2} \quad (4.1)$$

where c is the speed of the sound (343 m/s at standard temperature and pressure) and the factor of 2 converts the round-trip travel distance to a distance measurement [183].

The I2CXL-MaxSonar-EZ2 ultrasound sensor (Figure 4.3a, see Appendix B.1) was employed as a distance measurement sensor in the Mark-II Tactile Helmet. It is small ($19.9 \times 22.1 \times 13.64$ mm) and lightweight (5.9 grams) for easy mounting on the helmet. This ultrasound sensor features the I2C interface that allows rapid control of multiple sensors with only two wires. This sensor has high acoustic power output along with real-time auto calibration for changing conditions (voltage and acoustic or electrical noise) that ensures receiving the most reliable ranging data for every reading taken. The sensor's low power (3 V-5.5 V) operation provides very short to long-range detection. The practical measuring range is between 20 cm and 765 cm with 1 cm resolution. If an obstacle is detected closer than 20 cm, the sensor will typically report the distance as 20 cm. This ultrasound sensor offers a good balance between wide or narrow beams with a beam angle of approximately 40 degrees.

The sonar sensor arrangement for the Mark-II Tactile Helmet is shown in Figure 4.3b. It comprises a ring of 12 ultrasound sensors mounted evenly 30 degrees apart around a helmet. An array of sonars is a common means to scan the entire environment around the user or robot [184]. This 30 degrees spacing allows an overlap

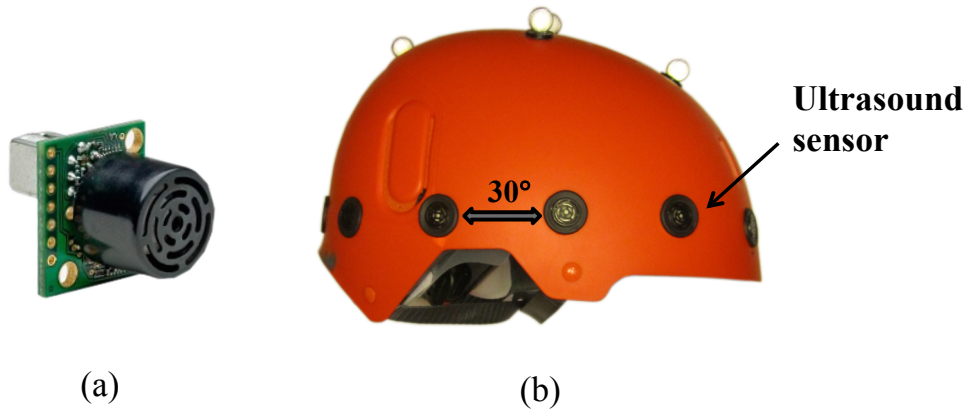


Fig. 4.3 (a): Ultrasound sensor (Model I2CXL-MaxSonar-EZ2 by MaxBotic), (b): Ultrasound sensors arrangement on the Mark-II Tactile Helmet.

between two adjacent sonar beams so at least one of the sonars will detect a strong reflecting object. The sonars in the ring are employed sequentially one at a time. In order to make measurements more stable against ultrasonic reflections, additionally a minimum pulse-pause time of 50 ms is maintained between consecutive readings. This value was determined experimentally in a preliminary study. Using a 50 ms pulse-pause time, a complete environmental scan is accomplished every 0.6 s.

4.1.2 Inertial Measurement Unit (IMU)

The Mark-II Tactile Helmet also contains a 9 Degrees of Freedom (DoF) Razor Inertial Measurement Unit (IMU) as shown in Figure 4.1. This IMU incorporates three sensors - a MEMS triple-axis gyroscope, a triple-axis accelerometer, and a triple-axis magnetometer (see Appendix B.2). The IMU is connected to the same I2C bus as the ultrasound sensors. The output of this sensor is processed by the microcontroller board and then transmitted over WiFi to a computation unit for further processing. However, in this

thesis the IMU data is bypassed and substituted based on information measured from a motion capture system. Detailed information about the motion capture system is presented in Chapter 5.

4.1.3 Vibrotactile display

The Mark-II Tactile Helmet provides navigational information to the user via a vibrotactile display similar to that investigated in terms of psychophysics in Chapter 3. In this section, the structure of the vibrotactile display fitted to the Mark-II Tactile Helmet is explained.

The display consists of seven Eccentric Rotating Mass (ERM) vibration motors (Figure 4.4a) with 10 mm body diameter and 3.4 mm body length, 3 V operating voltage and about 200 Hz operating frequency at 3 V. As shown in Figure 4.4b, these vibration motors are mounted on a neoprene fabric and attached to a plastic sheet with 2.5 cm inter-tactor spacing. The choice of 2.5 cm inter-tactor spacing is based on the psychophysical results in Chapter 3 as being a distance that will support experience of a funneling illusion.

The position of the vibrotactile display can easily be adjusted inside the helmet to increase the comfort and attenuate vibration along the forehead. Figure 4.4c shows the vibrotactile display attached inside the helmet. The vibration motors are controlled using an Arduino Yún based microcontroller which is explained in the next section.

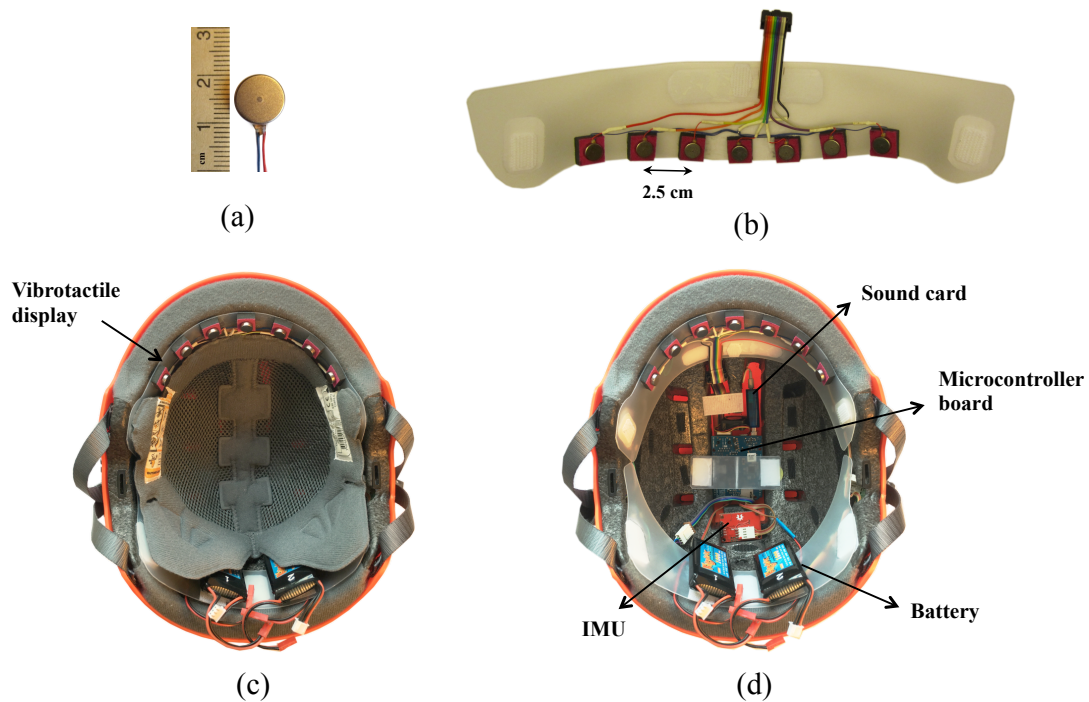


Fig. 4.4 (a): Eccentric Rotating Mass (ERM) vibration motor (Model 310-113 by Precision Microdrives (see Appendix B.3), (b): Vibrotactile display interface, (c): Vibrotactile display position inside the helmet, (d): Microcontroller, IMU, sound card, and batteries position inside the helmet.

4.1.4 Controlling unit and power supply

The controlling unit of the Mark-II Tactile Helmet is an Arduino Yún based microcontroller board which is mounted inside the helmet as shown in Figure 4.4d. The Arduino Yún is the combination of a microcontroller board based on the Atmega32U4 processor and the Atheros AR9331. The two processors communicate together using a bridge library that enables Arduino sketches to communicate with network interfaces and receive information from the Atheros processor. The board has 20 digital input/output pins of which 7 can be used as Pulse Width Modulation (PWM) outputs and 12 as analog inputs, and built-in Ethernet and WiFi support which

enable wireless communication. The datasheet of the Arduino Yún is presented in Appendix [B.4](#).

Ultrasound sensors, IMU and vibration motors are connected to various microcontroller pins. For instance, the twelve ultrasound sensors and IMU are connected to SCL and SDA (I2C interface) pins on the microcontroller to trigger the measurements while the seven vibration motors are connected to seven PWM pins on the microcontroller.

A sound card is connected to the microcontroller USB port (shown in Figure [4.4d](#)) and is employed in Chapter [6](#) to produce audio feedback. Two polymer lithium ion batteries (7.4 V, 1000 mAh) are mounted on the back side of the helmet as system power supplies (see Figure [4.4d](#)). Battery One provides the power for the microcontroller board, ultrasound sensors and IMU, and battery Two provides the power for the vibration motors. The system can work continuously for about one hour with a single charge.

4.2 System data flow

The data flow diagram of the Mark-II Tactile Helmet is shown in Figure [4.5](#). First, the ultrasound sensors and IMU measurement data are sent to the controlling unit through the I2C bus. The controlling unit reads the sensor values and sends them to the computation unit wirelessly using its built-in WiFi support. The computation unit receives the sensor values and generates commands for the tactors sending them back to the controlling unit wirelessly for onward transmission to the vibrotactile display. A prototype schematic of the Mark-II Tactile Helmet is presented in Appendix [B.6](#).

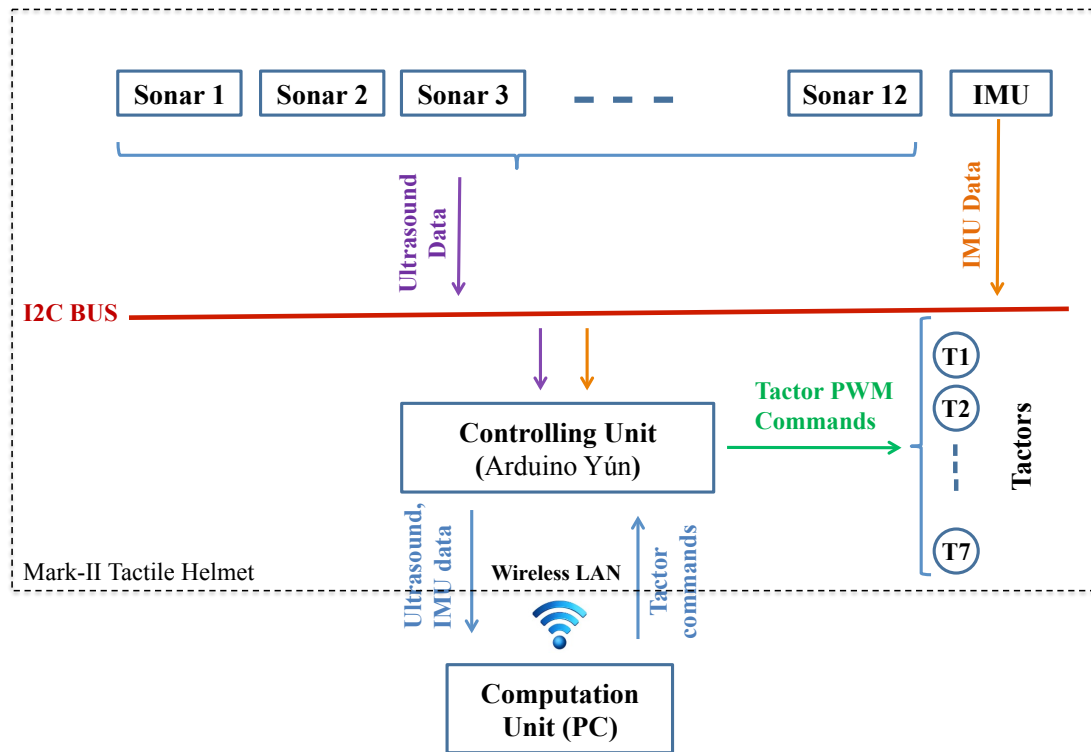


Fig. 4.5 Data flow diagram of the Mark-II Tactile Helmet.

This chapter has described the design of the Mark-II Tactile Helmet. This head-mounted sensory augmentation system is employed as an apparatus for the experiments in Chapter 5 and 6.

Chapter 5

Designing a Tactile Language for a Head-mounted Sensory Augmentation System

I have summarized previous work on the design of tactile languages for the communication of navigation commands through haptic displays in Section 2.6. As explained in that review, different body locations such as torso, waist, wrist and head can be utilized for the haptic presentation of navigation information. The torso, waist and wrist are the most commonly used body locations and also have been extensively investigated in a variety of studies. However, the head location that should allow fast reaction times has not been fully evaluated. Furthermore, results obtained from one area of the body may not necessarily transfer elsewhere due to the varying density of mechanoreceptors in the skin, concentration of different tissues (e.g. fat, bone, muscle) that can amplify or mask signals, the ability to move the display area relative to the rest of the body, and speed of transmission to the brain.

This chapter explores the design of a tactile language for effective communication in a navigation task using a head-mounted display, specifically focusing on the potential of signals that can be inter-

preted quickly and intuitively in stressful situations such as inside a smoked-filled building.

The experimental design is presented in Section 5.1. Section 5.2 describes the methods including the participants (5.2.1), apparatus and materials (5.2.2), and procedure (5.2.3). Finally, results and summary are presented in Sections 5.3 and 5.4, respectively.

5.1 Experimental design

In low visibility environments, firefighters navigate using the existing infrastructure such as walls and doors. These reference points help them to stay oriented and make a mental model of the environment [9].

In order to motivate the design of a tactile language, a navigation task is described on this challenge of moving through a building without the aid of vision. To support a navigation behaviour that follows the contour of nearby walls, a wall-following approach inspired by algorithms developed in mobile robotics (see Section 2.8) is used that combines steering-in, steering-out and moving forward commands [185]. Specifically, to navigate the user along the wall, three commands are employed: turn-left, turn-right, and go-forward. The turn-left/right commands are intended to induce a rotation around self (left/right rotation) in order to control the orientation of the user; the go-forward command is designed to induce forward motion in the current orientation.

Haptic commands

Figure 5.1 illustrates the position of tactors in the tactile display and the vibrotactile patterns used to present the different com-

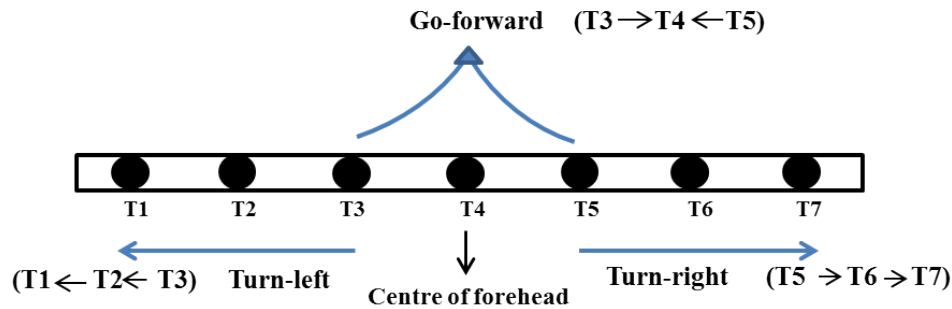


Fig. 5.1 Vibrotactile patterns for turn-left, turn-right and go-forward commands in the tactile display.

mands. Note that tactor 4 is placed in the center of the forehead. Commands are distributed spatially in the tactile display, using multiple tactors, in order to convey rich vibrotactile patterns to the user [144]. The turn-left command starts from tactor 3 and ends with tactor 1 while turn-right starts from tactor 5 and finishes with tactor 7. The go-forward command starts from tactor 3 and tactor 5 simultaneously and ends with tactor 4.

The utility and user experience of these commands was investigated using the combination of two command presentation modes, *continuous* and *discrete*, and two command types — *single* and *recurring*.

The *continuous* presentation mode takes advantage of the phenomenon of tactile apparent movement (see Section 2.2.2.3) [73]. As previously explained, Duration of Stimulus (DoS) and Stimulus Onset Asynchrony (SOA) [74] are two of the most important parameters in generating a feeling of apparent motion and different combinations of these parameter values were previously investigated in Section 3.2.4. There it was shown that a strong impression of movement on the forehead can be generated using a DoS of 400 ms and

an SOA of 100 ms. This results in a total rendering time of 600 ms for the turn-left/right commands and 500 ms for the go-forward command. To illustrate, a schematic representation of the turn-left command is presented in Figure 5.2a.

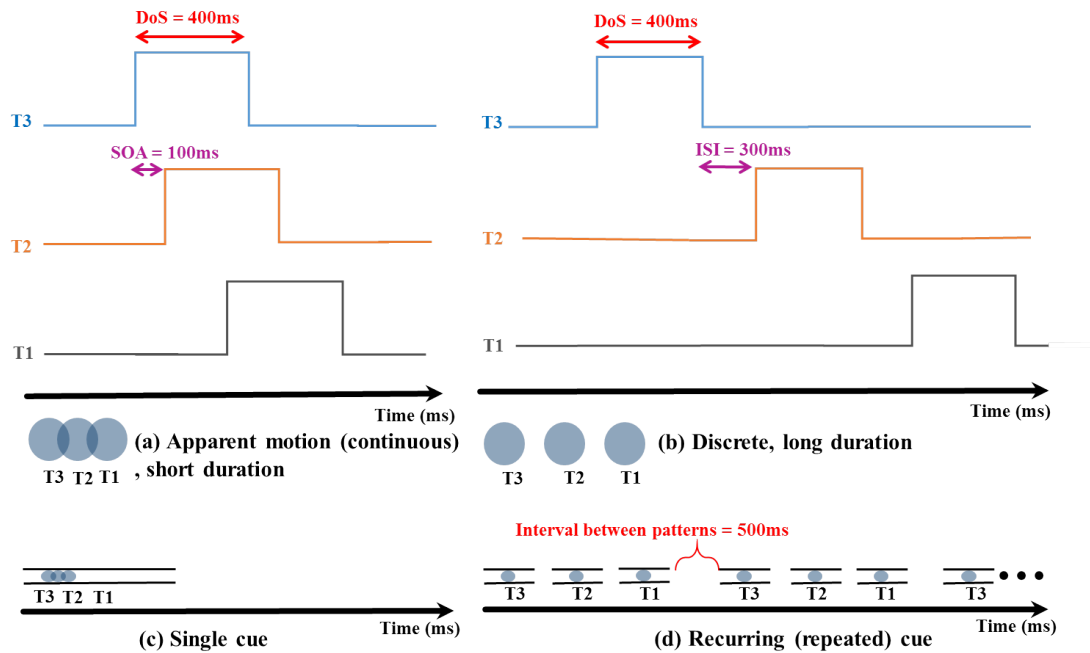


Fig. 5.2 Schematic representation of the tactile language employed in this study. (a) Continuous presentation. (b) Discrete presentation. (c) Single cue. (d) Recurring cue.

In the *discrete* presentation mode, the factors are activated sequentially with no stimulus overlap. For the current study, the DoS was set at 400 ms for each factor with an Inter-Stimulus Interval (ISI) of 300 ms between consecutive stimuli in a pattern. This results in a total rendering time of 1800 ms for the turn-left/right commands and 1100 ms for the go-forward command. As expected from the experimental results described in Chapter 3, this mode creates the experience of discrete motion across the forehead for

all three commands. Figure 5.2b shows an example of discrete presentation method for the turn-left command. Tactor stimulation intensity was the same in both presentation modes — 255 Pulse Width Modulation (PWM) intensity at 3 V — which is a level that was shown in Chapter 3 to be easily detectable and well tolerated.

This experiment also used two command types: *single* and *recurring*. In *single* conditions, the tactile command is presented to the user’s forehead just once when there is a change in the command. For *recurring* conditions, the tactile command is presented repeatedly with an interval between patterns of 500 ms until a new command is received. Figure 5.2c and Figure 5.2d show schematics of these two types of command, respectively.

I hypothesized that the *continuous* commands would be more effective than *discrete* at communicating direction information since apparent motion can provide a strongly intuitive direction signal (see literature reviewed in Section 2.6.2). I also anticipated that the *recurring* commands would lead to better navigation performance than *single* commands since it avoids the need for the user to remember the current navigation command.

User experience was evaluated using Likert-type scales [186] (see Section 5.2.3 below). I did not predict a preference for either *continuous* or *discrete* commands, but I thought it was possible that users might find the *recurring* commands more distracting or irritating than the *single* commands.

5.2 Methods

5.2.1 Participants

Eighteen naive participants including 9 women and 9 men with average age of 24 voluntarily participated in the experiment with no previous experience of navigation using a haptic aid. All participants were university students or staff. The study was approved by the University of Sheffield Ethics Committee. Informed consent form was obtained from all the participants (see Appendix A.3), and they were informed of the option of withdrawing from the experiment at any time. None of the participants reported any known abnormalities with haptic perception.

5.2.2 Apparatus and materials

Mark-II Tactile Helmet

The Mark-II Tactile Helmet (shown in Figure 4.3b and previously described in Chapter 4) was employed as an apparatus in this experiment. The helmet can use its ultrasound sensors to detect distances to nearby surfaces that can be displayed to the user through its vibrotactile display. However, for this study, the direct generation of tactor commands was disabled and signals were substituted based on information from a motion capture system that is explained in the next section.

Tracking system

In order to track the user's position and orientation, a Vicon motion capture system was employed as a precise optical marker tracking system that offers millimeter resolution of 3D spatial displacements.

This consisted of 10 Vicon MX T-Series (T160) cameras, each of which was capable of recording up to 120 Hz with images of 16 megapixel resolution. As shown in Figure 5.3, the cameras are connected to a controlling hardware module which is connected to a host PC through a Gigabyte Ethernet interface. The Vicon Tracker software on the host PC enables the experimenter to view and track global position values and the global rotation values of the object within the capture room. Furthermore, the Vicon DataStream created by the Vicon Tracker software streams in real time to a third-party software such as MATLAB on a control PC. This means that tactile commands can be generated based on information about the position and orientation of the user and sent wirelessly to the Mark-II Tactile Helmet to help the user navigate within the capture room.

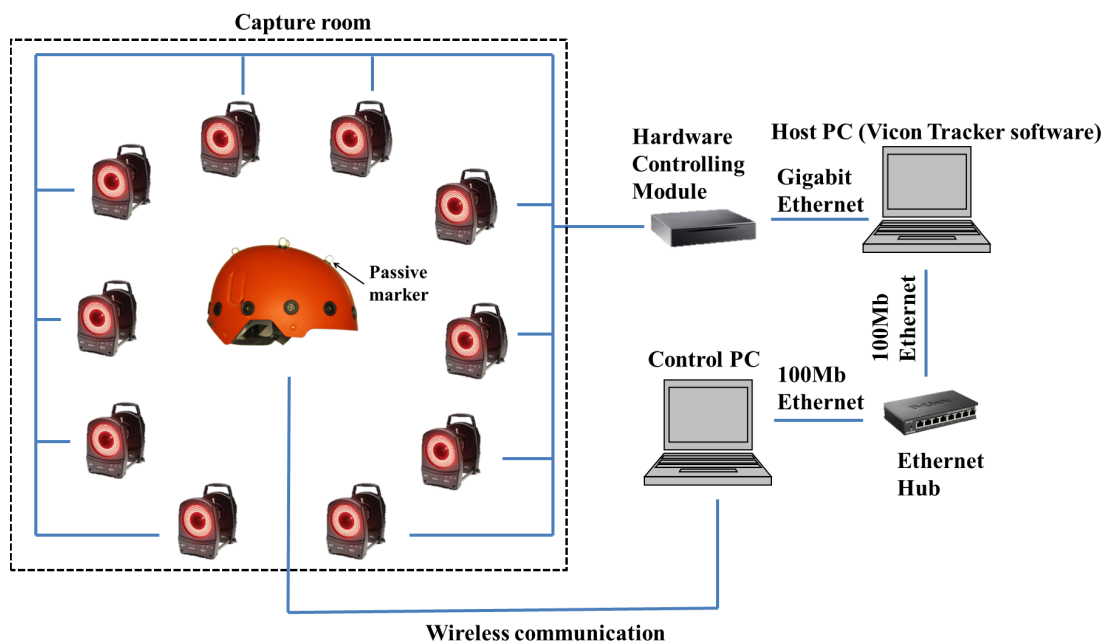


Fig. 5.3 Basic Vicon system structure.

The Mark-II Tactile Helmet, whose motion is to be captured by the cameras, has five reflective passive markers attached to its surface (shown in Figure 5.3). Figure 5.4 shows the 3D perspective of the capture room from the Tracker software and a screen shot of the 3D perspective of the Mark-II Tactile helmet as an object in the Tracker software.

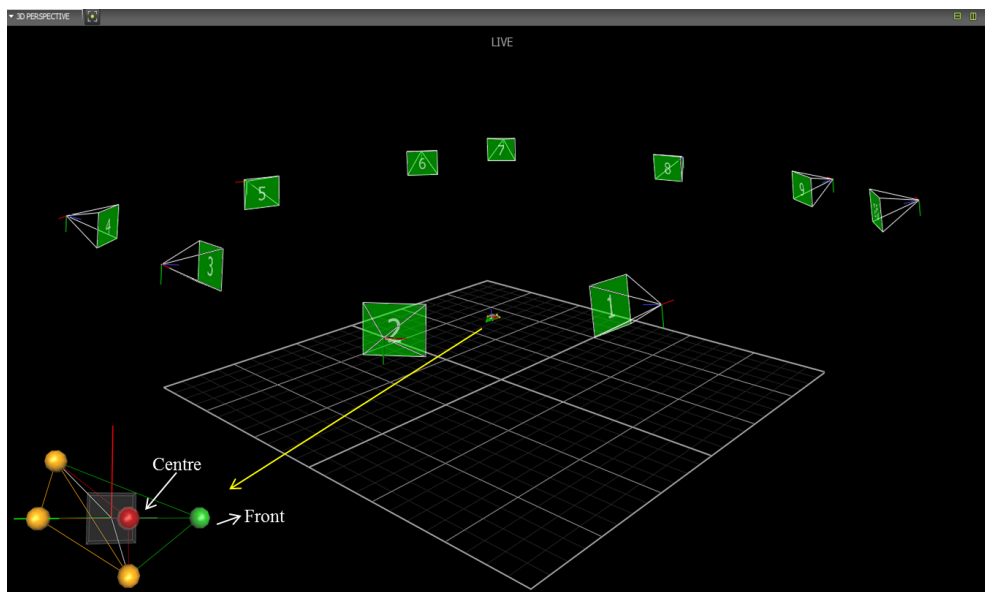


Fig. 5.4 3D perspective of the capture room from the perspective of the Vicon Tracker software [187] and representation of the Mark-II Tactile Helmet as an object within the capture room (bottom left). Ten cameras (green boxes) cover the experimental environment with the size of $3 \times 5 \text{ m}^2$.

Experimental set-up

To create an environment in which to explore a tactile language relevant to such settings, virtual walls were used to simulate the challenge faced by a firefighter seeking to follow walls within a building. Users navigated in a space of $3 \times 5 \text{ m}^2$ relative to three different virtual walls on either their left or right-hand side as illustrated in Figure 5.5. The experiment was performed in a motion capture

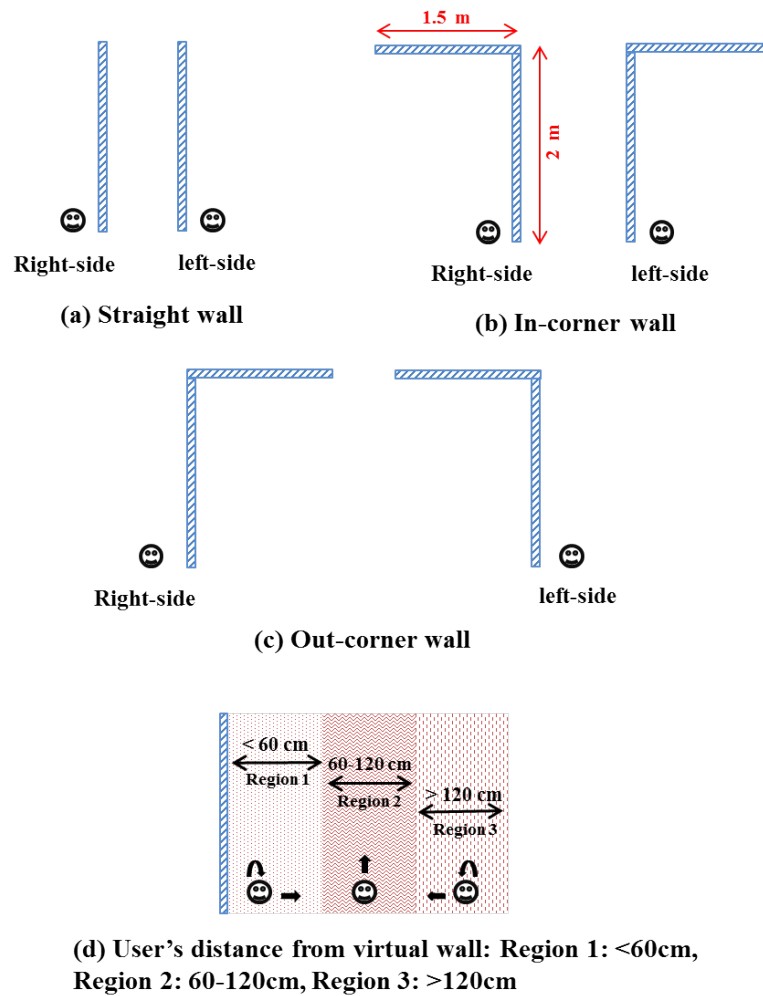


Fig. 5.5 Schematic of the virtual walls and the user in the right and left side of them.

room at the Sheffield Robotics laboratory in the UK. A picture of this experimental set-up is shown in Figure 5.6.

5.2.3 Procedure

Design

A within-subjects repeated measure design was employed in this study. All four possible combinations of the two presentation modes and command types were tested, giving the following four condi-



Fig. 5.6 Experimental environment: $3 \times 5 \text{ m}^2$ free space. A volunteer is walking along a virtual wall in the capture room.

tions: Recurring Continuous (RC), Recurring Discrete (RD), Single Continuous (SC), and Single Discrete (SD).

General procedure

At the beginning of the experiment, each participant was invited into the motion capture room and asked to put on the Mark-II Tactile Helmet. Participants were told that they would be using vibrotactile commands, relayed through the helmet, to follow a path at a fixed distance relative to a virtual wall. It was explained that the vibrotactile commands would help them to stay on the course either by turning to the left or right or by maintaining a forward path. The participants were instructed to follow the commands as closely as possible. A short training session was then provided to familiarize the participants with the tactile language, and with the experimental set-up. At this stage, each of the vibrotactile commands was presented sequentially and the experimenter explained the required response to each command. Finally, the participants were asked to keep their heads oriented in the direction of travel

while walking and to avoid making unnecessary sideways head movements.

Before the experiment, the participants performed five practice trials. During the experiment, they were asked to wear headphones playing white noise to mask the sound created by the tactors. In each trial, the participant started from a fixed position in the motion capture room and navigated with respect to a virtual wall either to the left or right hand side. Since the walls were virtual, they were permitted to move with their eyes open. Participants were allowed to rest after each trial and started the next trial whenever they were ready.

In total, each participant performed 72 trials ($3 \times$ different virtual walls $\times 2$ for left and right-hand wall-following $\times 4$ types of haptic command $\times 3$ repeats) in a pseudo-random order.

After completing all trials, participants were given a questionnaire consisting of fifteen Likert-type scales [186] (see Appendix C.1), where for each question then provided a rating of between 1 ('strongly disagree') and 7 ('strongly agree'). As shown in Table 5.1, responses assessed the extent to which participants considered the helmet to be comfortable and easy to use and vibration motors to be irritating, and, for each of the four conditions whether the commands were considered to be (i) easy to distinguish, (ii) effective for navigation along the virtual wall, and (iii) provided a comfortable and tolerable experience. Finally, participants were also asked to choose their preferred tactile language. The maximum duration of the experiment was approximately one hour.

Table 5.1 User's experience evaluation for 18 participants.

Questions	Median	SD
1. The helmet was comfortable.	5	1.1
2. It was easy to move while wearing the helmet.	6	1
3. The vibration motors were noisy and irritating.	4	0.9
4. RC command was easy to distinguish.	6	0.7
5. RD command was easy to distinguish.	5	0.9
6. SC command was easy to distinguish.	5	1.2
7. SD command was easy to distinguish.	5	1.3
8. RC command was effective for navigation.	6	0.5
9. RD command was effective for navigation.	5	1
10. SC command was effective for navigation.	5	1.1
11. SD command was effective for navigation.	5	1.1
12. RC command was comfortable.	5	1.2
13. RD command was comfortable.	5	0.9
14. SC command was comfortable.	4	1.1
15. SD command was comfortable.	4	1.2

Procedure within a trial

Throughout each trial, the user's position and orientation were obtained from the motion capture system and mapped into one of three following regions relative to the virtual wall (see Figure 5.5d) in order to calculate the haptic commands that were relayed to the helmet. This mapping was modelled based on robot wall-following navigation as summarized in Section 2.8.

- **Region 1:** less than 60 cm. In this region the user was too close to the wall and needed to turn away from it. In this case, the user's head orientation was checked and then the turn-left/right command activated to encourage the user to rotate around his/herself (left/right) until the go-forward command was received. By following these instructions the user should enter region 2.

- **Region 2:** between 60 and 120 cm. In this region the user was within a ‘good’ range of values, and could go straight. In this case, the go-forward command was activated if the user’s orientation value was within the range of a predetermined threshold, otherwise the turn-left/right command was activated to rotate the user toward that threshold.
- **Region 3:** greater than 120 cm. In this region the user was too far from the wall and needed to turn towards it. As in region 1, the turn-left/right command was activated and the user encouraged to rotate around his/herself until the go-forward command was received. By following these instructions the user should enter region 2.

As an illustration, Figure 5.7 shows tracked positions (black dashed line) and orientation (red arrow) of one participant while walking along an out-corner wall. This experiment started from region 2 (between 60 and 120 cm) and the user therefore initially received the go-forward command. When the user passed the vertical wall, the turn left command was activated and the user rotated until the go-forward command was triggered. By following this command, the user reached the area of the horizontal wall. Here, the user was too close to the wall and needed to turn away from it, so the turn-right command was activated. The user continued to navigate following the different commands until the finish point was reached where all of the vibration motors were activated simultaneously to indicate the end of the experiment.

- **Reaction time(s)** defined as elapsed time between finishing the display of the vibrotactile command and the moment that participant has turned left /right for turning commands and has walked toward forward direction in go-forward command.
- **Smoothness of the user's trajectory(cm)** defined as the Mean Absolute Deviation (MAD) of the path followed by the user compared to an ideal path following parallel to the virtual walls at a fixed distance.
- **Average walking speed(ms^{-1})** defined as the total distance traveled along the virtual walls (m) divided by the elapsed time (s).

5.3 Results

An alpha value of 0.05 was chosen as the threshold for statistical significance, all reported p-values are two-tailed. A Shapiro-Wilk test showed that data were normally distributed. A two-way repeated measure Multivariate Analysis of Variance (MANOVA) was employed to test the objective measures. Box's Test indicated that assumption of equality of covariance matrices was met ($p = 0.15$). Levene's test showed that the assumption of equality of error variance was met ($p > .05$, for all the dependent variables). Measures of command recognition accuracy, reaction time to the tactile command, smoothness of the user trajectory, and walking speed are shown in Figure 5.8 and 5.9 for each of the four conditions, respectively. Next, results for each of these quantitative measures are summarized in turn followed by the subjective reports (Likert-type scales).

Two-way repeated measure MANOVA showed no significant interaction effect between command type and command presentation

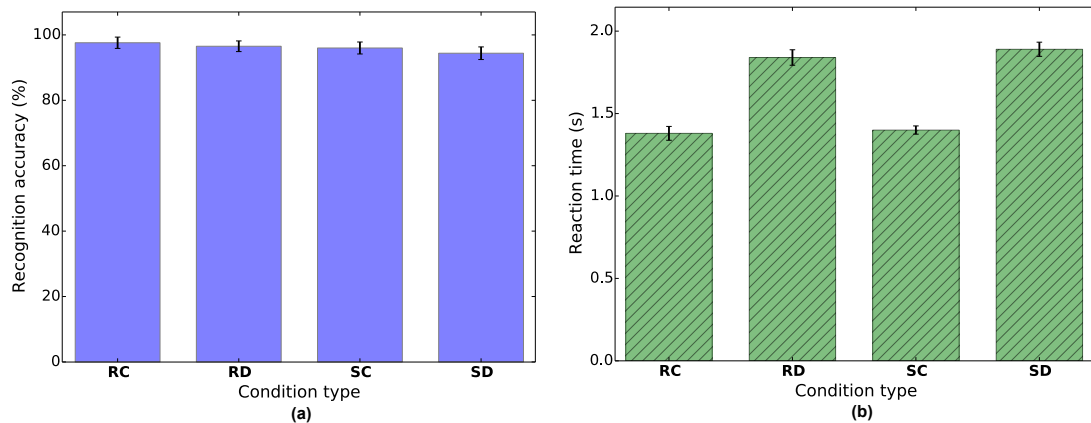


Fig. 5.8 (a) Recognition accuracy (%) for each condition, (b) Reaction time (s) for each condition, $n=1296$ samples. Error bars indicate standard error.

on the combined dependent variables, $F(4, 14) = 1.622$, $p = 0.224$; Wilks' $\Lambda = 0.683$.

Overall recognition accuracy rate from a total of 1296 trials was 96% with a standard deviation of 8%. The MANOVA revealed no significant main effect on recognition accuracy of command presentation mode ($F(1, 17) = 1.735$, $p = 0.205$) or command type ($F(1, 17) = 3.476$, $p = 0.08$).

Mean reaction time from a total of 1296 trials was 1.63 s (standard deviation: 0.31 s). The MANOVA showed a significant main effect on reaction time for command presentation mode ($F(1, 17) = 122.56$, $p < 0.001$) but no main effect for command type ($F(1, 17) = 0.812$, $p = 0.325$).

As can be seen in Figure 5.8b, reaction times were fastest when commands were presented continuously compared to when they were presented discretely. Additionally, it was found that reaction time differed significantly between turn-left, turn-right, and go-forward commands ($F(1.949, 33.140) = 159.957$, $p < 0.001$). Post hoc test using the Bonferroni correction revealed that there

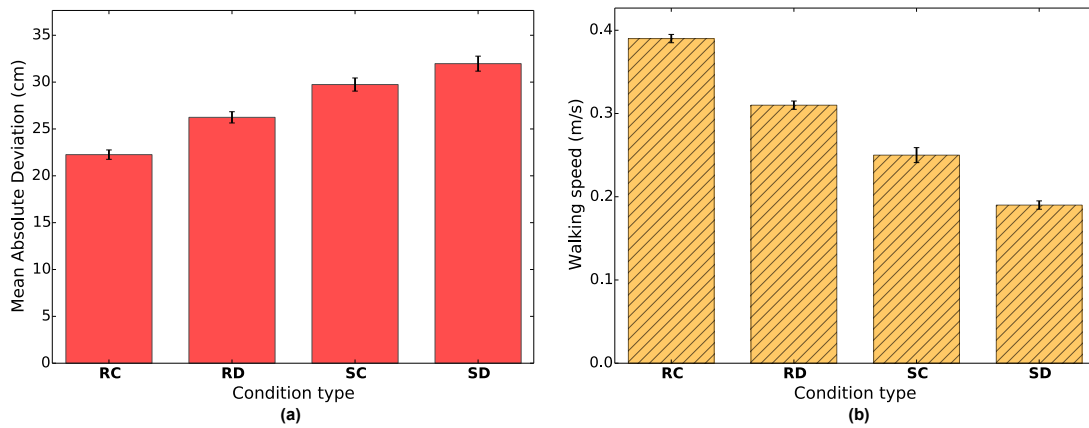


Fig. 5.9 (a) Smoothness of users' trajectory measured by Mean Absolute Deviation (MAD), (b) Walking speed for each condition, $n=1296$ samples. Error bars indicate standard error.

was a significant difference in reaction time between the go-forward and turn-left commands ($p = 0.0005$), and between the go-forward and turn-right commands ($p = 0.0005$) but no significant differences found between turn-left and turn-right commands ($p = 0.217$).

The effectiveness of the commands was evaluated according to the smoothness of the user's trajectory as measured by the Mean Absolute Deviation (MAD) from the ideal path. A two-way repeated measure MANOVA found a significant main effect on MAD score for both command presentation mode ($F(1, 17) = 22.362$, $p < 0.001$) and for command type ($F(1, 17) = 80.012$, $p < 0.001$). Figure 5.9a shows the MAD for each condition, indicating that MAD increases from RC to SD command, that is, participants navigated with the lowest route deviation using RC (Recurring Continuous) command. This same pattern is evident in Figure 5.10 that shows the trajectory of the users along the out-corner virtual walls for each of the four conditions.

Average walking speed was also calculated for each condition. A two-way repeated measures MANOVA found a significant main ef-

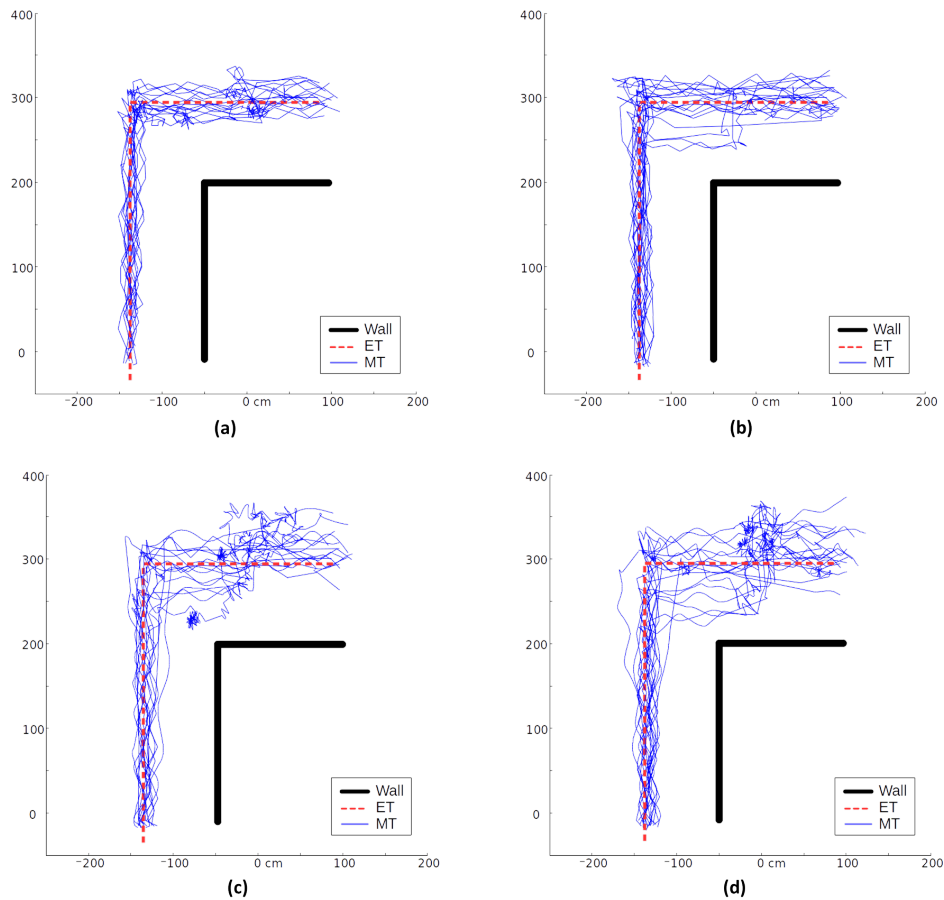


Fig. 5.10 Users' trajectory with: (a) Recurring Continuous (RC), (b) Recurring Discrete (RD), (c) Single Continuous (SC), and (d) Single Discrete (SD) command. Blue lines show users' Motion Trajectory (MT) and red dashed lines show users' Expected Trajectory (ET). In each command, the presented trajectories were chosen randomly from each of 18 participants.

fect on walking speed for command presentation mode ($F(1, 17) = 75.177, p < 0.001$) and for command type ($F(1, 17) = 128.402, p < 0.001$). As shown in Figure 5.9b, users had maximum walking speed with the RC command suggesting that participants were more confident in responding to tactile commands in this condition.

In the Likert-scale data, participants reported that helmet was comfortable, that it was easy to move while wearing the helmet, and that the vibration motors were not irritating. A Friedman test revealed that there was a significant difference between the

four conditions (RC, RD, SC and SD) for ease of distinguishability ($\chi^2(3) = 19.075$, $p < 0.001$) and effectiveness for navigation ($\chi^2(3) = 32.813$, $p < 0.001$), while no significant difference was found for comfort ($\chi^2(3) = 6.025$, $p = 0.17$). Post hoc analysis with Wilcoxon signed-rank test was conducted with a Bonferroni correction, resulting in an adjusted significance level ($p = 0.0083$, calculated by utilizing Sidak Correction [181]). As shown in Table 5.2, for ease of distinguishability, there was a significant difference between RC and RD, RC and SC, and between RC and SD, while no significant difference was found between RD and SC, RD and SD, and SC and SD. In terms of effectiveness for navigation, there was a significant difference between RC and RD, RC and SC, and RC and SD, while no significant difference was found between RD and SC, RD and SD, and SC and SD.

Table 5.2 Post hoc test for condition types comparison in terms of being easy to distinguish and effective for navigation.

Condition type comparison	Easy to distinguish	Effective for navigation
RC/RD	$Z = -2.730$, $p = 0.004^*$	$Z = -2.292$, $p = 0.002^*$
RC/SC	$Z = -3.066$, $p = 0.002^*$	$Z = -3.002$, $p = 0.003^*$
RC/SD	$Z = -2.648$, $p = 0.008^*$	$Z = -3.204$, $p = 0.001^*$
RD/SC	$Z = -2.352$, $p = 0.19$	$Z = -1.053$, $p = 0.293$
RD/SD	$Z = -1.509$, $p = 0.131$	$Z = -2.701$, $p = 0.091$
SC/SD	$Z = -1.250$, $p = 0.12$	$Z = -1.992$, $p = 0.176$

In sum, participants reported that Recurring Continuous (RC) commands were the easiest to distinguish, the most effective for navigation and the most preferred command. This agrees with the quantitative measures, which showed that RC command led to faster and more accurate navigation compared to the other commands.

5.4 Summary

This chapter has presented a ‘tactile language’ for communicating navigation commands to the Mark-II Tactile Helmet as a head-mounted vibrotactile sensory augmentation prototype. An experiment was performed in a structured environment in which the user navigated along a virtual wall whilst the position and orientation of the user’s head was tracked in real time by a motion capture system. Navigation commands in the form of vibrotactile guidance signals were presented according to the user’s distance from the virtual wall and their head orientation. Four possible combinations of two command presentation modes (*continuous, discrete*) and two command types (*recurring, single*) were tested. The effectiveness of these navigation commands was evaluated according to the users’ walking speed, the smoothness of their trajectory parallel to the virtual wall, and commands recognition accuracy and reaction time.

Overall recognition accuracy for all commands was high, and did not distinguish between different modes and types of tactile command. However, consistent with the hypothesis, it was found that tactile commands that exploit continuous signals creating an apparent motion effect were more effective in indicating desired movement direction than discrete patterns of stimulation. This was shown in the measured reaction times to command signals, in the smoothness of the user trajectory and in the walking speed. It was also found that navigation was more effective when commands were presented repeatedly, rather than only when a change of movement direction was needed. Furthermore, the helmet was well tolerated by users, and interestingly, users did not specifically report the re-

curing stimuli as being particularly irritating or burdensome. In sum, Recurring Continuous (RC) commands allowed users to navigate with lowest route deviation and highest walking speed and participants preferred it over other commands.

Chapter 6

Evaluation of Navigation Performance in a Physical Environment

Chapter 5 has shown that a haptic interface can be used as a sensory augmentation device to aid navigation in low visibility environments. For this purpose, sound could provide an alternative to touch through acoustic waveforms or synthetic speech [188]. In order to enable the comparative assessment of the tactile language developed in Chapter 5, audio guidance as a baseline is employed in this chapter in an experiment using the Mark-II Tactile Helmet.

This chapter starts by describing some background comparative studies of haptic and audio guidance in a number of augmented navigation tasks in Section 6.1. Following that, Section 6.2 introduces the haptic and audio guidance system employed in the current study. The experimental method including participants, apparatus and material, and the applied procedure is explained in Section 6.3. Section 6.3.4 describes a Multi-Layer Perceptron (MLP) neural network as a classification algorithm that is applied to classify ultrasound data to generate the three navigation commands used in the haptic and audio guidance. The data collection procedure for the MLP training (6.3.4.1), the proposed MLP structure and clas-

sification results (6.3.4.2) are then presented. The results of the audio vs haptic comparison are described in Section 6.4. Finally, Section 6.5 presents the summary of this chapter.

6.1 Haptic and audio guidance

Vibrotactile displays as a type of non-visual interfaces can provide useful navigational information in the form of haptic feedback when other communication channels such as vision and hearing are overloaded or limited. Auditory guidance in the form of non-verbal acoustic sound [189–191] or synthetic speech [188] is another means for providing augmented navigation information for people with visual impairments or for rescue workers in low visibility environments.

The effectiveness of haptic and audio guidance has been compared in a number of augmented navigation tasks with mixed results. For example, Flores et al. [188] compared audio and haptic interfaces for way-finding by blind pedestrians and it was found that haptic guidance resulted in closer path-following compared to audio feedback. Marston et al. [192] also evaluated nonvisual route-following with guidance from audio and haptic display. Their results showed that haptic feedback produced slightly faster path completion time and shorter distance, however, these differences between the audio and haptic modalities were not significant. Hara et al. [193] have investigated multimodal feedback strategies such as haptic, audio and combined feedback for navigation. Whilst there were no significant differences between modalities in navigation performance, participants reported that the audio guidance was less comfortable than others. Kaul et al. [153] evaluated audio and

haptic guidance in a 3D virtual object acquisition task using HapticHead (a cap consisting of vibration motors) as a head-mounted display. User studies indicated that haptic feedback was faster and more precise than auditory feedback for virtual object finding in 3D space around the user. Finally, in [194] haptic and audio modalities were compared in terms of cognitive workload, in a short-range navigation task, finding that workload was lower in haptic feedback compared to audio for blind participants.

6.2 Experimental design

As already explained in Chapter 5, firefighters navigate in low visibility environments using reference points such as walls and doors to stay oriented and make a mental model of the environment [9]. The current experiment employed a wall-following approach inspired by mobile robots to assist this navigation behavior which, as in Chapter 5, combined steering-in, steering-out and moving forward commands [185]. Specifically, the three navigation commands (i.e. turn-left, turn-right, and go-forward) were used to navigate users along a wall by inducing a rotation around the user in turn-left/right commands and forward movement in go-forward command. These three commands were presented in the form of either haptic or audio guidance signals.

Haptic guidance in the form of vibrotactile patterns was used to present the commands to the user through the employed vibrotactile display in the Mark-II Tactile Helmet. The vibrotactile patterns for presenting these three navigation commands are presented in Figure 5.1. The utility and user experience of these commands was already investigated in Chapter 5 using the combination of

two command presentation modes — *continuous* and *discrete* and two command types — *recurring* and *single* as tactile languages. It was found that ‘Recurring Continuous (RC)’ command led to better performance than other commands and also users preferred it over other commands. A schematic representation of the *continuous* command presentation mode and the *recurring* command type for the turn-left command is presented in Figure 5.2. The RC command was utilized for haptic guidance in this study.

The audio guidance also used three commands to navigate the user along the wall, delivered using synthetic speech and the spoken commands: ‘go-forward’, ‘turn-right’ and ‘turn-left’. The duration of each synthetic speech segment was equal to its equivalent haptic command and the interval between patterns was 500 ms like the *recurring* command type in the haptic commands.

6.3 Methods

6.3.1 Participants

Ten participants consisting of 4 men and 6 women with average age of 25 participated in this experiment. All participants were university students or staff. The experiment was approved by the University of Sheffield Ethics Committee, and participants signed the informed consent form before starting the experiment (see Appendix A.4). They did not report any tactile sensory disorder. Participation in this experiment was voluntarily and participants were informed that they were allowed to withdraw from the experiment at anytime.

6.3.2 Apparatus and material

This experiment employed the Mark-II Tactile Helmet (Figure 4.3b) and Vicon motion capture system (Section 5.2.2) to navigate a user along the wall. Unlike the experiment described in Chapter 5, here ultrasound sensors were utilized to measure the user's distance to the walls. However, the Vicon motion capture system was used to track the user's position and orientation as before. In order to produce synthetic speech, a sound card as shown in Figure 4.4d was connected to the microcontroller board inside the helmet.

6.3.3 Procedure

A path consisting of several cardboard walls was created in the experiment room as shown in Figure 6.1a. The motion capture cameras were placed next to the walls to track the participant's position and orientation during navigation. At the beginning of the experiment, each participant was invited into the experiment room and asked to wear the Mark-II Tactile Helmet and a blindfold. They were not allowed to see the experiment set-up and cardboard walls

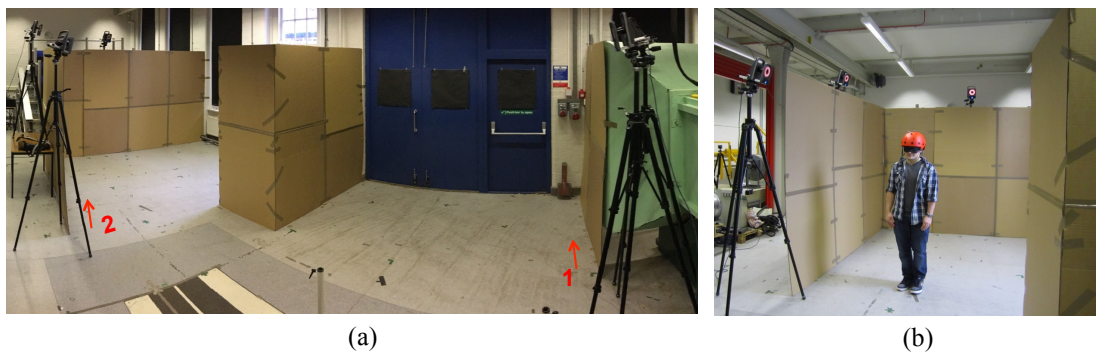


Fig. 6.1 (a) Overhead view of the experimental set-up consisting of cardboard walls and motion capture cameras, position 1 and 2 show the trial starting points. The length of the walls from the start point to the end is 20 m. (b) A participant is navigating along the wall.

before starting the experiment. Participants were told that haptic/audio guidance would assist them to follow the walls either by turning to the left or right or by maintaining a forward path. Participants were also asked to wear headphones playing white noise to mask any sounds from tactors during navigation with haptic guidance. Furthermore, participants were asked to keep their head oriented in the direction of travel and to avoid making unnecessary sideways head movements. A short training session was provided to familiarize participants with the haptic and audio guidance commands, and with the experimental set-up. Once the participant felt comfortable, the trial phase was started. Two different starting points were used (1 and 2 as shown in Figure 6.1a) in order to discourage participants from memorizing the paths. Blindfolded participants as illustrated in Figure 6.1b started the first trial from position 1 and the second trial from position 2 and repeated this sequence for the third and fourth trial. When each trial finished, participants were stopped by the experimenter. Participants were allowed to rest after each trial and started the next trial whenever they were ready. The maximum duration of the experiment was approximately 20 minutes.

Each participant performed 4 trials including 2 guidance types (haptic and audio), each for two times in a pseudo-random order. Task completion time, travel distance and route deviation were measured for each trial. After finishing the experiment, participants were asked to complete a paper and pencil version of the NASA Task Load Index (TLX) [195] (see Appendix C.2) to measure subjective workload. This scale consists of six dimensions covering mental demand, physical demand, temporal demand, performance,

effort and frustration with 21 gradations. Additionally, participants were asked to rate their preference for completing the task with either audio or haptic guidance.

6.3.4 A multi-layer perceptron classifier for computing navigation commands

As previously described in Section 2.8, different controllers have been used for solving the problem of robot wall-following. Figure 2.19 shows a neural network controller as one of the common techniques used to map distance sensor data into a set of discrete robot actions [158]. This study takes a similar approach by using a Multi-Layer Perceptron (MLP) algorithm which classifies ultrasound data into three navigation commands (turn-left, turn-right, and go-forward), then provide haptic or audio guidance to navigate a user along a wall. The next sections present data collection procedure, structure of the employed MLP algorithm and classification results, respectively.

6.3.4.1 Data collection procedure

In order to collect data for training the MLP algorithm, the experimenter wore the Mark-II Tactile Helmet and kept a laptop (running code that saved the ultrasound data in every scan) in her hands and followed the cardboard walls slowly in the experiment room without wearing a blindfold. The arrangement of the cardboard walls for data collection is shown in Figure 6.2. The dataset was the collection of ultrasound readings generated when the experimenter followed the walls in both clockwise and anti-clockwise directions, for 8 rounds each. The data collection was performed at a sample

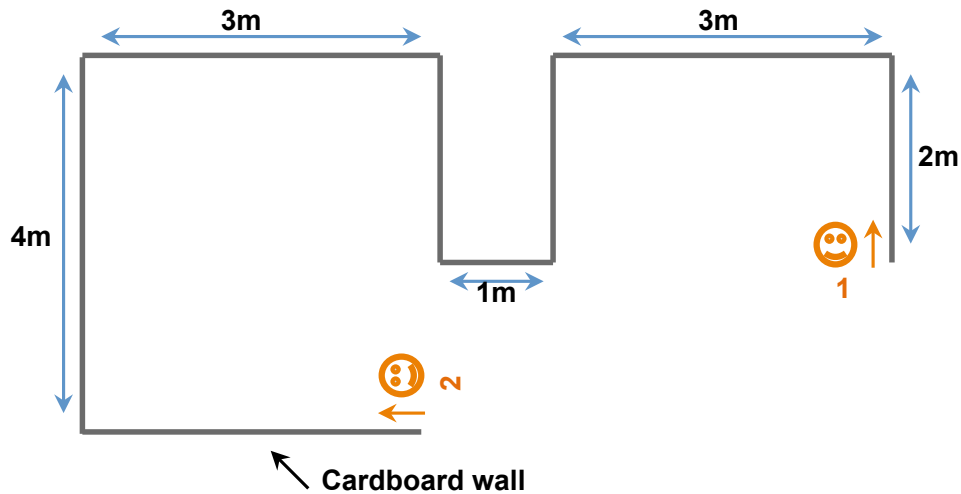


Fig. 6.2 Sketch of the data collection environment. Experimenter's start position for collecting data in anti-clockwise (1) and clockwise (2) direction is presented.

rate (for all 12 ultrasound sensors) of 0.6 seconds and generated a database with 4051 samples. Data were labeled during data collection by pressing the arrow key on the laptop keyboard when turning left/right or going forward was appropriate (pressing left/right arrow key button for turn-left/right and up arrow key button for go-forward). Ultrasound data in every scan were saved with a related label in a file. Three classes were considered in all the files which contained go-forward, turn-left and turn-right. Then, these classes were used to train the MLP classifier as presented in next section.

6.3.4.2 Proposed MLP algorithm

The proposed MLP consists of three layers: input layer, a hidden layer, and output layer as illustrated in Figure 6.3. The input layer consists of 12 neurons which represent distance measurements from 12 ultrasound sensors. In order to find out the optimum number of hidden neurons that enable a suitable class separation, a

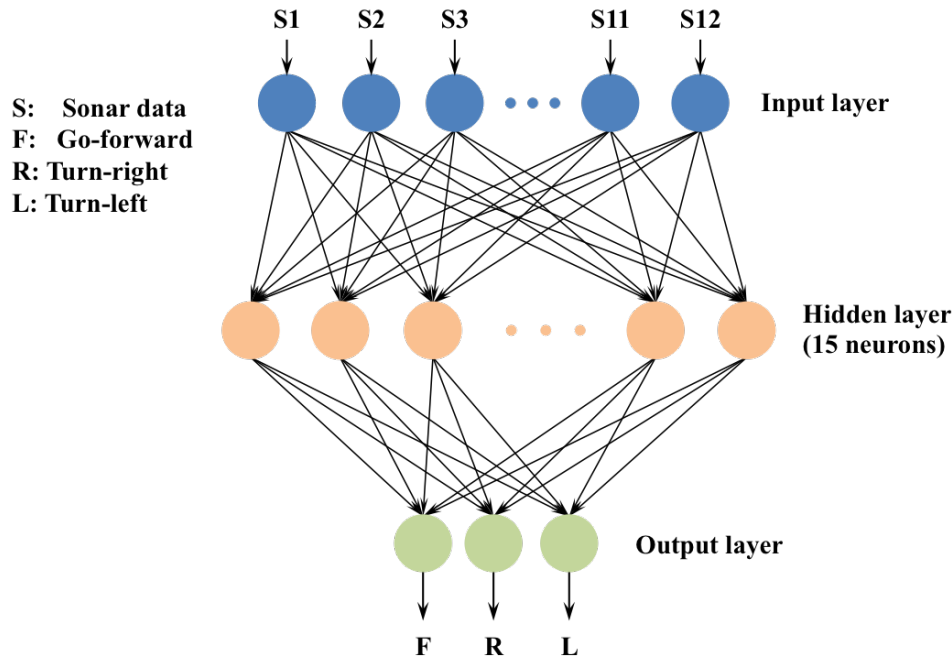


Fig. 6.3 The structure of the proposed MLP. It consists of 12 input neurons, 15 hidden neurons and 3 outputs.

preliminary experiment was performed. The training process was completed for MLPs with different numbers of hidden neurons (1 : 30) by achieving the minimum performance for the validation set. Due to random initialization of neural networks, for each number of hidden neurons, the training process was repeated 20 times to determine the accuracy as a function of hidden neurons by averaging the results. Figure 6.4 illustrates that minimum error was achieved with 15 neurons in the hidden layer. Furthermore, alternative MLPs were trained with different transfer functions in the hidden layer such as Hyperbolic tangent sigmoid (Tansig), Pureline and Log-sigmoid (Logsig). Table 6.1 shows that minimal error was achieved using the Tansig transfer function in the hidden layer with 15 hidden neurons. The output layer has three neurons corresponding to the three navigation commands: go-forward, turn-left, and

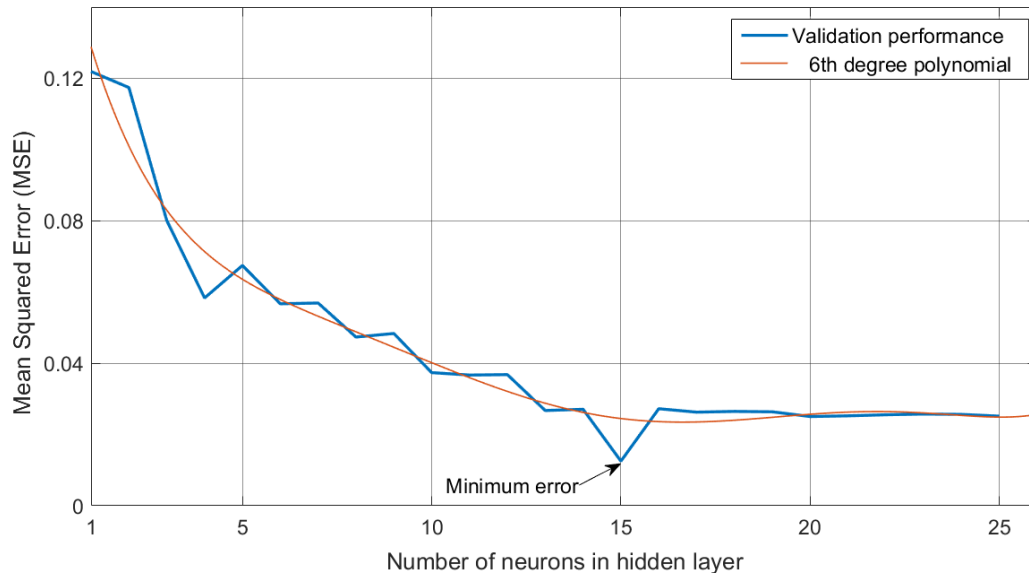


Fig. 6.4 Mean Squared Error (MSE) as a function of hidden neurons.

turn-right. The Log-sigmoid was considered as the transfer function for the output layer.

Table 6.1 Performance of the trained MLP with different transfer functions. Std and perf stand for standard deviation and performance, respectively.

Transfer function	Best perf	Avg perf	Std perf
Tansig	0.0744	0.0879	0.0112
Pureline	0.1361	0.1415	0.0164
Logsig	0.5483	0.5542	0.0185

Evaluation was performed using 10 times 10-Folds cross-validation. Back propagation algorithm with adaptive learning rate and momentum [196] was utilized as a learning technique for the MLP algorithm. Figure 6.5 shows network training, testing and validation performance during 66 learning epochs.

Analyses of data to evaluate statistical differences by navigation commands have been conducted in terms of precision and recall.

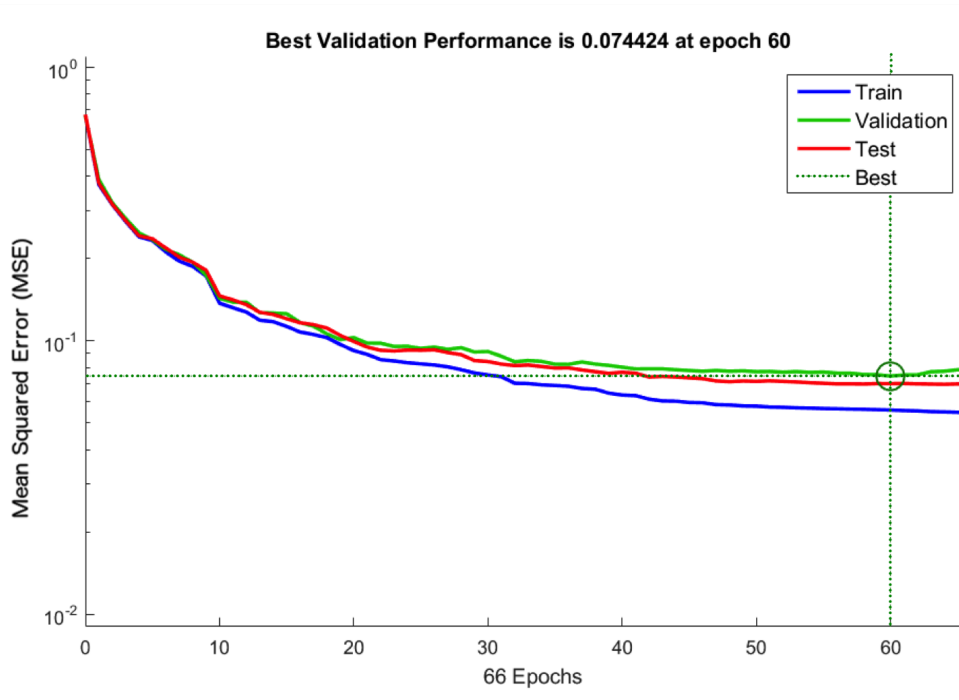


Fig. 6.5 The MLP best validation performance.

Precision and recall of the MLP algorithm for recognizing the commands (c) such as go-forward (F), turn-left (L) and turn-right (R) are computed as:

$$Precision_c = TP_c / (TP_c + FP_c) \quad \forall c \in [F, L, R] \quad (6.1)$$

$$Recall_c = TP_c / (TP_c + FN_c) \quad \forall c \in [F, L, R] \quad (6.2)$$

where TP_c (True Positive) corresponds to successfully classify the commands (i.e. go-forward, turn-left and turn-right), FP_c (False Positive) corresponds to erroneously classify the commands, and FN_c (False Negative) corresponds to the missed commands.

The overall accuracy of the MLP is 94.9%. Table 6.2 presents the results of precision and recall of the MLP algorithm for recognizing the go-forward and turning commands. Although participants were

Table 6.2 Precision and recall of the MLP algorithm for recognizing the go-forward, turn-left and turn-right commands.

	Go-forward	Turn-left	Turn-right
Precision (%)	96.6	90.6	92.1
Recall (%)	95.9	90.6	95.3

asked to keep their heads in the direction of motion, the tolerance of the MLP is 15 degrees relative to the motion capture origin if the user does not keep his head in the direction of motion.

During wall-following by participants, new ultrasound data was obtained from the helmet and was then classified by the trained MLP in order to obtain navigation commands for either haptic or audio guidance.

6.4 Results

An alpha value of 0.05 was chosen as the threshold for statistical significance, all reported p-values are two-tailed. Shapiro-Wilk test showed that data are normally distributed ($p = 0.523$). Task completion time (minute), travel distance (meter) and route deviation (meter) for haptic and audio guidance were measured as objective measures. Task completion time was recorded as the time that a participant took to navigate along the wall from the start point to the end point. As shown in Figure 6.6a, participants navigated faster with haptic guidance, however, paired t-test showed no significant difference in task completion time between the haptic and audio guidance system ($t(9) = -1.287$, $p = 0.33$). Travel distance, the distance that the participants walked along the wall, was measured using the motion capture system described in Section (5.2.2).

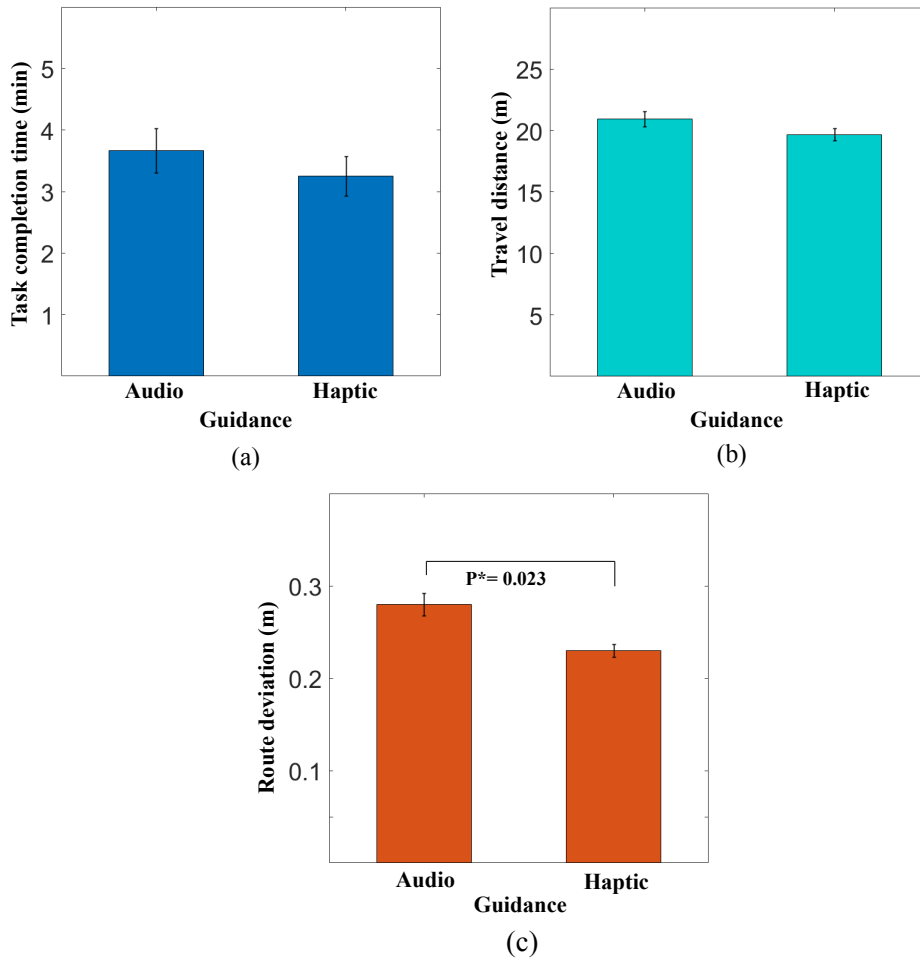


Fig. 6.6 Objective measures. (a) Task completion time, (b) Travel distance, (c) Route deviation, $n=40$ samples. The unit of task completion time is in the minute and unit of travel distance and route deviation is in the meter. Error bars show standard error.

As shown in Figure 6.6b, the participants travelled a shorter distance with the haptic guidance, however, a paired t-test revealed no significant difference in travel distance between the haptic and audio guidance ($t(9) = 2.024$, $p = 0.074$). Finally, the participants also had lower route deviation, relative to the walls, when navigating with the haptic guidance (Figure 6.6c). Here, a paired t-test showed that this difference was significant ($t(9) = 2.736$, $p = 0.023$).

After completing the experiment, subjective workload for each guidance system was measured by asking the participants to answer the NASA TLX questionnaire. As shown in Figure 6.7, physical and temporal demand did not vary much between two guidance systems which showed both of them were able to navigate the participants. However, the participants rated that mental demand and effort were higher when navigating with audio guidance. It seems plausible that the higher mental workload and effort were because the participants had to concentrate more to process the audio guidance to navigate successfully along the wall. The participants also rated better performance and lower frustration with the haptic guidance, which showed the capability of the haptic guidance for navigation along the wall as already shown by the objective measures. Finally, the participants were asked to rate their preference for navigation

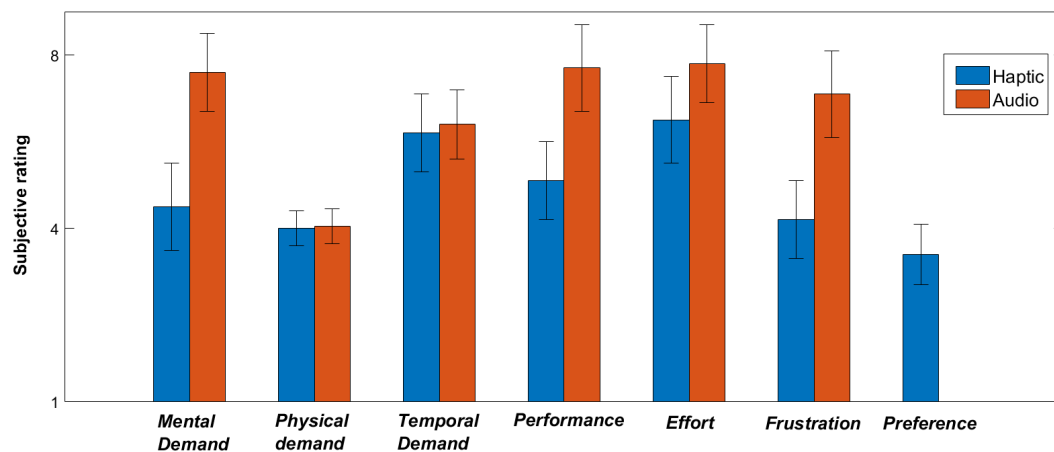


Fig. 6.7 Questionnaire feedback. The first six bar plots represent the NASA TLX score for the audio and haptic guidance. The rating scale is 1-21, where 1 represents no mental, physical and temporal demand, best performance, no effort required to complete the task and, no frustration. The last bar plot shows the participants' preference for navigation with the haptic guidance. The error bars indicate standard error.

with the haptic and audio guidance. This preference was rated on a scale of 1-21 to keep continuity with the NASA TLX, where (1) represents a strong preference for navigation with the haptic feedback and (21) represents a strong preference for navigation with the audio feedback. As illustrated in Figure 6.7, the average preference rate of 3.4 shows that the participants preferred haptic guidance.

6.5 Summary

This chapter has compared the effectiveness of haptic and audio guidance systems for navigation without vision along a wall using the Mark-II Tactile Helmet. The haptic guidance employed ‘Recurring Continuous (RC)’ command that was developed as a tactile language in Chapter 5, while audio guidance used synthetic speech to present navigation commands. In the experiment, participants navigated along a wall relying on either the haptic or audio feedback to guide navigation. The haptic/audio feedback was presented to the participants according to the information measured from the walls using a set of 12 ultrasound sensors placed around the Mark-II Tactile Helmet and a classification algorithm using an MLP neural network. The MLP algorithm classified the ultrasound data into the three navigation commands (go-forward, turn-left, and turn-right) with an overall classification accuracy of 94.9%. Objective measures indicated that the haptic guidance led to significantly lower route deviation. Although the participants also had faster task completion time and lower travel distance with the haptic guidance, no significant difference was found between these two guidance systems. Finally, results from the NASA TLX questionnaire showed that participants reported lower cognitive workload with the hap-

tic guidance although both guidance systems were able to navigate them along the wall. The results of this study show the effectiveness of haptic feedback for guiding navigation without vision.

Chapter 7

Conclusion and Future Work

This chapter summarizes the reported research and draws a conclusion with respect to the research questions laid out in Chapter 1. It also provides an outlook on a number of potential directions for future work.

7.1 Reviewing the scope of the thesis

This research was motivated by the need for augmenting the human sense to create new ways of experiencing and understanding the world within application domains such as firefighters' navigation. The primary aim of this thesis was to develop and investigate a head-mounted vibrotactile interface for sensory augmentation in low visibility environments.

The following steps were identified at the outset as necessary milestones to reach the target:

- Investigate the human perception of tactile signals delivered by a head-mounted vibrotactile display using a series of psychophysical experiments focusing on the vibrotactile absolute threshold, vibrotactile localization, the funneling illusion and the apparent motion illusion.

- Develop a 2nd generation head-mounted sensory augmentation prototype to overcome some of the limitations of the earlier prototype developed by Bertram et al. [6], particularly the low resolution of the tactile display and the size and weight of the on- and off-board electronics.
- Investigate the design space for display of haptic commands as tactile language, specifically focusing on the potential of signals that can be interpreted quickly and intuitively, and in the context of designing haptic navigation aids for firefighters.
- Evaluate the effectiveness of the developed tactile language compared with audio guidance for navigation without vision.

The forehead is a promising location for vibrotactile displays for navigation since a display can easily fit inside the headband of a hat or helmet, signals reach the brain quickly allowing quick responses, and an intuitive mapping can be created between sensed objects (such as obstacles) and stimulation of the head in the direction of the object. Key constraints for head-mounted vibrotactile displays design include the number and location of the tactors and appropriate use of tactile perceptual phenomena such as funneling illusion and apparent motion to improve the low resolution of the tactile display. In order to investigate the human tactile perception as the first objective in this thesis, four psychophysical experiments were performed using a 1-by-7 headband vibrotactile display (see Chapter 3):

- First, vibrotactile absolute threshold on the forehead was measured using the method of limits [11]. Level nine (PWM 98/255)

which is equal to acceleration 0.23 g, was achieved as the vibrotactile absolute threshold on the forehead.

- Second, vibrotactile localization accuracy on the forehead was evaluated. Whereas localization mean error seemed uniform across the forehead, a strong bias towards the forehead midline was found in localizing tactors that were away from the center of the forehead. This would appear to be an important design constraint for head-mounted displays. For instance, if an object is displayed as being to the side of the head by stimulation in that direction, a user of the device could experience the object as being more frontally-aligned than its true location. Unlike Dobrzynski et al. [197], who used a different method to measure localization accuracy and found poor localization at the center of the forehead, this study found the minimum localization mean error for midline tactor (front of the head) in the vibrotactile headband. This result, therefore, goes against the advice of the earlier paper that the center of the forehead is a less optimal location for vibrotactile stimulation.
- The third experiment was designed to evaluate the dependency of funneling illusion on inter-tactor spacing for head-mounted vibrotactile displays. Funneling can be used to increase localization accuracy [68] for a sparse array of actuators, or to communicate change of position [61] or movement [65], [67]. Results indicated that the funneling effect may occur primarily over fairly short distances on the forehead — It was found that only a small number of participants reported an experience of

funneling for inter-tactor distances of 5 cm or greater, whereas funneling was consistently reported (90%) for the smallest distance of 2.5 cm. By comparison, on the surface of the arm a strong experience of funneling has been reported as occurring in the range of 4-8 cm [65]. Here, these results do suggest that funneling could be a more localized effect on the forehead than elsewhere on the body. One possible explanation is that, compared to the arm, the skin of the forehead is stretched relatively tightly across the smooth surface of the skull with relatively little intervening fat/muscle. Furthermore, participants reported experiencing simultaneous stimuli at two locations as consistently closer to each other than their actual distance. The result of vibrotactile localization study whereby single stimulus is experienced as closer to the midline could partly explain this consistent under-estimating of inter-tactor spacing in the funneling study.

- Finally, the last psychophysical experiment was conducted to find the appropriate SOA and inter-tactor spacing which produce apparent motion illusion on the forehead. The highest rate of apparent motion on the forehead was found with an inter-tactor spacing of 5 cm and SOA value of 100 ms. It was shown that SOA values affect the apparent motion perception on the forehead. Similar to [77], it was found that inter-tactor spacing influences the perception of apparent motion although some studies [80, 81] reported that it has no significant effect on the apparent motion perception.

As a result of these experimental findings, inter-tactor spacing on the new helmet design was set at 2.5 cm, and SOA of 100 ms and inter-tactor spacing of 5 cm was used to create an apparent motion effect for communicating navigation commands.

In order to improve the Mark-I Tactile Helmet [6], particularly the low resolution of the tactile display and the size and weight of the on- and off-board electronics, the Mark-II Tactile Helmet as a 2nd generation sensory augmentation prototype was developed (see Chapter 4). More specifically, based on the psychophysics results in Chapter 3 and as summarized above, the number and positioning of the tactors, in the new helmet have been optimized for conveying navigation commands through spatiotemporal patterns that are well-tolerated and can induce the experience of apparent motion.

A ‘tactile language’ for communicating navigation commands to the Mark-II Tactile Helmet was developed (see Chapter 5). Four possible combinations of two command presentation modes (continuous, discrete) and two command types (recurring, single) in the form of vibrotactile feedback were examined for navigation along a virtual wall in a structured environment. This tactile language was evaluated in an experiment that measured users’ distance from a virtual wall and their head orientation tracked by a motion capture system in real time. The effectiveness of the tactile language was evaluated according to both objective measures of the command recognition accuracy, reaction time, the smoothness of the users’ trajectory and their walking speed, and subjective measures of their utility and comfort as determined using Likert-type rating scale. Results showed that overall recognition accuracy for all commands was high, and did not distinguish between different modes

and types of tactile command. However, consistent with the hypothesis presented in Chapter 5, tactile commands that exploit the continuous presentation mode, creating an apparent motion effect were more effective in navigation than discrete patterns of stimulation. This was shown in the measured reaction times to the tactile commands, in the smoothness of the user's trajectory and in the walking speed. In addition, navigation was more effective with recurring command types compared to the single command types. Likert-type scales results showed that helmet was well tolerated by the users, and interestingly, that users did not specifically report the recurring stimuli as being particularly irritating or burdensome. Overall, it was found that Recurring Continuous (RC) commands allowed users to navigate with lowest route deviation and highest walking speed. Additionally, participants preferred RC commands over other commands. These results provided new evidence that head-mounted tactile displays have promise as an intuitive means of displaying navigation signals and can improve spatial awareness in low visibility environments.

These results were obtained in a lab setting for a specific structured environment and should be viewed with caution in considering their application to everyday environments. For instance, in an environment with many distractions, such as a busy street or a building, recurring commands could be more distracting as previously suggested by Arab et al. [198]. Nevertheless, I hope that these results will be useful in formulating the design of tactile languages for future haptic augmentation devices for use in real-world settings.

This tactile language could provide firefighters with supplementary spatial information while navigating with the guide-rope specifically when their communication channels such as vision and hearing are overloaded. In addition, these navigation commands could be in control of firefighters through switching on the helmet guidance-mode (the helmet would have two modes: the guidance-mode when users need to receive the navigation commands and the off-mode when users do not need the navigation commands) to receive navigation commands when they get lost in the building during search and rescue missions. However, the system needs to be tested (for example in firefighters' training session) before using in a real situation to ensure that it does not make any problems for the firefighters and any accident is not the fault of the system.

The final milestone was achieved by comparing and evaluating the use of haptic and audio guidance signals for navigation in low visibility environments using the Mark-II Tactile Helmet (see Chapter 6). Haptic guidance utilized the proposed tactile language while the audio guidance applied synthetic speech. Navigation commands were generated according to distance information measured from the wall using the Mark-II Tactile Helmet ultrasound sensors and an MLP neural network as a classification algorithm. The MLP algorithm classified the ultrasound data into the three navigation commands (go-forward, turn-left, and turn-right) with an overall classification accuracy of 94.9%. It was found that haptic feedback led significantly to lower route deviation than audio feedback. Participants also had faster task completion time and lower travel distance when using the haptic guidance signals. The analysis using NASA TLX questionnaire indicated that haptic modality had lower

workload on the participants. The results of this study showed the effectiveness of haptic modality for guided navigation without vision.

In this study, data labeling for MLP training was performed in a structured environment (see Figure 6.2) by pressing the arrow key on the laptop keyboard when turning left/right or going forward was appropriate. However, in an unstructured environment a motion tracking system (such as Vicon/Inertial-based system) can be used to automatically label the action of the experimenter (turning left/right or going forward) while the experimenter is following the walls. Therefore, these labeled data could be used for training the MLP for wall-following navigation in an unstructured environment.

7.2 Answer to research questions

This thesis addressed the four research questions presented in Chapter 1. The first research question was: what form of a head-mounted vibrotactile display will be effective as a haptic interface for head-mounted sensory augmentation systems? It was shown in Chapter 3 that a 1-by-7 head-mounted vibrotactile display with 2.5 cm inter-tactor spacing, PWM 98/255 (equal to an acceleration value of 0.23 g) as vibrotactile absolute threshold, and inter-tactor spacing of 5 cm at 100 ms SOA to indicate direction with apparent motion illusion is effective as a haptic interface for head-mounted sensory augmentation systems. These results provide guidelines for the design of the vibrotactile headband displays.

The second research question was: given an initial head-mounted sensory augmentation prototype device, how can we identify and overcome its limitations? In order to overcome some of the limita-

tions of the Mark-I tactile helmet particularly the low resolution of the tactile display and the size and weight of the on- and off-board electronics, a 2nd generation tactile helmet called the Mark-II Tactile Helmet was developed as described in Chapter 4.

The third research question was: what are the vibrotactile parameters that can be manipulated to encode direction information as a tactile language for head-mounted sensory augmentation systems? A tactile language for communicating navigation commands to the Mark-II Tactile Helmet has been developed in Chapter 5. Four possible combinations of two command presentation modes (continuous, discrete) and two command types (recurring, single) were evaluated for navigation along a virtual wall in a structured environment. Recurring Continuous (RC) command that exploits the spatiotemporal patterns that induce the experience of apparent motion illusion while presenting the navigation commands repeatedly allowed users to navigate with lowest route deviation and highest walking speed and participants preferred it over other commands.

The last research question was: how should the proposed tactile language work in a navigation task? The proposed tactile language (RC) was compared with audio guidance using verbal instructions to investigate effectiveness in delivering navigation commands in a physical environment as described in Chapter 6. The results showed that haptic guidance leads to better performance as well as lower cognitive workload compared to auditory feedback. The results of this study showed the effectiveness of haptic feedback for guiding navigation without vision.

7.3 Future work

Evidence gathered throughout this research has shown that the proposed head-mounted sensory augmentation system could be used effectively to aid navigation in low visibility environments. Nevertheless, the findings lead to new questions and requirements for system improvement which are considered as future research directions as follows:

- Centralizing bias in the vibrotactile localization study could explain the consistent under-estimating of inter-tactor spacing in the funneling study. Further experiments will be required to dissect the contribution of the centralizing bias to this result.
- Extending the proposed tactile language to convey distance information as well as nonspatial information. Distance information is important as it can help firefighters to find obstacles and objects during search and rescue missions. Nonspatial information such as temperature of objects and ambient air is also crucial to firefighters since it provides an estimation of how close the fire is to them [110].
- One outstanding issue, which should be addressed in future studies, is the potential for separate movement of the head and body. In experiments in Chapter 5 and 6, participants were instructed to keep their head aligned with their body direction, however, in general navigation behaviour, head movement may be partially decoupled from the movement of the torso (for instance, looking around to explore a room) and this could

reduce the utility of the specific tactile command set tested in those experiments.

- As already mentioned, one limitation of this work is that the experiments in Chapter 5 and 6 have only been carried out in a lab setting, with the user's full attention on the task. In order to establish whether tactile language could be effective in real world applications such as firefighters' navigation, it will be necessary to carry out experiments in different environments and under different degrees of workload.
- Although ultrasound sensors are able to measure distances to objects through dense smoke [182], the high temperature in real firefighting scenario could change the speed of sound and therefore affects the sonar performance. In this condition, fusing sonar sensor information with other robust rangefinders such as microwave, radar and infrared cameras [199] can improve the system performance.
- Providing situation information by developing a local map of the environment estimated with the ultrasound sensors in place of the MLP algorithm. A local map of the environment is built using the Simultaneous Localization and Mapping (SLAM) techniques [200] which could provide the user with more detailed information about the environment such as their location in the building, escape routes and navigable paths in the form of haptic feedback.
- The Mark-II Tactile Helmet could also be used for active sensing [13] purpose to actively explore the environment using just

one ultrasound sensor and one tactor. In the current design, commands are distributed spatially in the vibrotactile display (see Figure 5.1), using multiple tactors, in order to convey rich vibrotactile patterns to the user [144] and 12 ultrasound sensors scan the entire environment around the user's head (It provides users with more information about the surrounding environment than a single ultrasound sensor). For the active sensing application, one tactor could be used for explorative scanning, but users will need to do a lot of head movements to explore the environment and therefore have to spend more time for scanning.

- Increasing the stress on the participants in order to get closer to the condition that firefighters are facing with that. This could be performed by generating an artificial stress situation [201] in which the participants are focused on a different task while receiving the navigation commands such as walking along a wall in a crowded pavement or moving the hands similar to the firefighters' building exploration task while navigating along the wall in a lab setting .

Finally, by addressing the future research envisaged by this study, I hope that the proposed head-mounted sensory augmentation system could be improved to be used as a navigation aid in a real firefighting scenario.

References

- [1] F. A. Geldard, “Adventures in tactile literacy.” *American Psychologist*, vol. 12, no. 3, p. 115, 1957.
- [2] F. A. Geldard, “Some neglected possibilities of communication.” *Science* 131, pp. 1583–1588, 1960.
- [3] L. A. Jones and S. J. Lederman, *Human hand function*. New York: Oxford University Press, 2006.
- [4] K. A. Kaczmarek and P. Bach-Y-Rita, *Tactile displays*. New York: Oxford University Press, 1995.
- [5] A. Cassinelli, C. Reynolds, and M. Ishikawa, “Augmenting spatial awareness with haptic radar,” in *10th IEEE International Symposium on Wearable Computers*, 2006, pp. 61–64.
- [6] C. Bertram, M. H. Evans, M. Javaid, T. Stafford, and T. Prescott, “Sensory augmentation with distal touch: the tactile helmet project,” in *Biomimetic and Biohybrid Systems*. Springer, 2013, pp. 24–35.
- [7] J. Van Erp, “Presenting directions with a vibrotactile torso display.” *Ergonomics*, vol. 48, no. 3, pp. 302–13, Feb. 2005.
- [8] L. A. Jones, B. Lockyer, and E. Piatetski, “Tactile display and vibrotactile pattern recognition on the torso,” *Advanced Robotics*, vol. 20, no. 12, pp. 1359–1374, 2006.
- [9] S. Deneff, L. Ramirez, T. Dyrks, and G. Stevens, “Handy navigation in ever-changing spaces: an ethnographic study of firefighting practices,” in *Proceedings of the 7th ACM conference on Designing interactive systems*, 2008, pp. 184–192.
- [10] C. Fischer and H. Gellersen, “Location and navigation support for emergency responders: A survey,” *IEEE Pervasive Computing*, vol. 9, no. 1, pp. 38–47, 2010.

-
- [11] G. A. Gescheider, “The Classical Psychophysical Methods,” in *Psychophysics: Method, Theory, and Application*, 2nd ed. Lawrence Erlbaum Associates, 1985.
- [12] J. M. Loomis and S. J. Lederman, “Tactual perception,” in *Handbook of perception and human performances*, 1986, p. 2.
- [13] J. J. Gibson, “Observations on active touch.” *Psychological review*, vol. 69, no. 6, p. 477, 1962.
- [14] J. Dargahi and S. Najarian, “Human tactile perception as a standard for artificial tactile sensing—a review,” *The International Journal of Medical Robotics and Computer Assisted Surgery*, vol. 1, no. 1, pp. 23–35, 2004.
- [15] University of Minnesota Duluth. (2014)., “lecture notes on somatosensation.” [Online]. Available: <http://www.d.umn.edu/~jfitzake/Lectures/DMED/Somatosensation/Somatosensation/Receptors.html>
- [16] S. J. Bolanowski, G. A. Gescheider, and R. T. Verrillo, “Hairy skin: psychophysical channels and their physiological substrates,” *Somatosensory and motor research*, vol. 11, no. 3, pp. 279–290, 1994.
- [17] D. G. Caldwell, N. Tsagarakis, and A. Wardle, “Mechanothermal and proprioceptor feedback for integrated haptic feedback,” in *Proceedings of IEEE International Conference on Robotics and Automation*, vol. 3, 1997, pp. 2491–2496.
- [18] D. A. Mahns, N. M. Perkins, V. Sahai, L. Robinson, and M. J. Rowe, “Vibrotactile frequency discrimination in human hairy skin,” *Journal of Neurophysiology*, vol. 95, no. 3, pp. 1442–1450, 2006.
- [19] H. R. Schiffman, *Sensation and perception: An integrated approach*. John Wiley & Sons, 1990.
- [20] S. Weinstein, “Intensive and extensive aspects of tactile sensitivity as a function of body part, sex and laterality,” in *the First Int’l symp on the Skin Senses*, 1968, pp. 195–222.
- [21] E. B. Goldstein, “The Cutaneous Sense,” in *Sensation and Perception*, 8th ed. Wadsworth Cengage Learning, 2010.

-
- [22] J. G. Betts and Others, “The Somatic Nervous System,” in *Anatomy and physiology*. OpenStax College, 2013, p. 596.
- [23] L. a. Jones and N. B. Sarter, “Tactile displays: guidance for their design and application.” *Human factors*, vol. 50, no. 1, pp. 90–111, 2008.
- [24] G. A. Gescheider, S. J. Bolanowski, J. V. Pope, and R. T. Verrillo, “A four-channel analysis of the tactile sensitivity of the fingertip: frequency selectivity, spatial summation, and temporal summation,” *Somatosensory and motor research*, vol. 19, no. 2, pp. 114–124, 2002.
- [25] R. W. Cholewiak, J. C. Brill, and A. Schwab, “Vibrotactile localization on the abdomen: Effects of place and space,” *Perception and Psychophysics*, vol. 66, no. 6, pp. 970–987, 2004.
- [26] J. W. Morley and M. J. Rowe, “Perceived pitch of vibrotactile stimuli: effects of vibration amplitude, and implications for vibration frequency coding.” *The Journal of physiology*, vol. 431, no. 1, pp. 403–416, 1990.
- [27] M. Rothenberg, R. T. Verrillo, S. A. Zahorian, M. L. Brachman, and S. J. Bolanowski Jr, “Vibrotactile frequency for encoding a speech parameter,” *The Journal of the Acoustical Society of America*, vol. 62, no. 4, pp. 1003–1012, 1977.
- [28] O. Franzén and J. Nordmark, “Vibrotactile frequency discrimination,” *Perception and Psychophysics*, vol. 17, no. 5, pp. 480–484, 1975.
- [29] G. D. Goff, “Differential discrimination of frequency of cutaneous mechanical vibration.” *Journal of experimental psychology*, vol. 74, no. 2p1, p. 294, 1967.
- [30] G. H. Mowbray and J. W. Gebhard, “Sensitivity of the skin to changes in the rate of intermittent mechanical stimuli,” *Science*, vol. 125, no. 3261, pp. 1297–1298, 1957.
- [31] C. E. Sherrick, “A scale for rate of tactual vibration,” *The Journal of the Acoustical Society of America*, vol. 78, no. 1, pp. 78–83, 1985.
- [32] G. Von Békésy, “Synchronism of neural discharges and their demultiplication in pitch perception on the skin and in hearing,”

- The Journal of the Acoustical Society of America*, vol. 31, no. 3, pp. 338–349, 1959.
- [33] R. W. Cholewiak and M. Wollowitz, “The design of vibrotactile transducers,” *Tactile aids for the hearing impaired*, pp. 57–82, 1992.
- [34] C. E. Sherrick and J. C. Craig, “The psychophysics of touch,” in *Tactual perception: A sourcebook*. Cambridge University Press, 1982, p. 55.
- [35] R. T. Verrillo and G. A. Gescheider, “Perception via the sense of touch,” *Tactile aids for the hearing impaired*, pp. 1–36, 1992.
- [36] R. W. Cholewiak, “Spatial factors in the perceived intensity of vibrotactile patterns.” *Sensory processes*, no. 3, pp. 141–156, 1979.
- [37] L. M. Brown, “Tactons: structured vibrotactile messages for non-visual information display,” Ph.D. dissertation, University of Glasgow, 2007.
- [38] Y. Kim, M. Harders, and R. Gassert, “Identification of Vibrotactile Patterns Encoding Obstacle Distance Information,” *IEEE Transactions on Haptics*, vol. 8, no. 3, pp. 298–305, 2015.
- [39] I. R. Summers, P. G. Cooper, P. Wright, D. A. Gratton, P. Milnes, and B. H. Brown, “Information from time-varying vibrotactile stimuli,” *The Journal of the Acoustical Society of America*, vol. 102, no. 6, pp. 3686–3696, 1997.
- [40] L. M. Brown, S. A. Brewster, and H. C. Purchase, “A first investigation into the effectiveness of tactons,” in *Proceedings of the 1st Joint Eurohaptics Conference and Symposium on Haptic Interfaces for Virtual Environment and Teleoperator Systems*, 2005, pp. 167–176.
- [41] J. B. F. van Erp, “Tactile navigation display,” in *Haptic human-computer interaction*. Springer, 2001, pp. 165–173.
- [42] H. Tan, R. Gray, J. J. Young, and R. Taylor, “A haptic back display for attentional and directional cueing,” *Haptics-e*, vol. 3, no. 1, 2003.

-
- [43] L. Jones, D. Held, I. Hunter, and Others, "Surface waves and spatial localization in vibrotactile displays," in *IEEE Haptics Symposium*, 2010, pp. 91–94.
- [44] R. W. Cholewiak and A. A. Collins, "Vibrotactile localization on the arm: Effects of place, space, and age," *Perception and psychophysics*, vol. 65, no. 7, pp. 1058–1077, 2003.
- [45] L. Jones, K. Ray, and Others, "Localization and pattern recognition with tactile displays," in *Symposium on haptic interfaces for virtual environment and teleoperator systems*, 2008, pp. 33–39.
- [46] R. W. Lindeman and Y. Yanagida, "Empirical studies for effective near-field haptics in virtual environments," in *Proceedings of IEEE Virtual Reality*, 2003, pp. 287–288.
- [47] H.-Y. Chen, J. Santos, M. Graves, K. Kim, and H. Z. Tan, "Tactor localization at the wrist," in *Haptics: Perception, Devices and Scenarios*. Springer, 2008, pp. 209–218.
- [48] I. Oakley, Y. Kim, J. Lee, and J. Ryu, "Determining the feasibility of forearm mounted vibrotactile displays," in *14th Symposium on Haptic Interfaces for Virtual Environment and Teleoperator Systems*, 2006, pp. 27–34.
- [49] R. T. Verrillo, *The effects of aging on the sense of touch*. Erlbaum: Hillsdale, NJ, 1993.
- [50] F. A. Geldard, "The mutability of time and space on the skin," *The Journal of the Acoustical Society of America*, vol. 77, no. 1, pp. 233–237, 1985.
- [51] J. Pasquero, "Survey on communication through touch," Tech. Rep., 2006.
- [52] R. W. Cholewiak and J. C. Craig, "Vibrotactile pattern recognition and discrimination at several body sites," *Perception and Psychophysics*, vol. 35, no. 6, pp. 503–514, 1984.
- [53] J. C. Craig, "Some factors affecting tactile pattern recognition," *International Journal of Neuroscience*, vol. 19, pp. 47–57, 1983.
- [54] S. J. Bensmaia, Y.-Y. Leung, S. S. Hsiao, and K. O. Johnson, "Vibratory adaptation of cutaneous mechanoreceptive afferents," *Journal of neurophysiology*, vol. 94, no. 5, pp. 3023–3036, 2005.

-
- [55] G. A. Gescheider, R. T. Verrillo, A. J. Capraro, and R. D. Hamer, "Enhancement of vibrotactile sensation magnitude and predictions from the duplex model of mechanoreception." *Sensory processes*, vol. 1, no. 3, pp. 187–203, 1977.
- [56] A. Gallace, M. Auvray, H. Z. Tan, and C. Spence, "When visual transients impair tactile change detection: A novel case of crossmodal change blindness?" *Neuroscience Letters*, vol. 398, no. 3, pp. 280–285, 2006.
- [57] A. Gallace, H. Z. Tan, and C. Spence, "Tactile change detection," in *Proceedings of the First World Haptic Conference*, 2005, pp. 12–16.
- [58] A. C. Guyton, "Sensory receptors, neuronal circuits for processing information," in *Textbook of Medical Physiology*, 2nd ed. W.B. Saunders Company, 1991, pp. 102–113.
- [59] Y. Kim, J. Lee, and G. J. Kim, "Designing of 2D illusory tactile feedback for hand-held tablets," in *Human-Computer Interaction*. Springer, 2015, pp. 10–17.
- [60] G. v. Bekesy, "Funneling in the nervous system and its role in loudness and sensation intensity on the skin," *The Journal of the Acoustical Society of America*, vol. 30, no. 5, pp. 399–412, 1958.
- [61] D. Alles, "Information Transmission by Phantom Sensations," *IEEE Transactions on Man Machine Systems*, vol. 11, no. 1, pp. 85–91, 1970.
- [62] G. Von Bekesy, "Similarities between hearing and skin sensations." *Psychological review*, vol. 66, no. 1, p. 1, 1959.
- [63] R. W. Cholewiak and A. A. Collins, "The generation of vibrotactile patterns on a linear array: Influences of body site, time, and presentation mode," *Perception and Psychophysics*, vol. 62, no. 6, pp. 1220–1235, 2000.
- [64] F. A. Geldard, *Sensory saltation: Metastability in the perceptual world*. Lawrence Erlbaum, 1975.
- [65] J. Cha, L. Rahal, and A. El Saddik, "A pilot study on simulating continuous sensation with two vibrating motors," in *IEEE*

- International Workshop on Haptic Audio visual Environments and Games*, 2008, pp. 143–147.
- [66] J. Lee, Y. Kim, and G. Kim, “Funneling and saltation effects for tactile interaction with virtual objects,” in *Proceedings of the SIGCHI Conference on Human Factors in Computing Systems*. ACM, 2012, pp. 3141–3148.
- [67] L. Rahal, J. Cha, and A. El Saddik, “Continuous tactile perception for vibrotactile displays,” in *IEEE International Workshop on Robotic and Sensors Environments*, 2009, pp. 86–91.
- [68] A. Barghout, J. Cha, A. El Saddik, J. Kammerl, and E. Steinbach, “Spatial resolution of vibrotactile perception on the human forearm when exploiting funneling illusion,” in *IEEE International Workshop on Haptic Audio visual Environments and Games*. IEEE, 2009, pp. 19–23.
- [69] F. A. Geldard and C. E. Sherrick, “The cutaneous" rabbit": A perceptual illusion,” *Science*, vol. 178, no. 4057, pp. 178–179, 1972.
- [70] T. Roady and T. K. Ferris, “An Analysis of Static, Dynamic, and Saltatory Vibrotactile Stimuli to Inform the Design of Efficient Haptic Communication Systems,” in *Proceedings of the Human Factors and Ergonomics Society Annual Meeting*, vol. 56, no. 1, 2012, pp. 2075–2079.
- [71] M. Miyazaki, M. Hirashima, and D. Nozaki, “The “cutaneous rabbit” hopping out of the body,” *The Journal of Neuroscience*, vol. 30, no. 5, pp. 1856–1860, 2010.
- [72] L. Kohli, M. Niwa, H. Noma, K. Susami, Y. Yanagida, R. W. Lindeman, K. Hosaka, and Y. Kume, “Towards effective information display using vibrotactile apparent motion,” in *14th Symposium on Haptic Interfaces for Virtual Environment and Teleoperator Systems*, 2006, pp. 445–451.
- [73] C. E. Sherrick and R. Rogers, “Apparent haptic movement,” *Perception and Psychophysics*, vol. 1, no. 3, pp. 175–180, 1966.
- [74] J. H. Kirman, “Tactile apparent movement: The effects of interstimulus onset interval and stimulus duration,” *Perception and Psychophysics*, vol. 15, no. 1, pp. 1–6, 1974.

-
- [75] C. E. Sherrick, "Bilateral apparent haptic movement," *Perception and Psychophysics*, vol. 4, no. 3, pp. 159–160, 1968.
- [76] M. Niwa, R. W. Lindeman, Y. Itoh, and F. Kishino, "Determining appropriate parameters to elicit linear and circular apparent motion using vibrotactile cues," in *Proceedings of World Haptics Conference (WHC)*, 2009, pp. 75–78.
- [77] A. Israr and I. Poupyrev, "Control space of apparent haptic motion," in *IEEE World Haptics Conference (WHC)*, 2011, pp. 457–462.
- [78] M. Niwa, Y. Yanagida, H. Noma, K. Hosaka, and Y. Kume, "Vibrotactile apparent movement by DC motors and voice-coil tactors," in *Proceedings of the 14th International Conference on Artificial Reality and Telexistence (ICAT)*, 2004, pp. 126–131.
- [79] J. H. Kirman, "The effect of number of stimulators on the optimal interstimulus onset interval in tactile apparent movement," *Perception and Psychophysics*, vol. 17, no. 3, pp. 263–267, 1975.
- [80] C. E. Sherrick, "Studies of apparent tactual movement," in *The skin senses*. CC Thomas: Springfield, IL, 1968, pp. 331–344.
- [81] V. Harrar, R. Winter, and L. R. Harris, "Visuotactile apparent motion," *Perception and Psychophysics*, vol. 70, no. 5, pp. 807–817, 2008.
- [82] R. H. Gibson, "Requirements for the use of electrical stimulation of the skin," in *Proceedings of the International Congress on Technology and Blindness*, vol. 2, 1963, pp. 183–207.
- [83] Y. Visell, "Tactile sensory substitution: Models for enactment in HCI," *Interacting with Computers*, vol. 21, no. 1-2, pp. 38–53, 2009.
- [84] K. A. Kaczmarek, J. G. Webster, P. Bach-y Rita, and W. J. Tompkins, "Electrotactile and vibrotactile displays for sensory substitution systems," *IEEE Transactions on Biomedical Engineering*, vol. 38, no. 1, pp. 1–16, 1991.
- [85] I. R. Summers, P. R. Dixon, P. G. Cooper, D. A. Gratton, B. H. Brown, and J. C. Stevens, "Vibrotactile and electrotactile perception of time-varying pulse trains," *The Journal of the*

- Acoustical Society of America*, vol. 95, no. 3, pp. 1548–1558, 1994.
- [86] K. A. Kaczmarek and S. J. Haase, “Pattern identification as a function of stimulation current on a fingertip-scanned electrotactile display,” *IEEE Transactions on neural systems and rehabilitation engineering*, vol. 11, no. 3, pp. 269–275, 2003.
- [87] S. Choi and K. J. Kuchenbecker, “Vibrotactile display: Perception, technology, and applications,” *Proceedings of the IEEE*, vol. 101, no. 9, pp. 2093–2104, 2013.
- [88] I. Poupyrev, S. Maruyama, and J. Rekimoto, “Ambient touch: designing tactile interfaces for handheld devices,” in *Proceedings of the 15th annual ACM symposium on User interface software and technology*. ACM, 2002, pp. 51–60.
- [89] P. B. Shull and D. D. Damian, “Haptic wearables as sensory replacement, sensory augmentation and trainer—a review,” *Journal of neuroengineering and rehabilitation*, vol. 12, no. 1, p. 1, 2015.
- [90] P. Bach-y Rita, C. C. Collins, F. A. Saunders, B. White, and L. Scadden, “Vision substitution by tactile image projection,” *Nature*, vol. 221, pp. 963–964, 1969.
- [91] P. Bach-y Rita and S. W. Kercel, “Sensory substitution and the human–machine interface,” *Trends in cognitive sciences*, vol. 7, no. 12, pp. 541–546, 2003.
- [92] H. Tang and D. J. Beebe, “An oral tactile interface for blind navigation,” *IEEE Transactions on Neural Systems and Rehabilitation Engineering*, vol. 14, no. 1, pp. 116–123, 2006.
- [93] J. Bliss, M. Katcher, C. Rogers, and R. Shepard, “Optical-to-Tactile Image Conversion for the Blind,” *IEEE Transactions on Man Machine Systems*, vol. 11, no. 1, pp. 58–65, 1970.
- [94] H. C. Stronks, A. C. Nau, M. R. Ibbotson, and N. Barnes, “The role of visual deprivation and experience on the performance of sensory substitution devices,” *Brain research*, vol. 1624, pp. 140–152, 2015.
- [95] T. McDaniel, S. Krishna, V. Balasubramanian, D. Colbry, and S. Panchanathan, “Using a haptic belt to convey non-verbal

- communication cues during social interactions to individuals who are blind,” in *IEEE International Workshop on Haptic Audio visual Environments and Games.*, 2008, pp. 13–18.
- [96] T. Amemiya, J. Yamashita, K. Hirota, and M. Hirose, “Virtual leading blocks for the deaf-blind: A real-time way-finder by verbal-nonverbal hybrid interface and high-density RFID tag space,” in *Proceedings of IEEE Virtual Reality*, 2004, pp. 165–287.
- [97] R. Velázquez and O. Bazán, “Preliminary evaluation of podotactile feedback in sighted and blind users,” in *Annual International Conference of the IEEE Engineering in Medicine and Biology*, 2010, pp. 2103–2106.
- [98] T. Froese, M. McGann, W. Bigge, A. Spiers, and A. K. Seth, “The enactive torch: a new tool for the science of perception,” *IEEE Transactions on Haptics*, vol. 5, no. 4, pp. 365–375, 2012.
- [99] F. A. Saunders, W. A. Hill, and B. Franklin, “A wearable tactile sensory aid for profoundly deaf children,” *Journal of Medical Systems*, vol. 5, no. 4, pp. 265–270, 1981.
- [100] A. Y. J. Szeto and R. R. Riso, “Sensory feedback using electrical stimulation of the tactile sense,” in *Rehabilitation Engineering*. R. V. Smith and J. H. Leslie Jr., Eds. Boca Raton, FL: CRC Press, 1990, pp. 29–78.
- [101] K. L. Galvin, G. Mavrias, A. Moore, R. S. C. Cowan, P. J. Blamey, and G. M. Clark, “A comparison of tactaid II and tactaid 7 use by adults with a profound hearing impairment,” *Ear and hearing*, vol. 20, no. 6, p. 471, 1999.
- [102] S. M. Kärcher, S. Fenzlaff, D. Hartmann, S. K. Nagel, and P. König, “Sensory augmentation for the blind,” *Frontiers in human neuroscience*, vol. 6, p. 37, 2012.
- [103] A. Carton and L. E. Dunne, “Tactile distance feedback for firefighters: design and preliminary evaluation of a sensory augmentation glove,” in *Proceedings of the 4th Augmented Human International Conference*. ACM, 2013, pp. 58–64.
- [104] C. Wall III and M. S. Weinberg, “Balance prostheses for postural control,” *IEEE Engineering in Medicine and Biology Magazine*, vol. 22, no. 2, pp. 84–90, 2003.

- [105] S. Gallo, D. Chapuis, L. Santos-Carreras, Y. Kim, P. Rertornaz, H. Bleuler, and R. Gassert, “Augmented white cane with multimodal haptic feedback,” in *3rd IEEE RAS and EMBS International Conference on Biomedical Robotics and Biomechatronics (BioRob)*, 2010, pp. 149–155.
- [106] S. K. Nagel, C. Carl, T. Kringe, R. Martin, and P. König, “Beyond sensory substitution—learning the sixth sense,” *Journal of neural engineering*, vol. 2, no. 4, pp. R13–R26, 2005.
- [107] K. Kaspar, S. König, J. Schwandt, and P. König, “The experience of new sensorimotor contingencies by sensory augmentation.” *Consciousness and cognition*, vol. 28, pp. 47–63, 2014.
- [108] J. K. O’Regan and A. Noë, “A sensorimotor account of vision and visual consciousness,” *Behavioral and brain sciences*, vol. 24, no. 05, pp. 939–973, 2001.
- [109] D. V. D. Heever, “Magnetoreception in humans,” *Transactions of Japanese Society for Medical and Biological Engineering*, vol. 51, no. Supplement, pp. R–22, 2013.
- [110] K. Walters, S. Lee, T. Starner, R. Leibbrandt, and M. Lawo, “Touchfire: Towards a glove-mounted tactile display for rendering temperature readings for firefighters,” in *International Symposium on Wearable Computers, ISWC*, 2010, pp. 1–4.
- [111] C. Wall III, M. S. Weinberg, P. B. Schmidt, and D. E. Krebs, “Balance prosthesis based on micromechanical sensors using vibrotactile feedback of tilt,” *IEEE Transactions on Biomedical Engineering*, vol. 48, no. 10, pp. 1153–1161, 2001.
- [112] A. A. Priplata, J. B. Niemi, J. D. Harry, L. A. Lipsitz, and J. J. Collins, “Vibrating insoles and balance control in elderly people.” *The Lancet*, vol. 362, no. 9390, pp. 1123–4, 2003.
- [113] F. B. Horak, M. Dozza, R. Peterka, L. Chiari, and C. Wall III, “Vibrotactile biofeedback improves tandem gait in patients with unilateral vestibular loss,” *Annals of the New York Academy of Sciences*, vol. 1164, no. 1, pp. 279–281, 2009.
- [114] L. J. F. Janssen, L. L. Verhoeff, C. G. C. Horlings, and J. H. J. Allum, “Directional effects of biofeedback on trunk sway during

- gait tasks in healthy young subjects,” *Gait and posture*, vol. 29, no. 4, pp. 575–581, 2009.
- [115] N. Rao and A. S. Aruin, “Auxiliary sensory cues improve automatic postural responses in individuals with diabetic neuropathy,” *Neurorehabilitation and neural repair*, vol. 25, no. 2, pp. 110–117, 2011.
- [116] E. van Wegen, C. de Goede, I. Lim, M. Rietberg, A. Nieuwboer, A. Willems, D. Jones, L. Rochester, V. Hetherington, H. Berendse, and Others, “The effect of rhythmic somatosensory cueing on gait in patients with Parkinson’s disease,” *Journal of the neurological sciences*, vol. 248, no. 1, pp. 210–214, 2006.
- [117] A. Jeffs and K. Warwick, “Sensory Perception through an Electro-tactile Stimulus Array on the Tongue,” in *IEEE International Conference on Systems, Man, and Cybernetics*, 2013, pp. 3549–3554.
- [118] A. Saig, A. Arieli, and E. Ahissar, “What is it like to be a rat? sensory augmentation study,” in *Haptics: Generating and Perceiving Tangible Sensations*. Springer, 2010, pp. 298–305.
- [119] H. Van Veen and J. B. F. Van Erp, “Providing directional information with tactile torso displays,” in *Proceedings of EuroHaptics*, 2003, pp. 471–474.
- [120] A. H. Rupert, “An instrumentation solution for reducing spatial disorientation mishaps,” *IEEE Engineering in Medicine and Biology Magazine*, vol. 19, no. 2, pp. 71–80, 2000.
- [121] J. L. Rochlis and D. J. Newman, “A tactile display for international space station (ISS) extravehicular activity (EVA).” *Aviation, space, and environmental medicine*, vol. 71, no. 6, pp. 571–578, 2000.
- [122] R. Traylor and H. Z. Tan, “Development of a wearable haptic display for situation awareness in altered-gravity environment: Some initial findings,” in *10th IEEE Symposium on Haptic Interfaces for Virtual Environment and Teleoperator Systems*, 2002, pp. 159–164.

-
- [123] R. W. Lindeman, J. L. Sibert, C. E. Lathan, and J. M. Vice, "The design and deployment of a wearable vibrotactile feedback system," in *Proceedings of the 8th IEEE International Symposium on Wearable Computers.*, 2004, pp. 56–59.
- [124] R. D. Gilson, E. S. Redden, and L. R. Elliott, "Remote tactile displays for future soldiers (ARL-SR-0152.)," Aberdeen Proving Ground, MD: Army Research Laboratory., Tech. Rep., 2007.
- [125] J. B. F. Van Erp, H. A. H. C. Van Veen, C. Jansen, and T. Dobbins, "Waypoint navigation with a vibrotactile waist belt," *ACM Transactions on Applied Perception (TAP)*, vol. 2, no. 2, pp. 106–117, 2005.
- [126] J. B. F. Van Erp and H. A. H. C. Van Veen, "Vibrotactile in-vehicle navigation system," *Transportation Research Part F: Traffic Psychology and Behaviour*, vol. 7, no. 4, pp. 247–256, 2004.
- [127] E. Giannopoulos, A. Pomes, and M. Slater, "Touching the void: exploring virtual objects through a vibrotactile glove," *The International Journal of Virtual Reality*, vol. 11, no. 2, pp. 19–24, 2012.
- [128] L. A. Jones, J. Kunkel, and E. Torres, "Tactile vocabulary for tactile displays," in *Second Joint EuroHaptics Conference and Symposium on Haptic Interfaces for Virtual Environment and Teleoperator Systems (WHC'07)*, 2007, pp. 574–575.
- [129] C. M. Reed, W. M. Rabinowitz, N. I. Durlach, L. D. Braida, S. Conway-Fithian, and M. C. Schultz, "Research on the Tadoma method of speech communication," *The Journal of the Acoustical society of America*, vol. 77, no. 1, pp. 247–257, 1985.
- [130] S. Brewster and L. M. Brown, "Tactons: structured tactile messages for non-visual information display," in *Proceedings of Australasian User Interface Conference*, 2004, pp. 15–23.
- [131] J. B. F. Van Erp, "Guidelines for the use of vibro-tactile displays in human computer interaction," in *Proceedings of eurohaptics*. Springer, 2002, pp. 18–22.

-
- [132] A. Riener and A. Ferscha, “Raising awareness about space via vibro-tactile notifications,” in *European Conference on Smart Sensing and Context*. Springer, 2008, pp. 235–245.
- [133] A. Riener and H. Hartl, “Personal Radar: a self-governed support system to enhance environmental perception,” in *Proceedings of the 26th Annual BCS Interaction Specialist Group Conference on People and Computers*. British Computer Society, 2012, pp. 147–156.
- [134] D. Dakopoulos and N. Bourbakis, “Towards a 2D tactile vocabulary for navigation of blind and visually impaired,” in *IEEE International Conference on Systems, Man and Cybernetics*. IEEE, 2009, pp. 45–51.
- [135] V. A. d. J. Oliveira, E. Marques, R. de Lemos Peroni, and A. Maciel, “Tactile Interface for Navigation in Underground Mines,” in *XVI Symposium on Virtual and Augmented Reality (SVR)*, 2014, pp. 230–237.
- [136] M. Straub, A. Riener, and A. Ferscha, “Distance encoding in vibro-tactile guidance cues,” in *Poster at the 6th Annual International Conference on Mobile and Ubiquitous Systems: Computing, Networking and Services (MobiQuitous)*, 2009, p. 2.
- [137] A. Asif, W. Heuten, and S. Boll, “Exploring distance encodings with a tactile display to convey turn by turn information in automobiles,” in *Proceedings of the 6th Nordic conference on human-computer interaction: Extending boundaries*. ACM, 2010, pp. 32–41.
- [138] S. Boll, A. Asif, and W. Heuten, “Feel your route: a tactile display for car navigation,” *IEEE Pervasive Computing*, vol. 10, no. 3, pp. 35–42, 2011.
- [139] H. Z. Tan and A. Pentland, “Tactual displays for wearable computing,” in *First International Symposium on Wearable Computers*, 1997, pp. 84–89.
- [140] K. Tsukada and M. Yasumura, “Activebelt: Belt-type wearable tactile display for directional navigation,” in *UbiComp: Ubiquitous Computing*. Springer, 2004, pp. 384–399.

- [141] W. Heuten, N. Henze, S. Boll, and M. Pielot, “Tactile wayfinder: a non-visual support system for wayfinding,” in *Proceedings of the 5th Nordic conference on Human-computer interaction: building bridges*. ACM, 2008, pp. 172–181.
- [142] M. Pielot, N. Henze, W. Heuten, and S. Boll, “Evaluation of continuous direction encoding with tactile belts,” in *International Workshop on Haptic and Audio Interaction Design*. Springer, 2008, pp. 1–10.
- [143] A. Cosgun, E. A. Sisbot, and H. I. Christensen, “Evaluation of Rotational and Directional Vibration Patterns on a Tactile Belt for Guiding Visually Impaired People,” in *IEEE Haptics Symposium (HAPTICS)*, 2014, pp. 367–370.
- [144] E. Hoggan, S. Anwar, and S. A. Brewster, “Mobile multi-actuator tactile displays,” in *International Workshop on Haptic and Audio Interaction Design*. Springer, 2007, pp. 22–33.
- [145] D. A. Ross and B. B. Blasch, “Wearable interfaces for orientation and wayfinding,” in *Proceedings of the fourth international ACM conference on Assistive technologies*, 2000, pp. 193–200.
- [146] A. Murata, S. Kemori, M. Moriwaka, and T. Hayami, “Proposal of automotive 8-directional warning system that makes use of tactile apparent movement,” in *International Conference on Digital Human Modeling and Applications in Health, Safety, Ergonomics and Risk Management*. Springer, 2013, pp. 98–107.
- [147] L. A. Jones, J. Kunkel, and E. Piatetski, “Vibrotactile pattern recognition on the arm and back,” *Perception*, vol. 38, no. 1, pp. 52–68, 2009.
- [148] S. Panëels, M. Anastassova, S. Strachan, S. P. Van, S. Sivacoumarane, and C. Bolzmacher, “What’s around me? Multi-actuator haptic feedback on the wrist,” in *IEEE World Haptics Conference (WHC)*, 2013, pp. 407–412.
- [149] S. Bosman, B. Groenendaal, J.-W. Findlater, T. Visser, M. de Graaf, and P. Markopoulos, “Gentleguide: An exploration of haptic output for indoors pedestrian guidance,” in *Human-computer interaction with mobile devices and services*. Springer, 2003, pp. 358–362.

-
- [150] B. Weber, S. Schätzle, T. Hulin, C. Preusche, and B. Deml, “Evaluation of a vibrotactile feedback device for spatial guidance,” in *IEEE World Haptics Conference (WHC)*, 2011, pp. 349–354.
- [151] T. Stafford, M. Javaid, B. Mitchinson, A. M. J. Galloway, and T. J. Prescott, “Integrating augmented senses into active perception: a framework,” in *Poster Presented at Royal Society meeting on Active Touch Sensing*, vol. 31, 2011.
- [152] S. Mann, J. Huang, R. Janzen, R. Lo, V. Rampersad, A. Chen, and T. Doha, “Blind navigation with a wearable range camera and vibrotactile helmet,” in *Proceedings of the 19th ACM international conference on Multimedia*, 2011, pp. 1325–1328.
- [153] O. B. Kaul and M. Rohs, “HapticHead: 3D Guidance and Target Acquisition through a Vibrotactile Grid,” in *Proceedings of the CHI Conference Extended Abstracts on Human Factors in Computing Systems*, 2016, pp. 2533–2539.
- [154] M. Berning, F. Braun, T. Riedel, and M. Beigl, “ProximityHat: a head-worn system for subtle sensory augmentation with tactile stimulation,” in *Proceedings of the ACM International Symposium on Wearable Computers*, 2015, pp. 31–38.
- [155] A. C. Marsalia, “Evaluation of Vibrotactile Alert Systems for Supporting Hazard Awareness and Safety of Distracted Pedestrians,” Ph.D. dissertation, Texas A&M University, 2013.
- [156] M. Katsev, A. Yershova, B. Tovar, R. Ghrist, and S. M. LaValle, “Mapping and pursuit-evasion strategies for a simple wall-following robot,” *IEEE Transactions on Robotics*, vol. 27, no. 1, pp. 113–128, 2011.
- [157] W. Tsui, M. S. Masmoudi, F. Karray, I. Song, and M. Masmoudi, “Soft-computing-based embedded design of an intelligent wall/lane-following vehicle,” *IEEE/ASME Transactions on Mechatronics*, vol. 13, no. 1, pp. 125–135, 2008.
- [158] A. L. Freire, G. A. Barreto, M. Veloso, and A. T. Varela, “Short-term memory mechanisms in neural network learning of robot navigation tasks: A case study,” in *Robotics Symposium (LARS), 6th Latin American*, 2009, pp. 1–6.

-
- [159] M. Lichman, “{UCI} Machine Learning Repository,” 2013. [Online]. Available: <http://archive.ics.uci.edu/ml>
- [160] T. Dash, T. Nayak, and G. Mishra, “Neural network approach to control wall-following robot navigation,” in *IEEE International Conference on Advanced Communications, Control and Computing Technologies*, 2014, pp. 1072–1076.
- [161] T. Dash, T. Nayak, and R. R. Swain, “Controlling wall following robot navigation based on gravitational search and feed forward neural network,” in *Proceedings of the 2nd International Conference on Perception and Machine Intelligence*. ACM, 2015, pp. 196–200.
- [162] E. Rashedi, H. Nezamabadi-Pour, and S. Saryazdi, “GSA: a gravitational search algorithm,” *Information sciences*, vol. 179, no. 13, pp. 2232–2248, 2009.
- [163] S. Grossberg, “Adaptive Resonance Theory: How a brain learns to consciously attend, learn, and recognize a changing world,” *Neural Networks*, vol. 37, pp. 1–47, 2013.
- [164] T. Dash, “Automatic navigation of wall following mobile robot using Adaptive Resonance Theory of Type-1,” *Biologically Inspired Cognitive Architectures*, vol. 12, pp. 1–8, 2015.
- [165] X. Wang, Z.-G. Hou, F. Lv, M. Tan, and Y. Wang, “Mobile robots modular navigation controller using spiking neural networks,” *Neurocomputing*, vol. 134, pp. 230–238, 2014.
- [166] L. A. Zadeh, “Fuzzy sets,” *Information and control*, vol. 8, no. 3, pp. 338–353, 1965.
- [167] G. Antonelli, S. Chiaverini, and G. Fusco, “A fuzzy-logic-based approach for mobile robot path tracking,” *IEEE Transactions on Fuzzy Systems*, vol. 15, no. 2, pp. 211–221, 2007.
- [168] J.-S. Lo, Chi-Wen and Wu, Kun-Lin and Liu, “Wall Following and Human Detection for Mobile Robot Surveillance in Indoor Environment,” in *IEEE International Conference on Mechatronics and Automation*, 2014, pp. 1696–1702.
- [169] S.-J. Li, T-HS and Chang, “Autonomous fuzzy parking control of a car-like mobile robot,” *IEEE Transactions on Systems*,

- Man and Cybernetics, Part A: Systems and Humans*, vol. 33, no. 4, pp. 451–465, 2003.
- [170] D. Hanafi, Y. M. Abueejela, and M. F. Zakaria, “Wall follower autonomous robot development applying fuzzy incremental controller,” *Intelligent Control and Automation*, vol. 4, no. 1, p. 18, 2013.
- [171] A. Zhu and S. X. Yang, “Neurofuzzy-based approach to mobile robot navigation in unknown environments,” *IEEE Transactions on Systems, Man, and Cybernetics, Part C: Applications and Reviews*, vol. 37, no. 4, pp. 610–621, 2007.
- [172] P. Rusu, E. M. Petriu, T. E. Whalen, A. Cornell, and H. J. W. Spoelder, “Behavior-based neuro-fuzzy controller for mobile robot navigation,” *IEEE Transactions on Instrumentation and Measurement*, vol. 52, no. 4, pp. 1335–1340, 2003.
- [173] A. Zhu, S. X. Yang, F. Wang, and G. S. Mittal, “A neuro-fuzzy controller for reactive navigation of a behaviour-based mobile robot,” in *International Symposium on Neural Networks*, Springer, Ed., 2005, pp. 259–264.
- [174] N. Zhang, D. Beetner, D. C. Wunsch, B. Hemmelman, A. Hasan, and Others, “An embedded real-time neuro-fuzzy controller for mobile robot navigation,” in *14th IEEE International Conference on Fuzzy Systems*, 2005, pp. 319–324.
- [175] J. Godjevac and N. Steele, “Neuro-Fuzzy Control for Basic Mobile Robot,” *Fuzzy Logic Techniques for Autonomous Vehicle Navigation*, vol. 61, p. 97, 2013.
- [176] S. F. Desouky and H. M. Schwartz, “Genetic based fuzzy logic controller for a wall-following mobile robot,” in *IEEE American Control Conference*, 2009, pp. 3555–3560.
- [177] R. Braunstingl, J. Mujika, and J. P. Uribe, “A wall following robot with a fuzzy logic controller optimized by a genetic algorithm,” in *Proceedings of 1995 IEEE International Conference on Fuzzy Systems*, vol. 5, 1995, pp. 77–82.
- [178] J. Nijhuis, S. Neuß er, L. Spaanenburger, J. Heller, and J. Spönnemann, “Evaluation of fuzzy and neural vehicle control,” in *Proceedings of Computer Systems and Software Engineering*, 1992, pp. 447–452.

- [179] L. Jones, H. Z. Tan, and Others, “Application of psychophysical techniques to haptic research,” *IEEE Transactions on Haptics*, vol. 6, no. 3, pp. 268–284, 2013.
- [180] National Instrument. (2016), “Understanding Resolution in High-Speed Digitizers/Oscilloscopes.” [Online]. Available: <http://www.ni.com/white-paper/4806/en/>
- [181] H. Abdi, “The Bonferonni and Šidák corrections for multiple comparisons,” *Encyclopedia of measurement and statistics*, vol. 3, pp. 103–107, 2007.
- [182] J. Sales, R. Marín, E. Cervera, S. Rodríguez, and J. Pérez, “Multi-sensor person following in low-visibility scenarios,” *Sensors*, vol. 10, no. 12, pp. 10 953–10 966, 2010.
- [183] B. Siciliano and O. Khatib, “Sonar Sensing,” in *Springer handbook of robotics*. Springer Science & Business Media, 2008.
- [184] S. Walter and Others, “The sonar ring: Obstacle detection for a mobile robot,” in *IEEE International Conference on Robotics and Automation.*, vol. 4, 1987, pp. 1574–1579.
- [185] Y. Ando and S. Yuta, “Following a wall by an autonomous mobile robot with a sonar-ring,” in *Proceedings of IEEE International Conference on Robotics and Automation*, vol. 3, 1995, pp. 2599–2606.
- [186] R. Likert, “A technique for the measurement of attitudes.” *Archives of psychology*, 1932.
- [187] Vicon. (2013), “Vicon software tracker.” [Online]. Available: <http://www.vicon.com/products/software/tracker>
- [188] G. Flores, S. Kurniawan, R. Manduchi, E. Martinson, L. M. Morales, and E. A. Sisbot, “Vibrotactile Guidance for Wayfinding of Blind Walkers,” *IEEE Transactions on Haptics*, vol. 8, no. 3, pp. 306–317, 2015.
- [189] S. Shoval, J. Borenstein, and Y. Koren, “Auditory guidance with the navbelt—a computerized travel aid for the blind,” *IEEE Transactions on Systems, Man, and Cybernetics, Part C: Applications and Reviews*, vol. 28, no. 3, pp. 459–467, 1998.

- [190] S. Holland, D. R. Morse, and H. Gedenryd, "AudioGPS: Spatial audio navigation with a minimal attention interface," *Personal and Ubiquitous computing*, vol. 6, no. 4, pp. 253–259, 2002.
- [191] J. M. Loomis, J. R. Marston, R. G. Golledge, and R. L. Klatzky, "Personal guidance system for people with visual impairment: A comparison of spatial displays for route guidance," *Journal of visual impairment and blindness*, vol. 99, no. 4, p. 219, 2005.
- [192] J. R. Marston, J. M. Loomis, R. L. Klatzky, and R. G. Golledge, "Nonvisual route following with guidance from a simple haptic or auditory display." *Journal of Visual Impairment and Blindness*, vol. 101, no. 4, pp. 203–211, 2007.
- [193] M. Hara, S. Shokur, A. Yamamoto, T. Higuchi, R. Gassert, and H. Bleuler, "Virtual environment to evaluate multimodal feedback strategies for augmented navigation of the visually impaired," in *Annual International Conference of the IEEE Engineering in Medicine and Biology Society (EMBC)*, 2010, pp. 975–978.
- [194] M. Martinez, A. Constantinescu, B. Schauerte, D. Koester, and R. Stiefelhagen, "Cognitive evaluation of haptic and audio feedback in short range navigation tasks," in *Computers Helping People with Special Needs*. Springer, 2014, pp. 128–135.
- [195] S. G. Hart and L. E. Staveland, "Development of NASA-TLX (Task Load Index): Results of empirical and theoretical research," *Advances in psychology*, vol. 52, pp. 139–183, 1988.
- [196] T. M. Mitchell, "Artificial Neural Networks," in *Machine learning*. McGraw-Hill, New York, 1997.
- [197] M. K. Dobrzynski, S. Mejri, S. Wischmann, and D. Floreano, "Quantifying information transfer through a head-attached vibrotactile display: principles for design and control," *IEEE Transactions on Biomedical Engineering*, vol. 59, no. 7, pp. 2011–2018, 2012.
- [198] F. Arab, S. Paneels, M. Anastassova, S. Cœugnet, F. Le Morellec, A. Dommès, and A. Chevalier, "Haptic patterns and older adults: To repeat or not to repeat?" in *IEEE World Haptics Conference (WHC)*, 2015, pp. 248–253.

-
- [199] J. W. Starr and B. Y. Lattimer, “Evaluation of navigation sensors in fire smoke environments,” *Fire Technology*, vol. 50, no. 6, pp. 1459–1481, 2014.
- [200] S. Thrun and Others, “Robotic mapping: A survey,” *Exploring artificial intelligence in the new millennium*, pp. 1–35, 2002.
- [201] A. Meier, D. J. C. Matthies, B. Urban, and R. Wettach, “Exploring vibrotactile feedback on the body and foot for the purpose of pedestrian navigation,” in *Proceedings of the 2nd international Workshop on Sensor-based Activity Recognition and Interaction*. ACM, 2015, pp. 1–11.

Appendix A

Participant consent forms

This appendix describes four employed consent forms for the experiments in this thesis. Consent form I corresponds to the vibrotactile absolute threshold, vibrotactile localization and funneling illusion experiments, and consent form II belongs to the apparent motion study in Chapter 3. Consent forms III and IV are for the experiments in Chapter 5 and Chapter 6, respectively.

A.1 Consent form I

You are being asked to take part in a psychophysics experiment. The aim of this research is to evaluate the perception of vibrotactile stimuli for a wearable haptic interface. This research is as a part of my PhD project under the supervision of Professor Tony Prescott and has received ethics approval from the department of psychology, University of Sheffield. Practice sessions will be given prior to the experiments. During the test please do not close your eyes and before you press the "Next" button, you can take a rest as long as you want. The total time required to complete the study should be approximately 45 minutes.

Procedure: If you agree to be in this study, you will be asked to do the following: First you need to sit in front of the computer screen and wear a headband which composes of a set of vibration motors. When you are ready, the experiment will start. It composes of three parts as follow:

Experiment 1:

- By pressing the start button in the GUI, the experiment will start.
- The stimuli is presented to the forehead midline: If it is sensible, you should press the "Yes" button in the GUI, otherwise press the "No" button.
- Repeat trials until you see the finish message.

Experiment 2:

- Press the start button in the GUI by clicking a mouse or a touch pad.
- Then, vibration is displayed to one part of the headband.
- You should respond to stimuli by pointing on the perceived location on your forehead using a pen while looking at the mirror.
- Press the "Next" key in the GUI for capturing the image while pointing on the perceived stimuli location and after hearing a shutter voice the next stimuli will start.
- Repeat trials until you see the finish message.

Experiment 3:

- By pressing the "Start" button in GUI, the experiment will start.
- Vibration is displayed to one or two parts of the headband: If one location was sensed, you should point to that with a pen while looking at the mirror. If two locations were sensed, you should point them with two pens while looking at the mirror.
- Press the "Next" key in the GUI with foot switch to capture the image while pointing on the perceived stimuli location and after hearing a shutter voice the next stimuli will start.
- Repeat trials until you see the finish message.

Participants' rights: Your participation in this study is entirely voluntary. You may decide to stop being a part of study at any time without explanation or refuse to answer any questions with which you are uncomfortable. The data will be accessible only to those working on the project.

Questions and contacts: At this time you may ask any questions you may have regarding this study. If you have questions later, you can contact:

Hamideh Kerdegari: h.kerdegari@sheffield.ac.uk

Participant's name and signature:

A.2 Consent form II

You are invited to take part in a psychophysics experiment. The aim of this research is to evaluate the perception of vibrotactile

stimuli for a wearable haptic interface. This research is as a part of my PhD project under the supervision of Professor Tony Prescott and has received ethics approval from the department of psychology, University of Sheffield. Practice sessions will be given prior to the experiments. During the test please do not close your eyes and before you press the "Next" button, you can take a rest as long as you want. The total time required to complete the study is approximately 15 minutes.

Procedure: First you need to sit in front of the computer screen and wear a headband which composes of a set of vibration motors. When you are ready, the experiment will start as follow:

- Press the start button in GUI by clicking a mouse.
- Then, vibration stimuli patterns are displayed to your headband and you should rate their perceived movement by choosing one of five buttons in the GUI.
- Press the "Next" button in the GUI for starting the next stimuli.
- Repeat trials until you see the finish message.

Participants' rights: Your participation in this study is entirely voluntary. You may decide to stop being a part of study at any time without explanation or refuse to answer any questions with which you are uncomfortable. The data will be accessible only to those working on the project.

Questions and contacts: At this time you may ask any questions you may have regarding this study. If you have questions later, you can contact:

Hamideh Kerdegari: h.kerdegari@sheffield.ac.uk

Participant's name and signature:

A.3 Consent form III

The aim of this research is to evaluate vibrotactile feedbacks for human navigation using a wearable haptic interface device (tactile helmet). This research is as a part of my PhD project under the supervision of Professor Tony Prescott and has received ethics approval from the department of psychology, University of Sheffield. Practice sessions will be given prior to the experiments. After each trial, you can take a rest as long as you want. During the test please do not close your eyes. The total time required to complete the study should be approximately one hour. At the end of the experiment you will be asked to fill a short questionnaire.

Procedure: If you agree to be in this study, you will be asked to do the following: First you need to wear the tactile helmet and stand in a fixed start point which already indicated in the motion capture room. When you are ready, the experiment will start. In this experiment, you will be navigated along virtual walls (you cannot see them) using tactile commands that present on your forehead. I have considered three simple navigation commands: turn-right, turn-left and go-forward commands. The turn-right/left command induces a rotation around self (right/left rotation); while the go-forward command induces a motion toward forward direction. After receiving each command, you should respond to it correctly by rotating around self in the turn-right/left commands or walking toward forward direction in the go-forward

commands. Finally, when you reach to the finish point, all the vibration motors are activated to show that the trial has finished. Then you have to come back to the start point and these trails will be repeated until the experimenter tells you that the experiment has finished.

Participants' rights: Your participation in this study is entirely voluntary. You may decide to stop being a part of study at any time without explanation or refuse to answer any questions with which you are uncomfortable. The data will be accessible only to those working on the project.

Questions and contacts: For further questions please contact:

Hamideh Kerdegari: h.kerdegari@sheffield.ac.uk

Participant's name and signature:

A.4 Consent form IV

The aim of this research is to evaluate tactile and audio feedbacks for human navigation using a wearable haptic interface device (tactile helmet). This research is as a part of my PhD project under the supervision of Professor Tony Prescott and has received ethics approval from the department of psychology, University of Sheffield. Practice sessions will be given prior to the experiments. After each trial, you can take a rest as long as you want. The total time required to complete the study should be approximately 20 minutes. At the end of the experiment you will be asked to fill a short questionnaire.

Procedure: You need to wear the tactile helmet and blindfold, and then stand in a fixed start point. When you are ready, the experiment will start. In this experiment you will be navigated along cardboard walls using tactile and audio commands that you receive. I have considered three simple commands: turn-right, turn-left and go-forward commands. The turn-right/left command induces a rotation around self (right/left rotation); while the go-forward command induces a motion toward forward direction. After receiving each command, you should respond to it correctly by rotating around self in the turn-right/left commands or walking toward forward direction in the go-forward commands. Finally, when you reach to the finish point, the experimenter let you know that experiment has finished.

Participants' rights: Your participation in this study is entirely voluntary. You may decide to stop being a part of study at any time without explanation or refuse to answer any questions with which you are uncomfortable. The data will be accessible only to those working on the project.

Questions and contacts: If you have questions later, you can contact:

Hamideh Kerdegari: h.kerdegari@sheffield.ac.uk

Participant's name and signature:

Appendix B

Hardware specification

This appendix presents the datasheet of all the employed electronic components in the Mark-II Tactile Helmet. They are explained as follows: ultrasound sensor, IMU (accelerometer, gyroscope and compass), vibration motor and microcontroller board. Furthermore, the datasheet of the employed accelerometer in the vibrotactile absolute threshold measurement experiment is also provided. At the end, schematic of the Mark-II Tactile Helmet is illustrated.

B.1 I2CXL-MaxSonar-EZ2 Ultrasound Sensor

The I2CXL-MaxSonar-EZ2 offers a good balance between wide and narrow beam sensors, and large and narrow object detection. The I2CXL-MaxSonar-EZ2 works for nearly all indoor applications where the wider or narrower beam of other models could be a problem, including people detection, large-target detection, long range detection, and applications requiring high noise tolerance. The I2CXL-MaxSonar-EZ2 detects objects from 0-cm to 765-cm (25.1 feet) and provides sonar range information from 20-cm or 25-cm out to 765-cm with 1-cm resolution. Objects from 0-cm to minimum distance typically range as minimum distance.

Features	Low Power Requirement	Applications and Uses
<ul style="list-style-type: none"> • I2C bus communication allows rapid control of multiple sensors with only two wires • High acoustic power output • Real-time auto calibration and noise rejection for every ranging cycle • Calibrated beam patterns • Continuously variable gain • Object presence information as close as 1-mm from the sensor. Range information starting at min. distance. • 3V to 5.5V supply with very low average current draw • Readings can occur up to every 25ms (40Hz rate) for up-close objects. 15Hz rate for full range. • Triggered operation provides a new range reading as desired • Ultrasonic signal frequency of 42KHz • Status pin available to determine sensor state • -40°C to +65°C operation 	<ul style="list-style-type: none"> • Wide, low supply voltage requirements eases battery powered design • Low current draw reduces current drain for battery operation • Fast first reading after power-up eases battery requirements <p>Benefits</p> <ul style="list-style-type: none"> • Acoustic and electric noise resistance • Reliable and stable range data • Low cost • Quality controlled beam characteristics • Very low power rangefinder, excellent for multiple sensor or battery based systems • Ranging is triggered externally • Fast measurement cycle • No power up calibration required • Perfect for when objects may be directly in front of the sensor during power up • Easy mounting 	<ul style="list-style-type: none"> • Multi-sensor arrays • Proximity zone detection • People detection • Robot ranging sensor • Autonomous navigation • Educational and hobby robotics • Environments with acoustic and electrical noise • Distance measuring • Long range object detection • Security systems • Motion detection • Landing flying objects • Collision avoidance

MB1222

I2CXL-MaxSonar®-EZ2™ Beam Pattern

Sample results for measured beam pattern are shown on a 30-cm grid. The detection pattern is shown for dowels of varying diameters that are placed in front of the sensor.

A 6.1-mm (0.25-inch) diameter dowel

B 2.54-cm (1-inch) diameter dowel

C 8.89-cm (3.5-inch) diameter dowel

Note: The maximum detected distance for 3.3V is ~720cm

D 11-inch wide board moved left to right with the board parallel to the front sensor face.

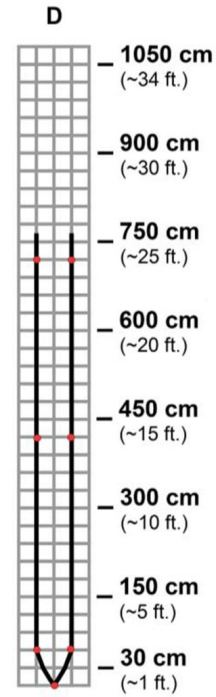
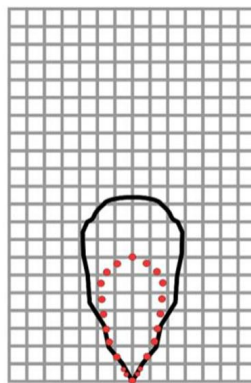
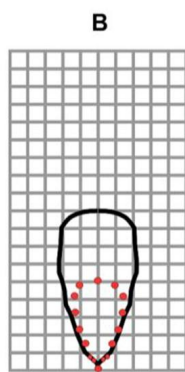
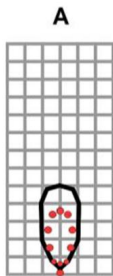
This shows the sensor's range capability.

Note: For people detection the pattern typically falls between charts A and B.

■ ■ Partial Detection

— 5.0 V

● 3.3 V



Beam Characteristics are Approximate

Beam Patterns drawn to a 1:95 scale for easy comparison to our other products.

B.2 IMU

B.2.1 ADXL345 accelerometer

Features:

- Ultralow power: as low as 40 μA in measurement mode and 0.1 μA in standby mode at $V_S = 2.5\text{ V}$ (typical)
- Power consumption scales automatically with bandwidth
- User-selectable resolution: Fixed 10-bit resolution. Full resolution, where resolution increases with g range, up to 13-bit resolution at $\pm 16\text{ g}$ (maintaining 4 mg/LSB scale factor in all g ranges)
- Embedded, patent pending FIFO technology minimizes host processor load
- Tap/double tap detection, Activity/inactivity monitoring, Free-fall detection
- Supply voltage range: 2.0 V to 3.6 V
- I/O voltage range: 1.7V to V_S
- SPI (3- and 4-wire) and I²C digital interfaces
- Wide temperature range (-40°C to $+85^\circ\text{C}$)
10,000 g shock survival Pb free/RoHS compliant
- Small and thin: 3 mm \times 5 mm \times 1 mm LGA package

Application:

Handsets

Personal navigation devices

Industrial Instrumentation

Gaming and pointing devices

Medical Instrumentation

Hard disk drive (HDD) protection

Fitness equipment

General Description:

The ADXL345 is a small, thin, low power, 3-axis accelerometer with high resolution (13-bit) measurement at up to $\pm 16\text{ g}$. Digital output data is formatted as 16-bit twos complement and is accessible through either a SPI (3- or 4-wire) or I²C digital interface.

The ADXL345 is well suited for mobile device applications. It measures the static acceleration of gravity in tilt-sensing applications, as well as dynamic acceleration resulting from motion or shock. Its high resolution (4 mg/LSB) enables measurement of inclination changes less than 1.0° .

Several special sensing functions are provided. Activity and inactivity sensing detect the presence or lack of motion and if the acceleration on any axis exceeds a user-set level. Tap sensing detects single and double taps. Free-fall sensing detects if the device is falling. These functions can be mapped to one of two interrupt output pins. An integrated, patent pending 32-level first in, first out (FIFO) buffer can be used to store data to minimize host processor intervention.

Low power modes enable intelligent motion-based power management with threshold sensing and active acceleration measurement at extremely low power dissipation. The ADXL345 is supplied in a small, thin, 3 mm \times 5 mm \times 1 mm, 14-lead, plastic package.

Specifications:

TA = 25°C, VS = 2.5 V, VDD I/O = 1.8 V, acceleration = 0 g, CS = 1 μF tantalum, CIO = 0.1 μF, unless otherwise noted.

Parameter	Test Conditions	Min	Typ	Max	Unit
SENSOR INPUT					
Measurement Range	Each axis User selectable		±2, ±4, ±8, ±16		g
Nonlinearity	Percentage of full scale		±0.5		%
Inter-Axis Alignment Error			±0.1		Degrees
Cross-Axis Sensitivity ²			±1		%
OUTPUT RESOLUTION					
All g Ranges	Each axis 10-bit resolution		10		Bits
±2 g Range	Full resolution		10		Bits
±4 g Range	Full resolution		11		Bits
±8 g Range	Full resolution		12		Bits
±16 g Range	Full resolution		13		Bits
SENSITIVITY					
Sensitivity at X _{OUT} , Y _{OUT} , Z _{OUT}	Each axis ±2 g, 10-bit or full resolution	232	256	286	LSB/g
Scale Factor at X _{OUT} , Y _{OUT} , Z _{OUT}	±2 g, 10-bit or full resolution	3.5	3.9	4.3	mg/LSB
Sensitivity at X _{OUT} , Y _{OUT} , Z _{OUT}	±4 g, 10-bit resolution	116	128	143	LSB/g
Scale Factor at X _{OUT} , Y _{OUT} , Z _{OUT}	±4 g, 10-bit resolution	7.0	7.8	8.6	mg/LSB
Sensitivity at X _{OUT} , Y _{OUT} , Z _{OUT}	±8 g, 10-bit resolution	58	64	71	LSB/g
Scale Factor at X _{OUT} , Y _{OUT} , Z _{OUT}	±8 g, 10-bit resolution	14.0	15.6	17.2	mg/LSB
Sensitivity at X _{OUT} , Y _{OUT} , Z _{OUT}	±16 g, 10-bit resolution	29	32	36	LSB/g
Scale Factor at X _{OUT} , Y _{OUT} , Z _{OUT}	±16 g, 10-bit resolution	28.1	31.2	34.3	mg/LSB
Sensitivity Change Due to Temperature			±0.01		%/°C
0 g BIAS LEVEL					
0 g Output for X _{OUT} , Y _{OUT}	Each axis	-150	±40	+150	mg
0 g Output for Z _{OUT}		-250	±80	+250	mg
0 g Offset vs. Temperature for x-, y-Axes			±0.8		mg/°C
0 g Offset vs. Temperature for z-Axis			±4.5		mg/°C
NOISE PERFORMANCE					
Noise (x-, y-Axes)	Data rate = 100 Hz for ±2 g, 10-bit or full resolution		<1.0		LSB rms
Noise (z-Axis)	Data rate = 100 Hz for ±2 g, 10-bit or full resolution		<1.5		LSB rms
OUTPUT DATA RATE AND BANDWIDTH					
Measurement Rate ³	User selectable	6.25		3200	Hz
SELF-TEST⁴					
Output Change in x-Axis	Data rate ≥ 100 Hz, 2.0 V ≤ VS ≤ 3.6 V	0.20		2.10	g
Output Change in y-Axis		-2.10		-0.20	g
Output Change in z-		0.30		3.40	g
POWER SUPPLY					
Operating Voltage Range (VS)		2.0	2.5	3.6	V V
Interface Voltage Range (VDD I/O)	VS ≤ 2.5 V	1.7	1.8	VS	μA
	VS ≥ 2.5 V	2.0	2.5	VS	μA
Supply Current	Data rate > 100 Hz		145		μA
	Data rate < 10 Hz		40		ms
Standby Mode Leakage Current			0.1	2	
Turn-On Time ⁵	Data rate = 3200 Hz		1.4		
Operating Temperature Range		-40		+85	°C
Device Weight			20		mg

¹ All minimum and maximum specifications are guaranteed. Typical specifications are not guaranteed.

² Cross-axis sensitivity is defined as coupling between any two axes.

³ Bandwidth is half the output data rate.

⁴ Self-test change is defined as the output (g) when the SELF_TEST bit = 1 (in the DATA_FORMAT register) minus the output (g) when the SELF_TEST bit = 0 (in the DATA_FORMAT register). Due to device filtering, the output reaches its final value after $4 \times \tau$ when enabling or disabling self-test, where $\tau = 1/(\text{data rate})$.

⁵ Turn-on and wake-up times are determined by the user-defined bandwidth. At a 100 Hz data rate, the turn-on and wake-up times are each approximately 11.1 ms. For other data rates, the turn-on and wake-up times are each approximately $\tau + 1.1$ in milliseconds, where $\tau = 1/(\text{data rate})$.

B.2.2 ITG-3200 3-Axis Gyro Evaluation Board

ITG-3200 3-Axis Gyro Evaluation Board provides three axes of motion processing, comprised of:

- X-, Y-, and Z-Axis gyros with $\pm 2,000$ °/sec full-scale range;
- 16-bit digital data measured using on-chip ADCs, transmitted over I²C interface.

The Evaluation board may be used independently with the I²C serial communications interface. Alternatively, it may be connected to InvenSense's ARM Evaluation Board (INV-ARMEVB) for connectivity to a host Windows PC using the USB interface.

ITG-3200 3-Axis EVB Overview:

The ITG-3200 3-Axis EVB contains the ITG-3200 3-axis digital gyroscope and its interface circuitry. It contains removable and 'solder-across' jumper points that permits several circuit configurations.

Referring to Figure 1, the EVB is populated on its top side only for ease of measurement access. The 20-pin (10 x 2-pin) Main header connector is designed to interface with the InvenSense INV-ARM EVB, which is a host microcontroller board useful for adapting the ITG-3200 3-Axis EVB to a personal computer via its USB port.

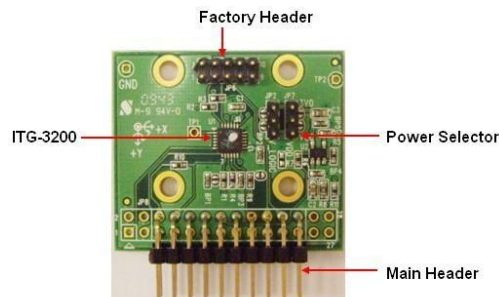
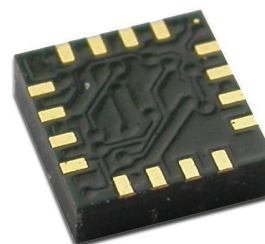


Figure 1. Top side of the ITG-3200 3-Axis EVB

B.2.3 3-Axis Digital compass IC HMC5883L

The Honeywell HMC5883L is a surface-mount, multi-chip module designed for low-field magnetic sensing with a digital interface for applications such as low-cost compassing and magnetometry. The HMC5883L includes our state-of-the-art, high-resolution HMC118X series magneto-resistive sensors plus an ASIC containing amplification, automatic degaussing strap drivers, offset cancellation, and a 12-bit ADC that enables 1° to 2° compass heading accuracy. The I²C serial bus allows for easy interface. The HMC5883L is a 3.0x3.0x0.9mm surface mount 16-pin leadless chip carrier (LCC). Applications for the HMC5883L include Mobile Phones, Netbooks, Consumer Electronics, Auto Navigation Systems, and Personal Navigation Devices.



The HMC5883L utilizes Honeywell's Anisotropic Magnetoresistive (AMR) technology that provides advantages over other magnetic sensor technologies. These anisotropic, directional sensors feature precision in-axis sensitivity and linearity. These sensors' solid-state construction with very low cross-axis sensitivity is designed to measure both the direction and the magnitude of Earth's magnetic fields, from milli-gauss to 8 gauss. Honeywell's Magnetic Sensors are among the most sensitive and reliable low-field sensors in the industry.

FEATURES

- ▶ 3-Axis Magnetoresistive Sensors and ASIC in a 3.0x3.0x0.9mm LCC Surface Mount Package
- ▶ 12-Bit ADC Coupled with Low Noise AMR Sensors Achieves 2 milli-gauss Field Resolution in ±8 Gauss Fields
- ▶ Built-In Self Test
- ▶ Low Voltage Operations (2.16 to 3.6V) and Low Power Consumption (100 μA)
- ▶ Built-In Strap Drive Circuits
- ▶ I²C Digital Interface
- ▶ Lead Free Package Construction
- ▶ Wide Magnetic Field Range (+/-8 Oe)
- ▶ Software and Algorithm Support Available
- ▶ Fast 160 Hz Maximum Output Rate

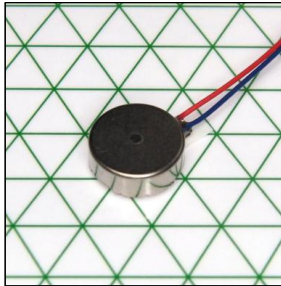
BENEFITS

- ▶ Small Size for Highly Integrated Products. Just Add a Micro-Controller Interface, Plus Two External SMT Capacitors Designed for High Volume, Cost Sensitive OEM Designs Easy to Assemble & Compatible with High Speed SMT Assembly
- ▶ Enables 1° to 2° Degree Compass Heading Accuracy
- ▶ Enables Low-Cost Functionality Test after Assembly in Production
- ▶ Compatible for Battery Powered Applications
- ▶ Set/Reset and Offset Strap Drivers for Degaussing, Self Test, and Offset Compensation
- ▶ Popular Two-Wire Serial Data Interface for Consumer Electronics
- ▶ RoHS Compliance
- ▶ Sensors Can Be Used in Strong Magnetic Field Environments with a 1° to 2° Degree Compass Heading Accuracy
- ▶ Compassing Heading, Hard Iron, Soft Iron, and Auto Calibration Libraries Available
- ▶ Enables Pedestrian Navigation and LBS Applications

SPECIFICATIONS (* Tested at 25°C except stated otherwise.)

Characteristics	Conditions*	Min	Typ	Max	Units
Power Supply					
Supply Voltage	VDD Referenced to AGND	2.16	2.5	3.6	Volts
	VDDIO Referenced to DGND	1.71	1.8	VDD+0.1	Volts
Average Current Draw	Idle Mode	-	2	-	µA
	Measurement Mode (7.5 Hz ODR; No measurement average, MA1:MA0 = 00) VDD = 2.5V, VDDIO = 1.8V (Dual Supply) VDD = VDDIO = 2.5V (Single Supply)	-	100	-	µA
Performance					
Field Range	Full scale (FS)	-8		+8	gauss
Mag Dynamic Range	3-bit gain control	±1		±8	gauss
Sensitivity (Gain)	VDD=3.0V, GN=0 to 7, 12-bit ADC	230		1370	LSb/gauss
Digital Resolution	VDD=3.0V, GN=0 to 7, 1-LSb, 12-bit ADC	0.73		4.35	milli-gauss
Noise Floor (Field Resolution)	VDD=3.0V, GN=0, No measurement average, Standard Deviation 100 samples (See typical performance graphs below)		2		milli-gauss
Linearity	±2.0 gauss input range			0.1	±% FS
Hysteresis	±2.0 gauss input range		±25		ppm
Cross-Axis Sensitivity	Test Conditions: Cross field = 0.5 gauss, Happlied = ±3 gauss		±0.2%		%FS/gauss
Output Rate (ODR)	Continuous Measurement Mode	0.75		75	Hz
	Single Measurement Mode			160	Hz
Measurement Period	From receiving command to data ready		6		ms
Turn-on Time	Ready for I2C commands		200		µs
	Analog Circuit Ready for Measurements		50		ms
Gain Tolerance	All gain/dynamic range settings		±5		%
I ² C Address	8-bit read address		0x3D		hex
	8-bit write address		0x3C		hex
I ² C Rate	Controlled by I ² C Master			400	kHz
I ² C Hysteresis	Hysteresis of Schmitt trigger inputs on SCL and SDA - Fall (VDDIO=1.8V)		0.2*VDDIO		Volts
	Rise (VDDIO=1.8V)		0.8*VDDIO		Volts
Self Test	X & Y Axes		±1.16		gauss
	Z Axis		±1.08		gauss
	X & Y & Z Axes (GN=5) Positive Bias X & Y & Z Axes (GN=5) Negative Bias	243 -575		575 -243	LSb
Sensitivity Tempco	T _A = -40 to 125°C, Uncompensated Output		-0.3		%/°C
General					
ESD Voltage	Human Body Model (all pins)			2000	Volts
	Charged Device Model (all pins)			750	Volts
Operating Temperature	Ambient	-30		85	°C
Storage Temperature	Ambient, unbiased	-40		125	°C

B.3 310-113 Vibration Motor



10mm Vibration Motor - 3mm Type
Shown on 6mm Isometric Grid



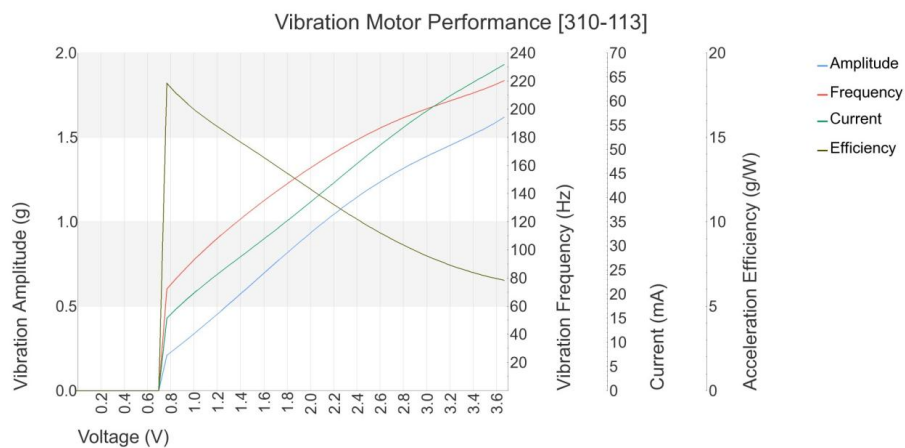
Product Data Sheet
Pico Vibe™

10mm Vibration Motor - 3mm Type

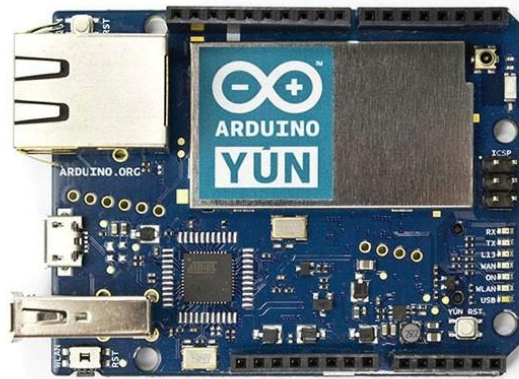
Model: 310-113

Key Features	
Body Diameter:	10 mm [± 0.1]
Body length:	3.4 mm [± 0.1]
Rated Operating Voltage:	3V
Rated Vibration Speed:	12,200 rpm [$\pm 2,500$]
Typical Rated Operating Current:	60 mA
Typical Normalized Amplitude:	1.34 G

Typical Vibration Motor Performance Characteristics

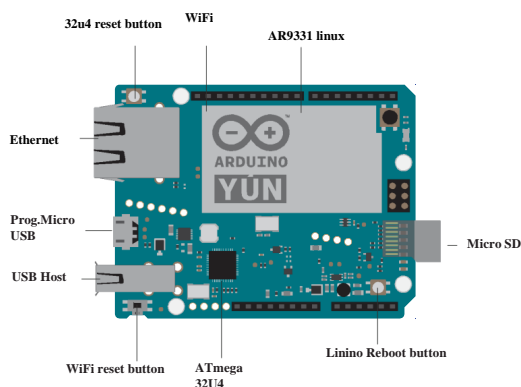


B.4 Arduino Yún microcontroller



Overview

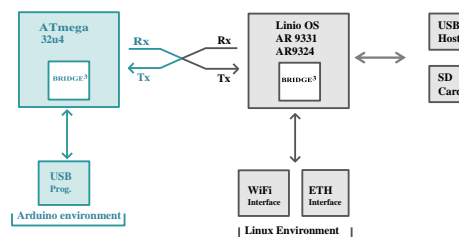
Arduino Yún is a microcontroller board based on the ATmega32u4 (datasheet) and the Atheros AR9331. The Atheros processor supports a Linux distribution based on OpenWrt named Linino OS. The board has built-in Ethernet and WiFi support, a USB-A port, micro-SD card slot, 20 digital input/output pins (of which 7 can be used as PWM outputs and 12 as analog inputs), a 16 MHz crystal oscillator, a micro USB connection, an ICSP header, and a 3 reset buttons.



The Yún distinguishes itself from other Arduino boards in that it can communicate with the Linux distribution onboard, offering a powerful networked computer with the ease of Arduino. In addition to Linux commands like cURL, you can write your own shell and python scripts for robust interactions.

The Yún is similar to the Leonardo in that the ATmega32u4 has built-in USB communication, eliminating the need for a secondary processor. This allows the Yún to appear to a connected computer as a mouse and keyboard, in addition to a virtual (CDC) serial / COM port.

The Bridge library facilitates communication between the two processors, giving Arduino sketches the ability to run shell scripts, communicate with network interfaces, and receive information from the AR9331 processor. The USB host, network interfaces and SD card are not connected to the 32U4, but the AR9331, and the Bridge library also enables the Arduino to interface with those peripherals.



Arduino Yun



Description

AVR Microcontroller

Microcontroller	ATmega32u4
Operating Voltage	5V
Input Voltage	5V
Digital I/O Pins	20
PWM Channels	7
Analog Input Channels	12
DC Current per I/O Pin	40 mA
DC Current for 3.3V Pin	50 mA
Flash Memory	32 KB (of which 4 KB used by bootloader)
SRAM	2.5 KB
EEPROM	1 KB
Clock Speed	16 MHz

Linux Microprocessor

Processor	Atheros AR9331
Architecture	MIPS @400MHz
Operating Voltage	3.3V
Ethernet	IEEE 802.3 10/100Mbit/s
WiFi	IEEE 802.11b/g/n
USB Type-A	2.0 Host
Card Reader	Micro-SD only
RAM	64 MB DDR2
Flash Memory	16 MB

B.5 ADXL325 Accelerometer

Features:

- 3-axis sensing
- Small, low profile package
- 4 mm × 4 mm × 1.45 mm
- LFCSP Low power: 350 μ A typical
- Single-supply operation: 1.8 V to 3.6 V
- 10,000 g shock survival
- Excellent temperature stability
- Bandwidth adjustment with a single capacitor per axis
- RoHS/WEEE lead-free compliant

Applications:

- Cost-sensitive, low power, motion- and tilt-sensing applications
- Mobile devices
- Gaming systems
- Disk drive protection
- Image stabilization
- Sports and health devices

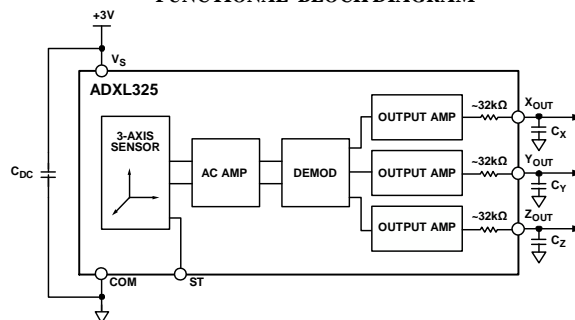
General Description:

The ADXL325 is a small, low power, complete 3-axis accelerometer with signal conditioned voltage outputs. The product measures acceleration with a minimum full-scale range of ± 5 g. It can measure the static acceleration of gravity in tilt-sensing applications, as well as dynamic acceleration, resulting from motion, shock, or vibration.

The user selects the bandwidth of the accelerometer using the CX, CY, and CZ capacitors at the XOUT, YOUT, and ZOUT pins. Bandwidths can be selected to suit the application with a range of 0.5 Hz to 1600 Hz for X and Y axes and a range of 0.5 Hz to 550 Hz for the Z axis.

The ADXL325 is available in a small, low profile, 4 mm × 4 mm × 1.45 mm, 16-lead, plastic lead frame chip scale package (LFCSP_LQ).

FUNCTIONAL BLOCK DIAGRAM



Specifications:

TA = 25°C, VS = 3 V, CX = CY = CZ = 0.1 µF, acceleration = 0 g, unless otherwise noted. All minimum and maximum specifications are guaranteed. Typical specifications are not guaranteed.

Parameter	Conditions	Min	Typ	Max	Unit
SENSOR INPUT					
Measurement Range	Each axis	±5	±6		g
Nonlinearity	Percent of full scale		±0.2		%
Package Alignment Error			±1		Degrees
Interaxis Alignment Error			±0.1		Degrees
Cross-Axis Sensitivity ¹			±1		%
SENSITIVITY (RATIOMETRIC)²					
Sensitivity at X _{OUT} , Y _{OUT} , Z _{OUT}	V _S = 3 V	156	174	192	mV/g
Sensitivity Change Due to Temperature ³	V _S = 3 V		±0.01		%/°C
ZERO g BIAS LEVEL (RATIOMETRIC)					
0 g Voltage at X _{OUT} , Y _{OUT} , Z _{OUT}	V _S = 3 V	1.3	1.5	1.7	V
0 g Offset vs. Temperature			±1		
NOISE PERFORMANCE					
Noise Density X _{OUT} , Y _{OUT} , Z _{OUT}			250		µg/√Hz rms
FREQUENCY RESPONSE⁴					
Bandwidth X _{OUT} , Y _{OUT} ⁵	No external filter		1600		Hz
Bandwidth Z _{OUT} ⁵	No external filter		550		Hz
R _{FILT} Tolerance			32 ± 15%		kΩ
Sensor Resonant Frequency			5.5		kHz
SELF TEST⁶					
Logic Input Low			+0.6		V
Logic Input High			+2.4		µA
ST Actuation Current			+60		mV
Output Change at X _{OUT}	Self test 0 to 1	-90	-190	-350	mV
Output Change at Y _{OUT}	Self test 0 to 1	+90	+190	+350	mV
Output Change at Z _{OUT}	Self test 0 to 1	+90	+320	+580	mV
OUTPUT AMPLIFIER					
Output Swing Low	No load		0.1		V
Output Swing High	No load		2.8		V
POWER SUPPLY					
Operating Voltage Range		1.8		3.6	V
Supply Current	V _S = 3 V		350		µA
Turn-On Time ⁷	No external filter		1		ms
TEMPERATURE					
Operating Temperature Range		-40		+85	°C

1 Defined as coupling between any two axes.

2 Sensitivity is essentially ratiometric to VS.

3 Defined as the output change from ambient-to-maximum temperature or ambient-to-minimum temperature.

4 Actual frequency response controlled by user-supplied external filter capacitors (CX, CY, CZ).

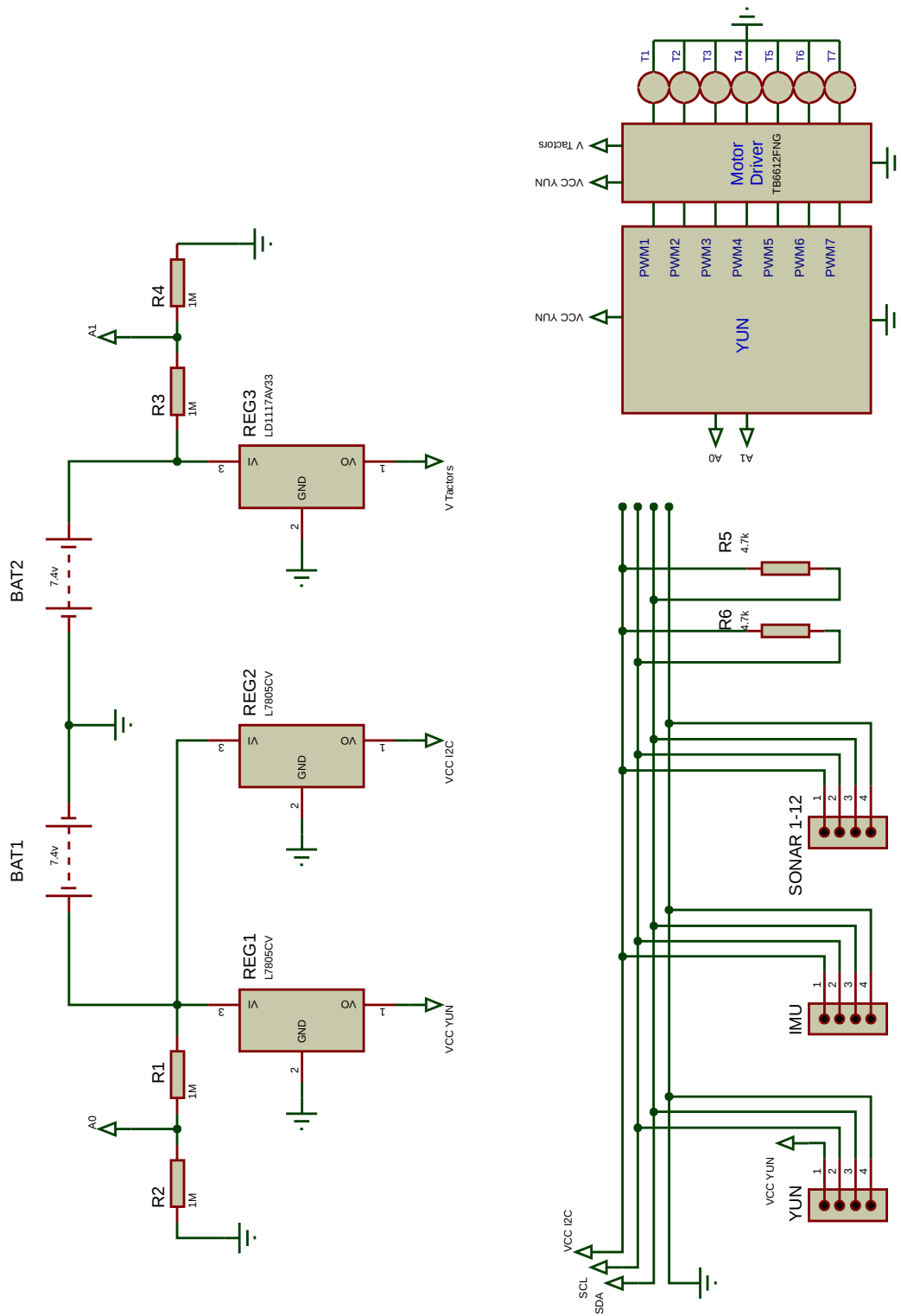
5 Bandwidth with external capacitors = $1/(2 \times \pi \times 32 \text{ k}\Omega \times C)$. For CX, CY = 0.003 µF, bandwidth = 1.6 kHz. For CZ = 0.01 µF, bandwidth = 500 Hz.

For CX, CY, CZ = 10 µF, bandwidth = 0.5 Hz.

6 Self test response changes cubically with VS.

7 Turn-on time is dependent on CX, CY, CZ and is approximately $160 \times CX$ or CY or $CZ + 1$ ms, where CX, CY, CZ are in µF.

B.6 Schematic of the Mark-II Tactile Helmet



Appendix C

Questionnaires

This section presents two employed questionnaires in this thesis. The first questionnaire is likert scale questionnaire that was used to measure participants' attitude toward the tactile languages in Chapter 5. The second one is NASA TLX questionnaire that was utilized to determine haptic and audio feedbacks workload for user's navigation along the wall in Chapter 6.

C.1 Likert Scale Questionnaire

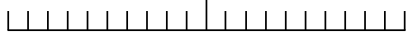
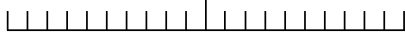
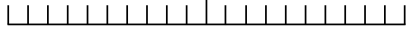
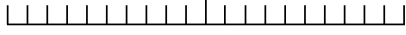

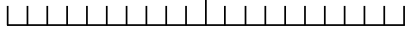
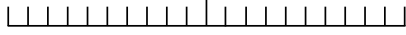
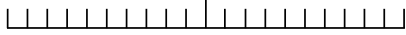

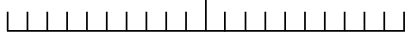


- Please answer these questions by rating them on a score from 1 to 7.

	1	2	3	4	5	6	7
	Strongly disagree	disagree	Somewhat disagree	Neither Agree or disagree	Somewhat Agree	Agree	Strongly Agree
1. The helmet was comfortable.							
2. It was easy to move while wearing the helmet.							
3. The vibration motors were noisy and irritating.							
4. Repeated continuous (RC) commands were easy to distinguish.							
5. Repeated discrete (RD) commands were easy to distinguish.							
6. Single continuous (SC) commands were easy to distinguish.							
7. Single discrete (SD) commands were easy to distinguish.							
8. Repeated continuous (RC) commands were effective to navigate you along the wall.							
9. Repeated discrete (RD) commands were effective to navigate you along the wall.							
10. Single continuous (SC) commands were effective to navigate you along the wall.							
11. Single discrete (SD) commands were effective to navigate you along the wall.							
12. Repeated continuous (RC) commands were comfortable.							
13. Repeated discrete (RD) commands were comfortable.							
14. Single continuous (SC) commands were comfortable.							
15. Single discrete (SD) commands were comfortable.							

C.2 NASA Task Load Index Questionnaire

RATING SCALE DEFINITIONS		
Title	Endpoints	Descriptions
Mental demand	<i>Low/High</i>	How much mental and perceptual activity was required (e.g., thinking, deciding, calculating, remembering, searching, etc.)? Was the task easy or demanding, simple or complex, exacting or forgiving?
Physical demand	<i>Low/High</i>	How much physical activity was required (e.g., pushing, pulling, turning, controlling, activating, etc.)? Was the task easy or demanding, slow or brisk, slack or strenuous, restful or laborious?
Temporal demand	<i>Low/High</i>	How much time pressure did you feel due to the rate or pace at which the tasks or task elements occurred? Was the pace slow and leisurely or rapid and frantic?
Effort	<i>Low/High</i>	How hard did you have to work (mentally and physically) to accomplish your level of performance?
Performance	<i>Good/Poor</i>	How successful do you think you were in accomplishing the goals of the task set by the experimenter (or yourself)? How satisfied were you with your performance in accomplishing these goals?
Frustration	<i>Low/High</i>	How insecure, discouraged, irritated, stressed and annoyed versus secure, gratified, content, relaxed and complacent did you feel during the task?

Name:	Date:
--------------	--------------

	Haptic	Audio
Mental Demand	 Very low Very high	 Very low Very high
Physical Demand	 Very low Very high	 Very low Very high
Temporal Demand	 Very low Very high	 Very low Very high
Performance	 Very good Very poor	 Very good Very poor
Effort	 Very low Very high	 Very low Very high
Frustration	 Very low Very high	 Very low Very high

- Which navigation methods do you prefer (haptic/audio)?

